NAVAL POSTGRADUATE SCHOOL

Monterey, California

THESIS

AN EXPERIMENTAL AND COMPUTER
MODELING STUDY OF STEPPED
RADIUS MONOPOLE ANTENNAS

by

Yim, Jae Yong

December 1988

Thesis Advisor: Richard W. Adler
Co-Advisor: James K. Breakall

Unclassified

security classification of this page

REPORT DOCUMENTATION PAGE

1a Report Security Classification Unclassified	1b Restrictive Markings
2a Security Classification Authority	3 Distribution Availability of Report Approved for public release; distribution is unlimited.
2b Declassification Downgrading Schedule	
4 Performing Organization Report Number(s)	5 Monitoring Organization Report Number(s)
6a Name of Performing Organization Naval Postgraduate School / 6b Office Symbol *(if applicable)* 62	7a Name of Monitoring Organization Naval Postgraduate School
6c Address *(city, state, and ZIP code)* Monterey, CA 93943-5000	7b Address *(city, state, and ZIP code)* Monterey, CA 93943-5000
8a Name of Funding Sponsoring Organization / 8b Office Symbol *(if applicable)*	9 Procurement Instrument Identification Number
8c Address *(city, state, and ZIP code)*	10 Source of Funding Numbers Program Element No / Project No / Task No / Work Unit Accession No

11 Title *(include security classification)*
AN EXPERIMENTAL AND COMPUTER MODELING STUDY OF STEPPED RADIUS MONOPOLE ANTENNAS

12 Personal Author(s) Yim, Jae Yong

13a Type of Report	13b Time Covered	14 Date of Report *(year, month, day)*	15 Page Count
Master's Thesis	From To	December 1988	163

16 Supplementary Notation The views expressed in this thesis are those of the author and do not reflect the official policy or position of the Department of Defense or the U.S. Government.

17 Cosati Codes

Field	Group	Subgroup

18 Subject Terms *(continue on reverse if necessary and identify by block number)*
Monopole Antennas, Stepped Radius, Computer Simulation, Impedance Measurements

19 Abstract *(continue on reverse if necessary and identify by block number)*
This thesis compares the input impedance numerically calculated by MININEC, NEC, and NECGS with experimental results on stepped radius monopole antennas for swept frequencies. This determines the limitation of computer codes and gives guidelines for Yagi and Log Periodic (LP) antenna designs which use Tapered Linear Antenna Elements (TLAE's).

NEC and MININEC, thin wire modeling codes, use different Electric Field Integral Equation (EFIE) formulations of the method of moments for the solution of currents. A cylindrical wire cage model is used via NECGS. Four groups of computer models are developed, varying the number of segments from 1 to 70 for 27-31 MHz. Reflection coefficients of seven experimental models are measured at the antenna feed point, and the input impedances are calculated by an auxiliary computer program. The input impedance is then analyzed by comparing the computer simulation results with measured results. Surprisingly, the input impedance of MININEC is closest to experimental results for monopoles which were constructed with ratios of radius-to-wavelength up to 0.0026. (KR)

20 Distribution Availability of Abstract ☒ unclassified unlimited ☐ same as report ☐ DTIC users	21 Abstract Security Classification Unclassified
22a Name of Responsible Individual Richard W. Adler	22b Telephone *(include Area code)* (408) 646-2352 / 22c Office Symbol 62Ab

DD FORM 1473,84 MAR — 83 APR edition may be used until exhausted. All other editions are obsolete — security classification of this page

Unclassified

Approved for public release; distribution is unlimited.

An Experimental and Computer
Modeling Study of Stepped
Radius Monopole Antennas

by

Yim, Jae Yong
Major, Korean Army
Korean Military Academy, 1978 Seoul

Submitted in partial fulfillment of the
requirements for the degree of

MASTER OF SCIENCE IN ELECTRICAL ENGINEERING

from the

NAVAL POSTGRADUATE SCHOOL
December 1988

Author: ______________________
Yim, Jae Yong

Approved by: ______________________
Richard W. Adler, Thesis Advisor

____
James K. Breakall, Co-Advisor

____
John P. Powers, Chairman.
Department of Electrical and Computer Engineering

____
Gordon E. Schacher,
Dean of Science and Engineering

ABSTRACT

This thesis compares the input impedance numerically calculated by MININEC, NEC, and NECGS with experimental results on stepped radius monopole antennas for swept frequencies. This determines the limitation of computer codes and gives guidelines for Yagi and Log Periodic (LP) antenna designs which use Tapered Linear Antenna Elements (TLAE's)

NEC and MININEC, thin wire modeling codes, use different Electric Field Integral Equation (EFIE) formulations of "the method of moments" for the solution of currents. A cylindrical wire cage model is used via NECGS. Four groups of computer models are developed, varying the number of segments from 1 to 70 for 27-31 MHz. Reflection coefficients of seven experimental models are measured at the antenna feed point, and the input impedances are calculated by an auxiliary computer program. The input impedance is then analyzed by comparing the computer simulation results with measured results. *Surprisingly, the input impedance* of MININEC is closest to experimental results for monopoles which were constructed with ratios of radius-to-wavelength up to 0.0026.

TABLE OF CONTENTS

LIST OF TABLES

LIST OF FIGURES

ACKNOWLEGEMENTS

The author wishes to express his most sincere appreciation to his advisor, Dr. Richard W. Adler, and to his co-advisor, Dr. James K. Breakall, both of whom are from the Department of Electrical and Computer Engineering of the Naval Postgraduate School, for their unfailing aid and encouragement throughout the course of this work. Their patience and guidance have been invaluable.

The author also wishes to thank his wife , Jae Sun, and his son , Hong Mook, for their encouragement and assistance throughout his graduate studies.

Finally, he wishes to thank the Korean people for having paid for his course of studies.

I. INTRODUCTION

A. NEED FOR THE STUDY

In recent years considerable effort has been expended developing general purpose computer codes capable of modeling complicated wire antenna structures via the method of moments [Ref. 1].

The power and flexibility of general purpose wire codes are largely due to the simplicity of wire problems, which in turn are simplified by the use of the so-called "thin-wire approximation", which is that current flowing on the surface of a wire is assumed to be circumferentially invariant. However, when this approximation is used, certain questions arise in the formulation as to the proper treatment of wire junctions, including junctions of wires of dissimilar radii.

Tapered (stepped) element Yagi and Log-Periodic (LP) antennas require proper current amplitude and phase for clean patterns with low sidelobes. These antennas use Tapered (stepped) Linear Antenna Elements (TLAE's) and need to be modeled correctly. Measurements of near fields and current distribution on conducting surfaces are very difficult, but gain and input impedance are easily obtained at all frequencies by swept frequency test equipment.

B. STATEMENT OF THE PROBLEM

There are several ways to study the validation of computer simulations in solving tapered (stepped) radius linear antenna elements. This thesis concentrates on the input impedance vs. swept frequency study of stepped (tapered) radius monopole antenna experiments and computer simulations because previous studies have been lacking or inconclusive in this area.

The purposes of this thesis are: to compare the results of the Numerical Electromagnetics Code (NEC) [Ref. 2], the Mini-Numerical Electromagnetic Code (MININEC) [Ref. 3] and the results of measurements on stepped (tapered) radius monopole antenna models; to determine and to develop methods of analysis for Tapered (stepped) Linear Antenna Elements (TLAE's); and to determine what range of thickness can be numerically modeled at present and what code modifications are needed for extending the range of applicability for Tapered (stepped) Linear Antenna Elements (TLAE's).

C. HISTORICAL BACKGROUND.

The following studies on Stepped (Tapered) Radius Antenna Elements have been conducted to date:

- In February 1975, C. M. Butler, B. M. Duff, R. W. P. King, E. K.Yung and S. Singarayer investigated junction conditions of thin wire structures [Ref. 4] by a theoretical and experimental study.
- In January 1976, T. T. Wu and R. W. P. King studied the nature of the required conditions for determining the analysis of the tapered antenna [Ref. 5] .
- In October 1976, W. L. Curtis investigated the charge distribution on a dipole with a stepped change in radius [Ref. 6] .
- In March 1979, Allen W. Glisson and Donald R. Wilton intensively studied the numerical procedures for handling current and charge on stepped-radius wire junctions [Ref. 7].
- In the fall of 1987, J. K. Breakall and R. W. Adler investigated the Stepped Radius Dipole antenna [Ref. 8] .

D. SCOPE AND LIMITATIONS

1. Scope of the Study

This thesis compares the results of the *impedance vs. frequency change* numerically calculated by MININEC, NEC, and NECGS and the experimental results on the Stepped Radius Monopole. Also it determines the limitation of computer codes for analysis of the Stepped Radius Monopole.

Four monopole models are investigated:

1. The constant radius quarterwave monopole antenna (8 feet in height : Model 1. See Figure 1).

2. The one stepped radius and two equal length sections quarterwave monopole antenna (8 feet in height : Model 2. See Figure 2).
3. The two stepped radii and three equal length sections quarterwave monopole antenna (8 feet in height : Model 3. See Figure 3).
4. The four stepped radii and five equal length sections quaterwave monopole antenna (8 feet in height : Model 4 See Figure 4).

Some models are investigated by experiments and all models are studied by computer simulations (NEC, NECGS and MININEC). There are two different simulations used in NEC , without EK card and with EK card [Appendix A.3]. The equivalent average constant radius cases are considered in Models 2, 3, and 4.

2. Limitation of the Study

This thesis develops four different models and considers mainly the performance vs. frequency changes for three antenna parameters: impedance, VSWR, and average power gain. The frequency range is limited from 27 MHz to 31 MHz (similar to a typical Yagi antenna operating frequency range) due to computer storage and processing time. Twenty one points of input impedance for each model will be simulated at 0.2 MHz frequency increments from 27 MHz to 31 MHz with various numbers of segments from 1 to 70 in all computer codes.

The radius vs. wavelength is smaller than 0.0026 for experiments, and the ratio of adjacent radii is smaller than 2. As frequency increases, the wavelength decreases, and the required number of segments required to model an antenna increases. All four computer models are over a perfect ground plane.

Five points of input impedance for each experimental model (see Chapter IV) on a 30×30 feet ground plane are measured at 1MHz increments from 27 MHz to 31 MHz.

The validity of a numerical model is determined in part by calculating the average power gain of the antenna. An average power gain of 2.0 represents a theoretical antenna radiating in a half space over a perfect ground plane.

In Chapter II, four different models are developed in detail and brief computer code descriptions are given.

In Chapter III, the experimental set up and results are presented.

In Chapter IV, the input impedance vs. swept frequency simulation results of NEC (without EK card and with EK card), NECGS, MININEC, and the experiment are presented. Then, an analysis of the results of the computer simulations and the experiments is given.

Finally, Chapter V summarizes the results, and compares the computer simulation and experimental results. Discussions, conclusions, and recommendations for future study are then presented.

The appendices include simulation data, such as geometry input data for each model, the convergence graph of the input impedance vs. frequency change and a detailed explanation of the computer codes (MININEC, NEC, and NECGS).

II. COMPUTER CODE DESCRIPTION AND COMPUTER MODEL DEVELOPMENT

This chapter presents a brief discussion of the computer codes (MININEC, NEC, and NECGS) and the results of the computer models developed in Chapter II. Each model was tested to find the differences among different computer codes. All models in this thesis have the same performance as a monopole antenna over a perfect ground. The geometry data sets are given in Appendix B. The data sets were run to evaluate the variation of input impedance of each computer model as a function of frequency. The results are indicated on two different curves, one for resistance (R), and the other for reactance (jX). The computer codes use 1 - 70 segments. Two different MININEC programs are used. The MININEC SYSTEM [Ref. 9], which is written in Quick Basic and menu driven, has a limitation of less than 50 segments. The MININEC 3.11 version is used for 50 to 70 segments.

A. COMPUTER CODE DESCRIPTION

The "MINI" Electromagnetics Code, or MININEC [Ref. 10], is a personal computer (PC) BASIC program for analysis of thin wire antennas using the method of moments. A Galerkin [Ref. 1] procedure is applied to an Electric Field Integral Equation (EFIE) to solve for the wire currents.

The Numerical Electromagnetics Code (NEC [Ref. 2]) is the most advanced computer Fortran program available for the analysis of thin wire antennas using the the Pocklington EFIE equation [Ref. 1] for the currents and is run on a mainframe computer.

NECGS is a special purpose version of NEC 3 for limited applications. It is very efficient and runs quickly, but is good only for structures having rotational symmetry about the Z-axis.

The following tables [Tables 1 and 2] show the capabilties and the limitations of MININEC, NEC, and NECGS respectively. A detailed description of the computer codes is given in Appendix A.

Table 1. THE CAPABILITIES OF MININEC, NEC, AND NECGS

Codes	Capabilities
MININEC	• Currents (Galerkin procedure for EFIE) • Impedance, E and H near fields • Patterns (Fresnel Reflection Coefficient and E field at specified range) • Lumped parameter loading (Series impedance, complex frequency domain impedance function) • Free space or perfect ground • Improved (faster) solution routine • Modular programming with comments • Written in BASIC for Personal Computers
NEC	• Currents (Pocklington procedure) • Impedance, E and H near fields • Straight segments modeling wires and flat patches for modeling surfaces • Patterns (Fresenel Reflection Coefficient and E field at specified range) • Lumped element loading, nonradiating networks, transmission lines • Directive and power gains • Free space, perfect ground, or imperfect ground based on the Sommerfeld integrals • Written in Fortran for 32 bit mainframe at NPS. • Includes the Numerical Green's Function. • The excitation may be an incident plane wave or a voltage source on wire
NECGS	• A very efficient and quick running special purpose version of NEC 3 for limited applications • Good for structures having special rotational symmetry

Table 2. THE LIMITATIONS OF MININEC, NEC, AND NECGS

Codes	Limitations
MININEC	• Only suitable for small problems (less than 75 unknown segments and 10 wires depending on the personal computer memory and BASIC program in computer.) • In this thesis, 50 unknowns (segments) for the MININEC SYSTEM, 70 *unknowns (segments) for* MININEC 3.11 • It is good for $\frac{r}{\lambda}$ smaller than 0.001.
NEC	• Mainframe computer is needed. • Although the upper limit is determined by the cost factors and memory size of the mainframe, a model containing up to 2000 unknown segments seems to be the practical limit. • It is valid if the ratio of the segment length to the wavelength ($\frac{\Delta}{\lambda}$) is 0.001 to 0.1 for a constant radius. • It is valid if the ratio of the segment length to radius is 8 without an EK card, 2 with an EK card respectively.
NECGS	• The number of input wire segments in a symmetrical section is limited to 150.

All three computer codes solve for current basis functions in the integral equations (see Appendix A). Then, matrix, charge, input impedance, E and H fields, etc.) are calculated. The impedance Z is easily calculated by the following equation:

$$[(Z)_{mn}][I_n] = [V_m] \qquad (1)$$

- n is the nth current segment on the wire surface,
- m is the mth observation point on the wire surface,

- V_m represents the incident electric field on the wire surface,
- $[(Z)_{mn}][I_n]$ represents the axial component of the scattered field at the surface of the mth wire segment due to the current on all of the segments,
- $[V_{mn}],[I_n]$ represent column matrices where n = 1, 2, 3,.......N, with N unknowns and N current segments,
- $(Z)_{mn}$ is a square matrix where m = 1, 2,3,.....N, with N unknowns and N current segments.

$$Z_{in} = R_{in} + jX_{in} \tag{2}$$

where :

- Z_{in} is the antenna impedance at its terminals,
- R_{in} is the antenna resistance at its terminals, and
- X_{in} is the antenna reactance at its terminals.

The resistive part alone consists of two components :

$$R_{in} = R_r + R_L \tag{3}$$

where :

- R_r is the radiation resistance of the antenna, and
- R_L is the loss resistance of the antenna.

Radiation resistance (R_r) represents power that leaves the antenna as radiation, while loss resistance (R_L) represents power dissipation in the antenna structure.

Different computer codes use different basis functions and weighting factors for formulation of Electric Field Integral Equations (EFIE). Because of this, the results of computer simulations may be different.

B. OVERVIEW OF MODELING

This and the following sections develop four different monopole computer models (see Table 3) which have different radii and various sub-models.

Model 1 is a case of constant radius. Model 2 is a case of one-step radii and equal length sub-sections. Model 3 is a case of two-step radii and equal length sub-sections. Model 4 is a case of four-step radii and equal length sub-sections. The models to be used for the investigation will be 8 feet (2.4384 meters) high, stepped or constant radius monopoles radiating above a perfectly conducting ground plane. The ground plane is located in the X-Y plane; the monopole is co-axial with the Z-axis. The antenna will be excited at its base with a magnitude of 1 Volt and 0 degrees phase. The excitation is at 27-31 Megahertz, or a wavelength (λ) of 36.45377661 - 30.75787402 feet (11.111111111 - 9.375 meters). All models are simulated by NEC, NECGS and MININEC . There are two different simulations in NEC; without the EK card and with the EK card [Ref. 2]. In simulating these models, NEC and MININEC require that the antennas be broken into short straight segments.

The MVS batch system [Ref. 11] was used on the mainframe IBM 3033 Network. NEC is designed for a 60 bit computer, and the IBM 3033 has 32 bits, so double precision is used. Each model is briefly explained in the following sections.

Table 3. **CONFIGURATION OF EACH MODEL**

Model Name	Wire No.	Freq. (MHz)	Radius (inch or λ)	Others
Model 1	1	27-31	$r = 10^{-5} - 1$ (λ)	Experiment, Simulation
Model 2-1	2	27-31	$r_1 = 1/4$ $r_2 = 1/8$ (inch)	Experiment, Simulation
Model 2-2	2	27-31	$r_1 = 1/2$ $r_2 = 1/4$ (inch)	Experiment. Simulation
Model 2-1-E	1	27-31	$r_e = 3/16$ (inch) Equivalent average radius of Model 2-1	Simulation
Model 2-2-E	1	27-31	$r_e = 3/8$ (inch) Equivalent average radius of Model 2-2	Simulation
Model 3-1	3	27-31	$r_1 = 1/4$ $r_2 = 3/16$ $r_3 = 1/8$ (inch)	Experiment, Simulation
Model 3-2	3	27-31	$r_1 = 1$ $r_2 = 15/16$ $r_3 = 7/8$ (inch)	Experiment. Simulation
Model 3-1-E	1	27-31	$r_e = 3/16$ (inch) Equivalent average radius of Model 3-1	Simulation
Model 3-2-E	1	27-31	$r_e = 15/16$ (inch) Equivalent average radius of Model 3-2	Simulation
Model 4-1	5	27-31	$r_1 = 3/8$ $r_2 = 5/16$ $r_3 = 1/4$ $r_4 = 3/16$ $r_5 = 1/8$ (inch)	Experiment. Simulation
Model 4-2	5	27-31	$r_1 = 1$ $r_2 = 15/16$ $r_3 = 7/8$ $r_4 = 13/16$ $r_5 = 3/4$ (inch)	Experiment. Simulation
Model 4-1-E	1	27-31	$r_e = 1/4$ (inch) Equivalent average radius of Model 4-1	Simulation
Model 4-2-E	1	27-31	$r_e = 7/8$ (inch) Equivalent average radius of Model 4-2	Simulation

C. MODEL DESCRIPTIONS FOR MININEC AND NEC

In simulating these models, NEC and MININEC require that the antenna be broken into short straight segments. In consonance with this requirement, the models are composed of 2 - 70 equal segments. There are 2, 4, 6, and 10 segment increments in Model 1, Model 2, Model 3, and Model 4, respectively. The 70 segments are limitations of MININEC, not NEC.

1. Model 1 (Constant Radius Monopole Models)

Model 1 (radius change from 10^{-5} λ to 1 λ, see Figure 1) are constant radius monopole models with a height of 8 feet (2.4384 meters), driven by a 1 volt source. Table 4 provides the geometry data for 3 different frequencies and 3 different segmentations. A total of 21 different radii are calculated for each sub-model (see Appendix C for input data). Three cases of segmentation are investigated: 6, 38, and 70 segments.

An experiment is performed with the radius equal to 1/8 inch.

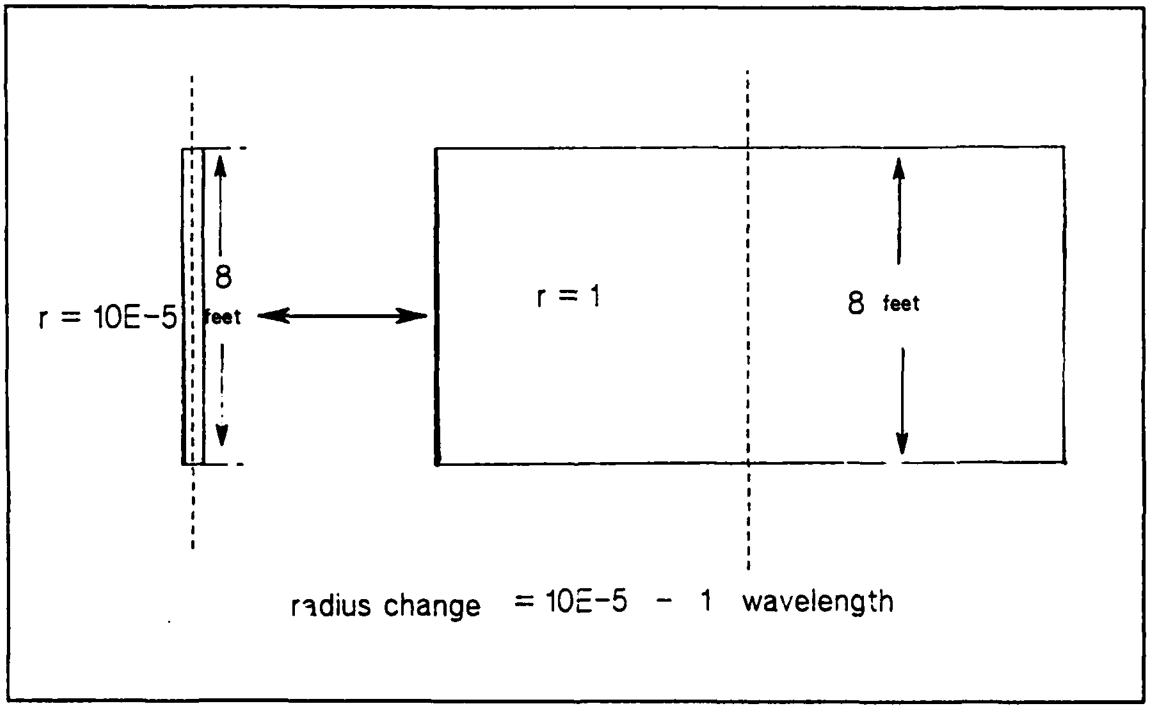

Figure 1. Model 1 (Constant Radius Monopoles)

Table 4. **MODEL 1 FREQUENCY AND GEOMETRY DATA IN WAVELENGTHS.**

Sub-Model	Frequency (MHz)	Number of Segments	$\frac{\Delta}{\lambda}$	r (λ)
Model 1-1-F1	29.757874	6	0.04034	10^{-5} - 1
Model 1-1-F2	30.757874	6	0.04169	10^{-5} - 1
Model 1-1-F3	31.757874	6	0.04305	10^{-5} - 1
Model 1-2-F1	29.757874	38	0.00637	10^{-5} - 1
Model 1-2-F2	30.757874	38	0.00658	10^{-5} - 1
Model 1-2-F3	31.757874	38	0.00680	10^{-5} - 1
Model 2-3-F1	29.757874	70	0.00346	10^{-5} - 1
Model 1-3-F2	30.757874	70	0.00357	10^{-5} - 1
Model 1-3-F3	31.757874	70	0.00369	10^{-5} - 1

2. Model 2 (One Stepped Radius and Equivalent Average Radius Monopoles)

Model 2 (see Figure 2) shows one stepped radius and equivalent average radius monopole models with a height of 8 feet (2.4384 meters). The dimensions of the antennas (1) and (2) are specified by the two lengths, L_1 and L_2, and by the two radii, r_1 and r_2. The lengths of L_1 and L_2 are both 4 feet. The two radii r_1 and r_2 of (1) are 1/8 inch and 1/4 inch respectively. The two radii r_1 and r_2 of (2) are 1/4 inch and 1/2 inch respectively. The ratio of the two radii, r_1/r_2, of (1) and (2) is 2.

The radius, r_{1e}, of (1-E) is 3/16 inch which is the average radius of r_1 and r_2 of (1). The radius, r_{2e}, of (2-E) is 3/8 inch which is the average radius of r_1 and r_2 of (2). The length of L in (1-E) and (2-E) is 8 feet long. Table 5 provides the geometry data for 27-31 MHz.

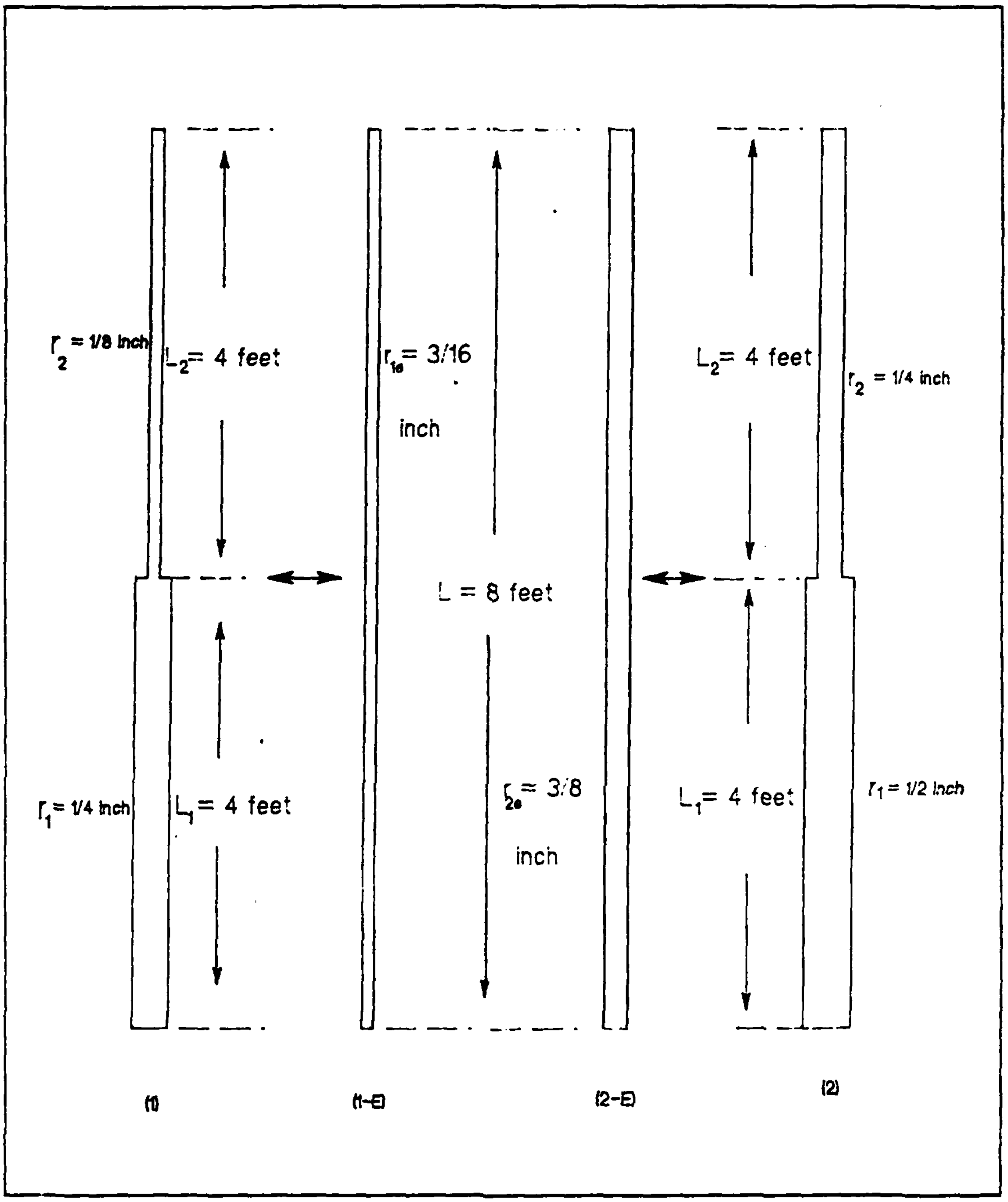

Figure 2. Model 2 (One Stepped Radius and Equivalent Average Radius Monopoles)

Table 5. MODEL 2 FREQUENCY AND GEOMETRY DATA IN WAVELENGTHS.

Sub-Model	Wire No.	Freq. (MHz)	Number of Segments	$\frac{\Delta}{\lambda}$	r (λ)
Model 2-1	2	27-31	2-70	0.0122 - 0.0036	r_1 = 5.715E-4 - 6.56166667E-4 r_2 = 2.8575E-4 - 3.280833333E-4
Model 2-2	2	27-31	2-70	0.0122 - 0.0036	r_1 = 1.143E-3 - 1.31233E-3 r_2 = 5.715E-4 - 6.561667E-4
Model 2-1-E	1	27-31	2-70	0.0122 - 0.0036	r_e = 4.28625E-4 - 4.92125E-4
Model 2-2-E	1	27-31	2-70	0.0122 - 0.0036	r_e = 8.5725E-4 - 9.842485E-4

3. Model 3 (Two Stepped Radii and Equivalent Average Radius Monopoles)

Model 3 (see Figure 3) shows two stepped radii and equivalent average radius monopole models with a height of 8 feet (2.4384 meter). The dimensions of the antennas (1) and (2) are specified by the three equal lengths, L_1 , L_2 , and L_3 , and by three different radii, r_1 , r_2 , and r_3 , where there is a 1/8 inch difference between adjacent radii. The length of L_1 , L_2 , and L_3 are all 8/3 feet for each model.

The three radii r_1, r_2, and r_3, of (1) are 1/4 inch, 3/16 inch, and 1/8 inch respectively. The ratios of radii r_1/r_2 , r_2/r_3 , and r_1/r_3 are 4/3 , 3/2 , and 2 respectively. The three radii r_1, r_2, and r_3 of (2) are 1 inch, 15/16 inch, and 7/8 inch respectively. The ratios of radii r_1/r_2 , r_2/r_3 , r_1/r_3 , of (2) are 16/15 , 15/14 , and 14/13 respectively. The radius, r_{1e}, of (1-E) is 1/4 inch which is the average of r_1, r_2, and r_3 of (1). The radius, r_{1e}, of (2-E) is 7/8 inch which is the average of r_1, r_2, and r_3 of (2). The length of L in (1-E) and (2-E) is 8 feet. Table 6 provides the geometry data for 27-31 MHz.

Table 6. MODEL 3 FREQUENCY AND GEOMETRY DATA IN WAVELENGTHS.

Sub-Model	Wire No.	Freq. (MHz)	Number of Segments	$\frac{\Delta}{\lambda}$	r (λ)
Model 3-1	3	27-31	3-69	0.07320 - 0.00318	r_1 = 5.715E-4 - 6.5616667E-4 r_2 = 4.28625E-4 - 4.92125E-4 r_3 = 2.86E-4 - 3.2808333E-4
Model 3-2	3	27-31	3-69	0.07320 - 0.00318	r_1 = 2.286E-3 - 2.62466667E-3 r_2 = 2.143125E-3 - 2.460625E-3 r_3 = 2.00025E-3 - 2.2965833E-3
Model 3-1-E	1	27-31	3-69	0.07320 - 0.00361	r_e = 4.28625E-4 - 4.9215E-4
Model 3-2-E	1	27-31	3-69	0.07320 - 0.00361	r_e = 2.143125E-3 - 2.460625E-3

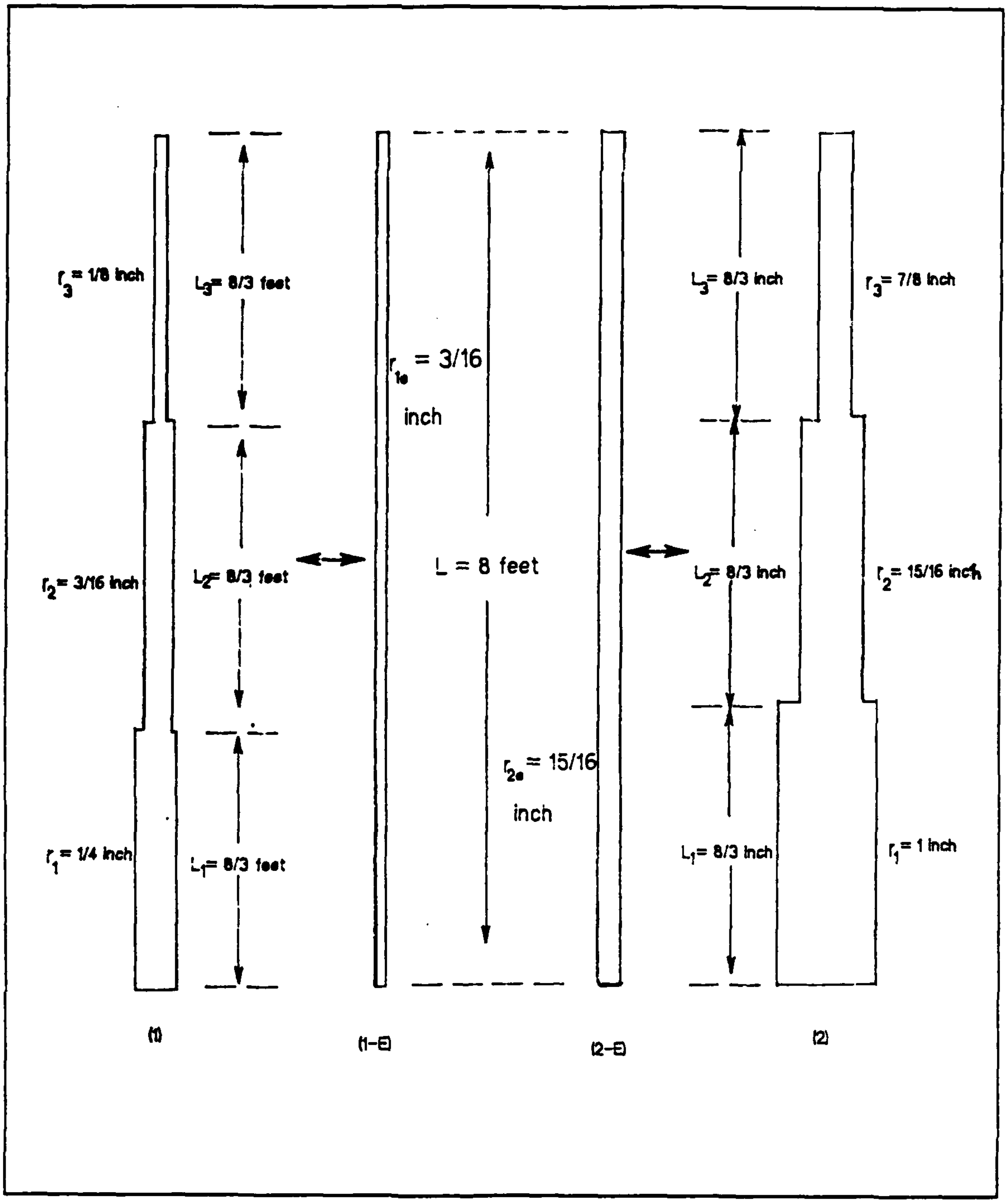

Figure 3. Model 3 (Two Stepped Radii and Equivalent Average Radius Monopoles)

4. Model 4 (Four Stepped Radii and Equivalent Average Radius Monopoles)

Model 4 (see Figure 4) is a four stepped and equivalent average radius monopole model with a height of 8 feet (2.4384 meters). The dimensions of the antennas (1) and (2) are specified by the five equal lengths, L_1 , L_2 , L_3 , L_4 , and L_5 , and by the five radii, r_1 , r_2 , r_3 , r_4 , and r_5 , where there is a 1/8 inch difference between the adjacent radii. The lengths of L_1 , L_2 , L_3 , L_4 , and L_5 are all 1.6 feet long for each model.

The five radii r_1, r_2, r_3, r_4 , and r_5 of (1) are 3/8 inch 5/16 inch, 1/4 inch, 3/16 inch, and 1/8 inch respectively. The ratios of adjacent radii r_1/r_2 , r_2/r_3 , r_3/r_4 , r_4/r_5 of (1) are 6/5 , 5/4 , 4/3 , and 3/2 respectively.

The five radii r_1, r_2, r_3, r_4 , and r_5 of (2) are 1 inch, 15/16 inch, 7/8 inch, 13/16 inch, and 3/4 inch respectively. The ratios of adjacent radii r_1/r_2 , r_2/r_3 , r_3/r_4 , r_4/r_5 of (2) are 16/15 , 15/14 , 14/13 , and 13/12 respectively. The radius, r_{1e}, of (1-E) is 1/4 inch which is the average of r_1, r_2, r_3, r_4 , and r_5 of (1). The radius, r_{2e}, of (2-E) is 7/8 inch which is the average of r_1, r_2, r_3, r_4 , and r_5 of (2). The length of L in (1-E) and (2-E) is 8 feet long. Table 7 provides the geometry data for 27-31 MHz.

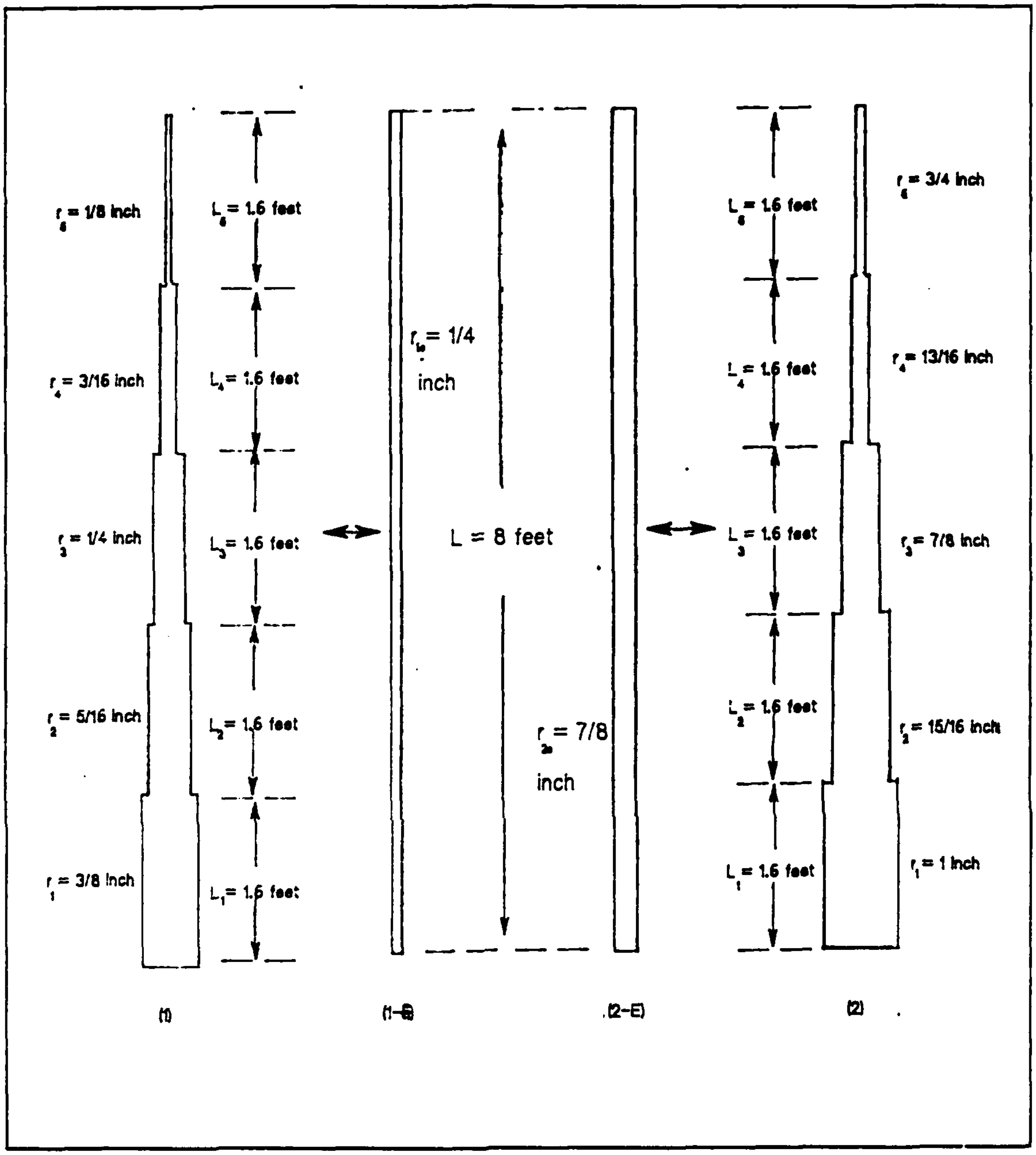

Figure 4. Model 4 (Four Stepped Radii and Equivalent Average Radius Monopoles)

Table 7. MODEL 4 FREQUENCY AND GEOMETRY DATA IN WAVELENGTHS.

Sub-Model	Wire No.	Freq. (MHz)	Number of segment	$\frac{\Delta}{\lambda}$	r (λ)
Model 4-1	5	27-31	5-70	0.04392 - 0.00334	r_1 = 8.5725E-4 - 9.8425E-4 r_2 = 4.14375E-4 - 8.202083333E-4 r_3 = 5.715E-4 - 6.561666 666E-4 r_4 = 4.28625E-4 - 4.92125E-4 r_5 = 2.8575E-4 - 3.280833333E-4
Model 4-2	5	27-31	5-70	0.04392 - 0.00334	r_1 = 2.2286E-3 - 2.624666667E-3 r_2 = 2.143125E-3 - 2.460625E-3 r_3 = 2.00025E-3 - 2.296583333E-3 r_4 = 1.857375E-3 - 2.132541667E-3 r_5 = 1.7145E-3 - 1.9685E-3
Model 4-1-E	1	27-31	5-70	0.04392 - 0.00334	r_e = 5.715E-4 - 6.561666667E-4
Model 4-2-E	1	27-31	5-70	0.04392 - 0.00334	r_e = 2.00025E-3 - 2.296583333E-3

D. MODEL DESCRIPTION OF NECGS

In this thesis, all monopole models stated in the above section (Model description of MININEC and NEC) are modeled with NECGS, using rotational symmetry with a wire cage equivalent to the actual models with wires across the annulus formed by the stepped transition in radii. In this section, modeling methods for Model 2-2 (see Figure 2) are explained in detail. The other models are modeled similarly.

The geometry is shown in a blown-up view in Figure 5.

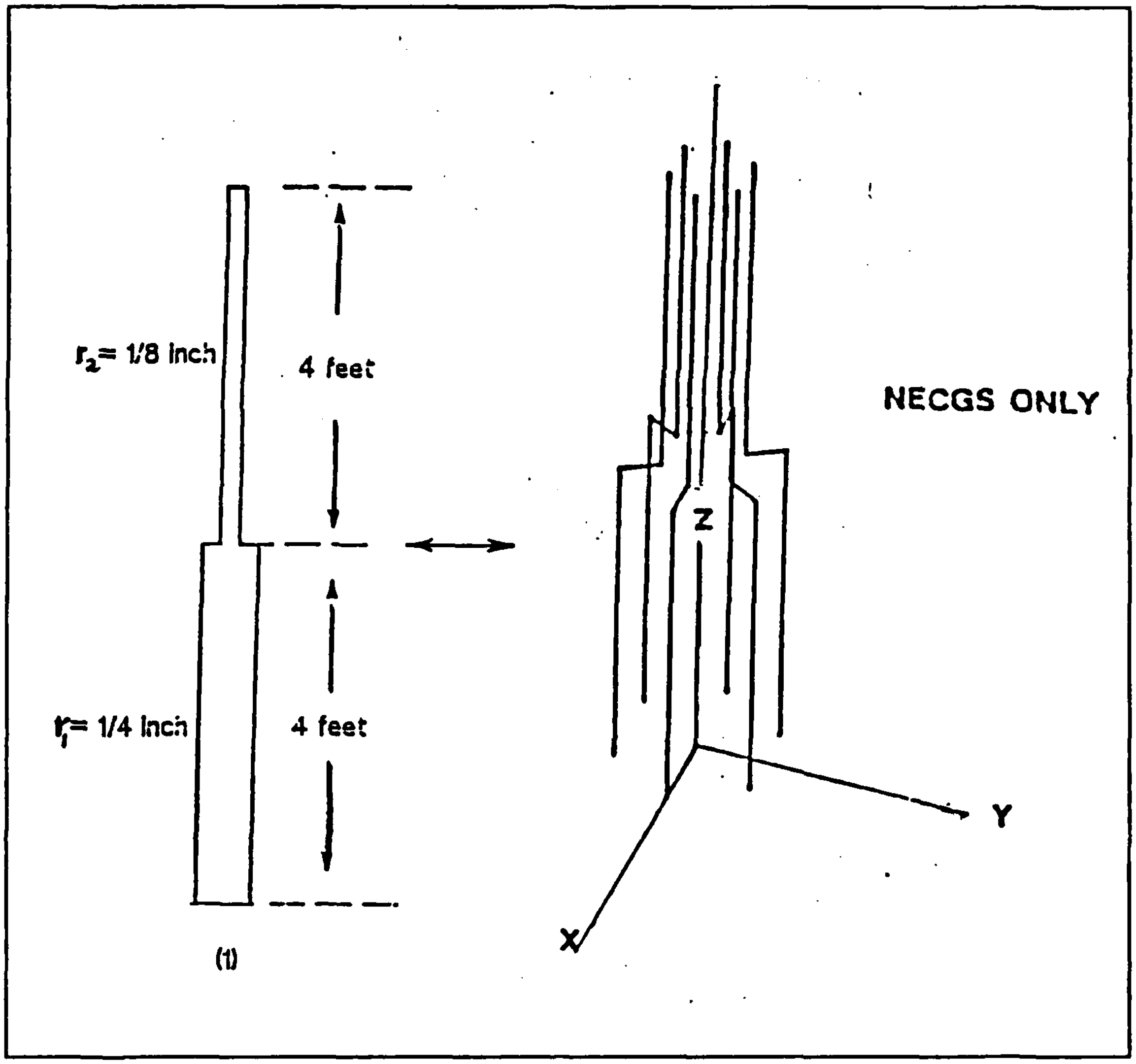

Figure 5. NECGS Model for Model 2 - 2

The equal area rule, which is used in this thesis states that the total surface area of the 6 cage wires would equal the same surface area of the actual antenna [Ref. 2]. The relationships between r_1 and r_A, the radius of the cage wires for section 1, and between r_2 and r_B, the radius of the cage wires for section 2, is 6 to 1; that is,

$$2\pi r_1 = 6(2\pi r_A) \tag{4}$$

$$2\pi r_2 = 6(2\pi r_B) \tag{5}$$

r_{AB} is the average of r_A and r_B. Then one continuous three section wire of different radii r_A, r_{AB}, and r_B is rotated 6 times about the Z-axis. The distance between the Z-axis and the center of wire r_A is the radius r_1 and to the center of wire r_B is r_2. Another method uses the average radius for r_A, r_{AB}, and r_B; that is,

$$r_A^{\prime} = r_{Ab}^{\prime} = r_B^{\prime} = \frac{r_A + r_{AB} + r_B}{3}$$

$$= \frac{r_A + \frac{(r_A + r_B)}{2} + r_b}{3} = \frac{\frac{3r_A + 3r_B}{2}}{3}$$

$$= \frac{3\frac{(r_A + r_B)}{2}}{3} = \frac{r_A + r_B}{2} \tag{6}$$

In this thesis, both cases are considered for each model. Additionally the case of an end cap on the top of the wire is considered. The modeling method for these cases uses tapering to increase the segment length, Δ , away from the step region, keeping a value less than 2 for the ratio of adjacent segment lengths. An auxiliary program RVAL [see Appendix D.2] is used to create the tapered length data required in NECGS.

III. EXPERIMENTAL SYSTEM AND RESULTS

A. GENERAL OPERATION

Figure 6 is a block diagram of the experimental system.

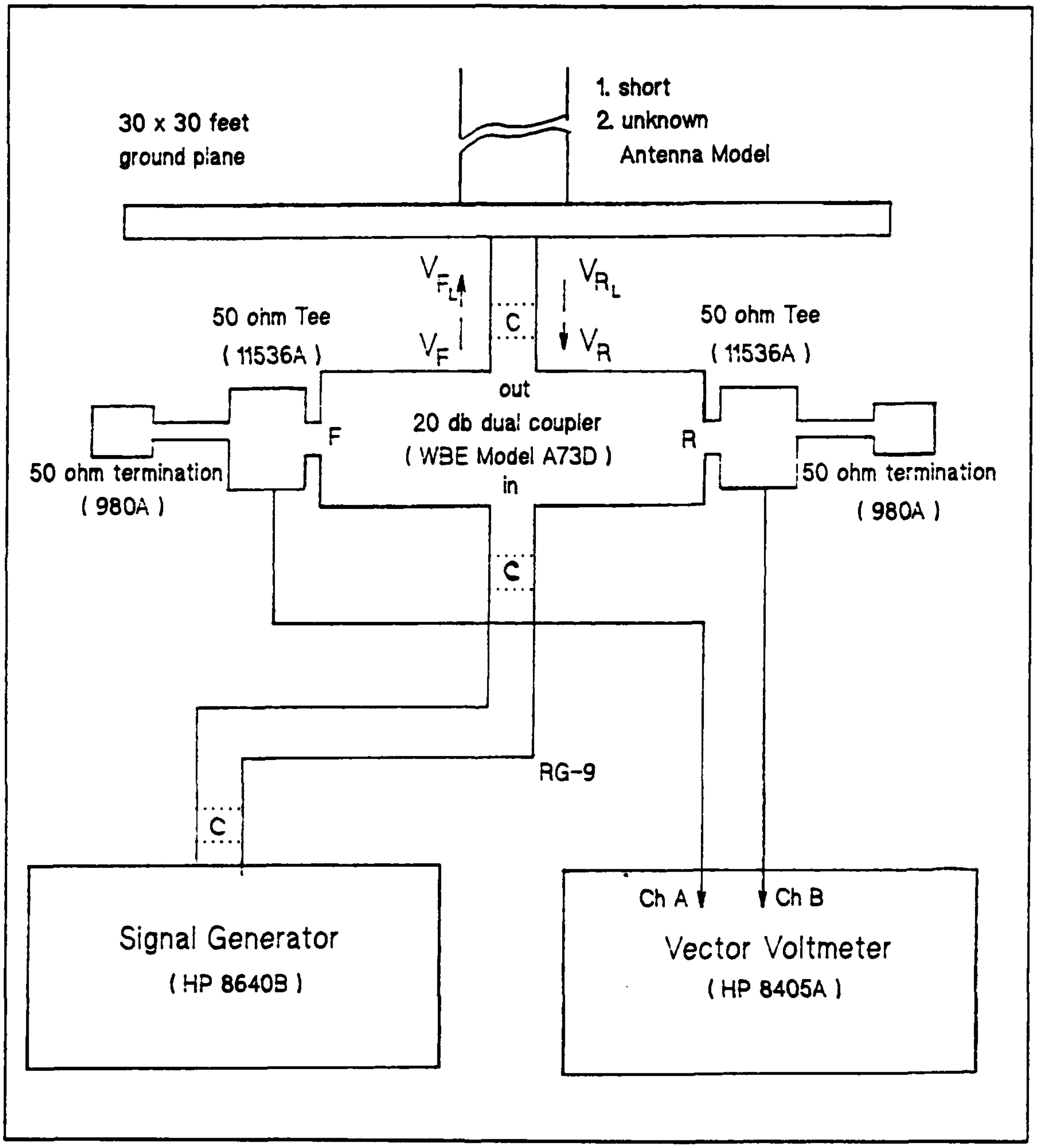

Figure 6. Block Diagram of the Experimental System

The input impedance Z_{in} of various models can be measured using a signal generator, vector voltmeter, 20 dB dual directional coupler (WBE Model A73D), various connectors and a RG-9 coaxial cable.

The signal generator (HP 8640B, Ref. [12]) operates from 0.45 MHz to 512 MHz and has a frequency readout of 10 Hz with a maximum output of 2 volts. In this experiment, a maximum output of 1 volt was used due to the vector voltmeter maximum limit and to achieve the best signal-to-noise ratio.

The vector voltmeter (HP 8405A, Ref. [13]) is a dual channel millivolt/phasemeter which operates over a three decade range from 1 to 1000 MHz. It measures both voltage and phase difference between its two input channels and also provides the phase angle between any two voltage vectors.

There are two connectors and one RG-9 coaxial cable between the signal generator and one 20 dB dual directional coupler. The RG-9 coaxial cable has a characteristic impedance Z_o of 50 ohms.

A vector voltmeter accessory kit 1157A [Ref. 14] is used for making all connections. The 11536A (Figure 6) is a 50 ohm Tee with type N RF fittings for monitoring signals in 50 ohm transmission lines. The 908A (Figure 6) is 50 ohm load for terminating 50 ohm coaxial systems in their characteristic impedance.

The 20 dB dual coupler has a 1-100 MHz operating range, a 45 dB separation between the forward and reverse channels, and 0.3 dB insertion loss. The 20 dB dual coupler is then connected by a connector to the antenna on a 30 × 30 feet ground plane.

The impedances of the 7 models (Model 1, Model 2-1, Model 2-2, model 3-1, Model 3-2, Model 4-1, and Model 4-2) are measured by sweeping frequencies from 27 MHz to 31 MHz. The results are then compared with the results of computer simulations.

B. THEORY

Input impedance Z_{in} can be obtained by measuring the reflection coefficient [Ref. 10]. The V_F signal from the signal generator propagates to the load through the transmission line. A portion, V_R, of the incident signal is phase shifted and reflected by the load. The directional coupler in this experiment is located at terminal A and provides samples of V_F and V_R to the vector voltmeter.

The relationships between input impedance and reflection coefficient are defined by the following equations (Figure 7):

$$V_{F_L} = V_F \exp^{-\alpha l - j\beta l} \tag{7}$$

$$V_R = V_{R_L} \exp^{-\alpha l - j\beta l} \tag{8}$$

$$\frac{V_R}{V_F} = \frac{V_{R_L} \exp^{-\alpha l - j\beta l}}{V_{F_l} \exp^{+\alpha l + j\beta l}} = \frac{V_{R_L}}{V_{F_L}} \exp^{-2\alpha l} \exp^{-j2\beta l} \tag{9}$$

$$\frac{V_{R_L}}{V_{F_L}} = \frac{V_R}{V_F} \exp^{+2\alpha l} \exp^{+j2\beta l} \tag{10}$$

Let

$$K_A = \frac{V_R}{V_F} \tag{11}$$

Let

$$K_B = \frac{V_{R_L}}{V_{F_L}} \tag{12}$$

where

- V_R is the reflection voltage at input terminal A, from load terminal B,
- V_F is the forward voltage at input terminal A,
- V_{F_L} is the forward voltage at the load terminal B,
- V_{R_L} is the reflected voltage at the load terminal B,
- α is the attenuation constant,

- β is the phase constant,
- ℓ is the distance between the input terminal A and the load terminal B (between the dual coupler and the antenna connecting point of ground plane in this experiment),
- K_A is the complex reflection coefficient at the input terminal A, and
- K_B is the complex reflection coefficient at the load terminal B (ground plane).

In this thesis, the K_B is calculated by measuring the K_A. Then, the input impedance, Z_{in}, is calculated by a computer program according to the following equation;

$$Z_{in} = Z_o \frac{1 + K_B}{1 - K_B} \tag{13}$$

where

Z_o is the characteristic impedance of transmission line.

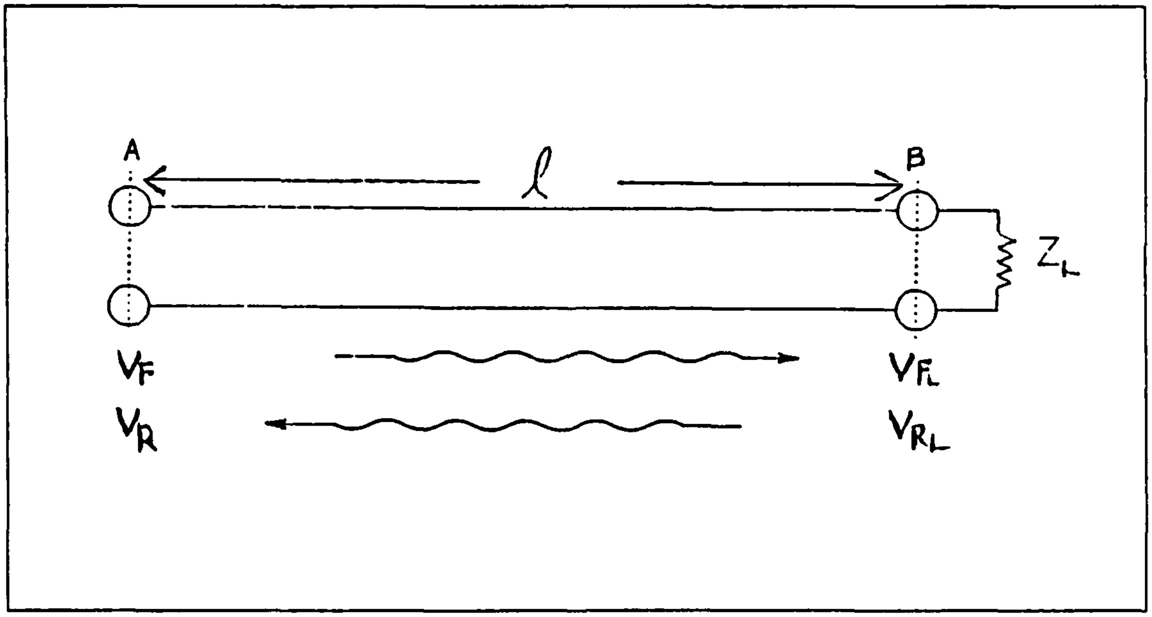

Figure 7. Input Impedance of a Line

C. EXPERIMENTAL MODELING AND MEASURMENT PROCEDURES.

All seven experimental models are measured.

1. Experimental Modeling

Model 1 (brass), Model 2-1 (aluminum), and Model 2-3 (aluminum) are solid rods. The other models (Model 3-1, Model 3-2, Model 4-1, and Model 4-2) use telescoping aluminum tubing (Figure 8). To support the connection point between the antenna and the 30 × 30 foot ground plane, plastic supports of 3.6 inch diameter and 2 inch height are used. For telescoping tubing, the different aluminum sections are joined together by hose clamps.

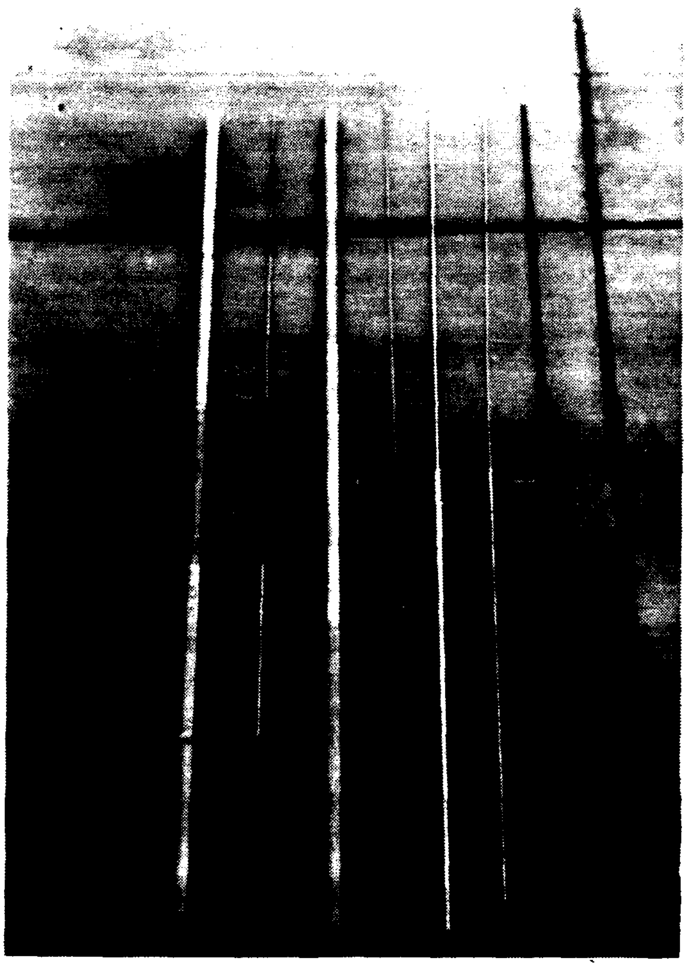

Figure 8. Photograph of all Models for Experiments

2. Measurement Procedures

Measurement procedures for input impedances are as follows:

1. Measure the lengths and diameters of seven monopole models
2. The system is calibrated prior to the measurements. A short circuit is placed at the monopole connection (at the 30 × 30 foot ground plane) and adjusted so that the phase angle is + 180 degrees at a reference of 29 MHz (the center frequency of the measurement) to account for any electrical distance between the 20 dB dual directional coupler and the monopole connection point. Then the generator frequency is varied from 27 to 31 MHz and measurements are made of the magnitude and phase of the reflection coefficient to compute the appropriate correction factors.
3. Connect one of seven monopole antennas to the ground plane and measure its reflection coefficient over the frequency range (27 - 31 MHz) in 1 MHz steps.
4. Repeat procedure 3 for the other antennas.
5. The real and imaginary input impedances for each antenna model are calculated by the computer program (Appendix D.1).

D. THE RESULTS OF THE EXPERIMENT

Measurements were made 4 times to test repeatability and the measured and average data are given in Table 8. The graphic results and analysis will be given in the next chapter comparing the measurements with computer simulation results. In the table, S means a short and L means a load.

Table 8. THE AVERAGE RESULTS OF FOUR REPETITIVE EXPERIMENTAL SOURCE MEASUREMENTS OF REFLECTION COEFFICIENT

Freq. (MHz)	27		28		29		30		31	
	Mag.	Phase	Mag.	Phase	Mag.	Phase	Mag.	Phase	Mag.	Phase
Model 1 (S)	0.99	181.7	0.99	180.9	0.988	180	0.987	179.3	0.987	178.6
Model 1 (L)	0.48	277.6	0.355	257.6	0.215	219.8	0.177	138.8	0.305	87.25
Model 2-1 (S)	0.99	181.7	0.99	180.9	0.988	180	0.987	179.3	0.987	178.6
Model 2-1 (L)	0.644	292.2	0.55	279.1	0.417	259.1	0.259	225.4	0.15	150
Model 2-2 (S)	0.99	181.65	0.99	180.9	0.988	180	0.987	179.3	0.987	178.6
Model 2-2 (L)	0.609	287.2	0.52	274.1	0.4	255.1	0.256	224.6	0.148	158.9
Model 3-1 (S)	0.99	181.6	0.992	180.8	0.992	180	0.995	179.2	0.992	178.6
Model 3-1 (L)	0.62	289.0	0.519	275.1	0.38	252.4	0.227	213	0.176	130.4
Model 3-2 (S)	0.99	181.6	0.992	180.8	0.992	180	0.995	179.2	0.992	178.6
Model 3-2 (L)	0.4	261	0.3	243.2	0.195	211.5	0.14	142.1	0.222	83.7
Model 4-1 (S)	0.991	181.6	0.99	180.8	0.992	180	0.99	179.3	0.991	178.5
Model 4-1 (L)	0.641	289.3	0.552	277.8	0.43	257.8	0.282	228.1	0.158	164.9
Model 4-2 (S)	0.991	181.6	0.99	180.8	0.992	180	0.99	179.3	0.991	178.5
Model 4-2 (L)	0.436	265.2	0.34	247.8	0.229	220	0.155	161.3	0.198	94.2

IV. COMPUTER SIMULATION, EXPERIMENTAL RESULTS, AND ANALYSIS

This chapter presents the results of the computer models developed in Chapter II and those of the experiment explained in Chapter III. Each model was tested by changing the number of segments or radius and the frequency to find the input impedance.

The results of the different computer codes are compared with the experimental results. The input geometry data sets are given in Appendix B. MININEC results have been shown to be valid when the ratio of radius to wavelength is smaller than 0.001 [Ref. 8].

The graphs of the input convergence test of Model 2-2 for MININEC and NEC are given in Appendix C. MININEC results always converge faster than those of NEC.

The results of the experiment are used to verify the computer simulations. In the following sections the results of different computer codes for Model 1 (constant radius of 1/8 inch) are compared with the results of the experiments. It is well known that the average gain of monopoles on perfect ground is 2.0 and azimuth radiation patterns are omni-directional [Ref. 16].

A. MODEL 1 RESULTS

First, Model 1 data sets (see Appendix C) were run to find the input impedance changes. The results of MININEC, NEC (without EK card and with EK card), and NECGS are plotted in Figures 9 and 10 to show the real (input resistance) and imaginary part (input reactance) of the input impedance. The radius was changed from 0.001 λ to 1 λ at a frequency of 29.7578 MHz with different number of segments for each model equal to 6, 38, and 70 segments. The real part of the input impedance has smaller variations than the imaginary part as frequency is swept. Comparing Figures 9, 11, and 13 (the input resistances, real part), variations of computer code results are greater as frequency moves away from resonance (29.22 MHz). When the radius is larger than 0.001 λ , the variations are even greater. The results of input impedance at these larger are therefore not as accurate. Comparing the reactance (the imaginary part of the input impedance), Figures 10, 12, and 14, the results are more sensitive than the those of input resistance, especially versus frequency.

Next, the experimental results for Model 1 (radius of 1/8 inch) are presented. Figures 15 and 16 show the results of the computer simulation and the experiment. The results for just 1 segment for all computer simulations are far from convergence. For the other cases of segmentation as compared to experiment, the results are almost coincidental for the real part, and almost in exact agreement with the input reactances except at low frequencies.

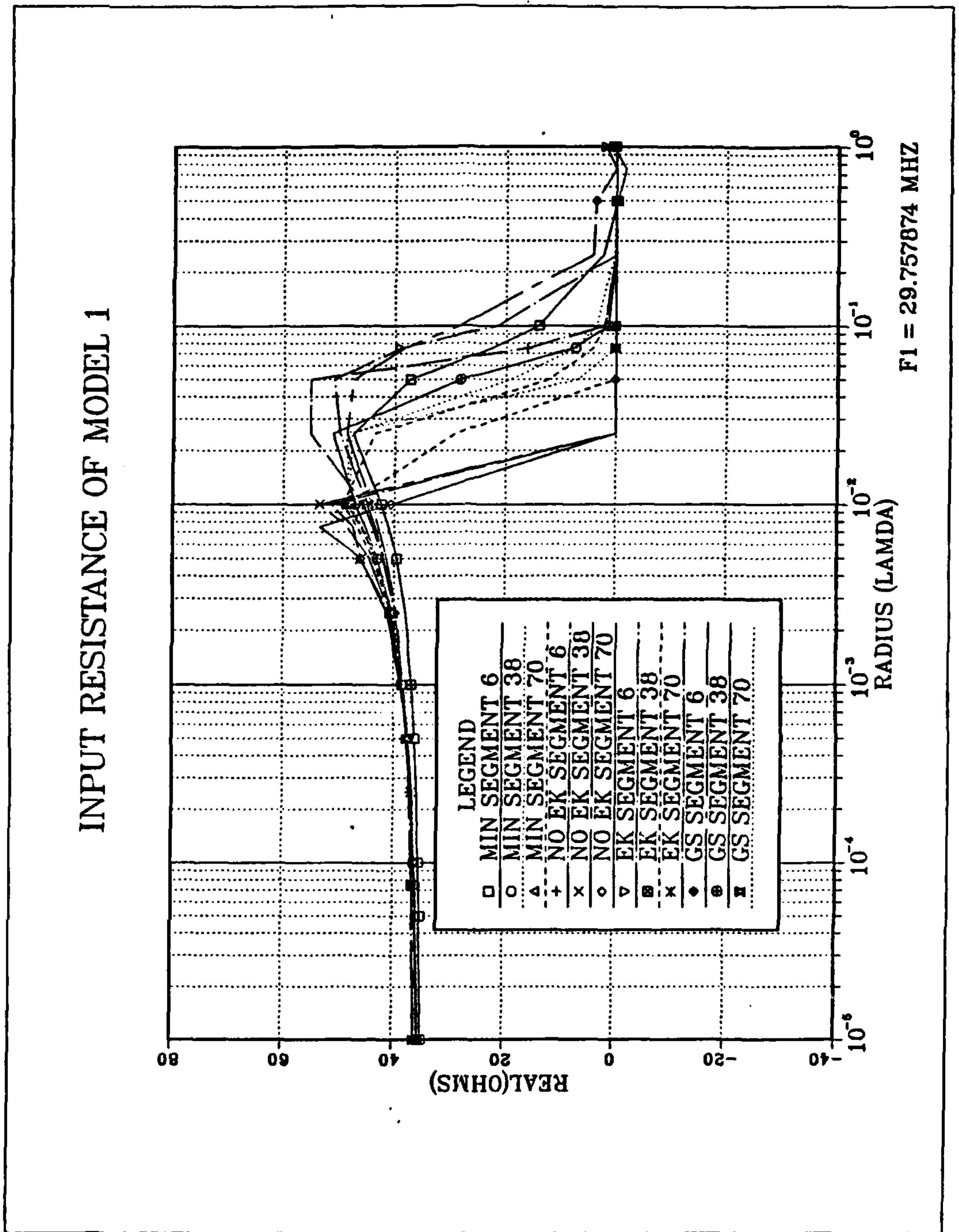

Figure 9. Model 1-1-F1, 1-2-F1, and 1-3-F1 Showing Input Resistance vs. Radius

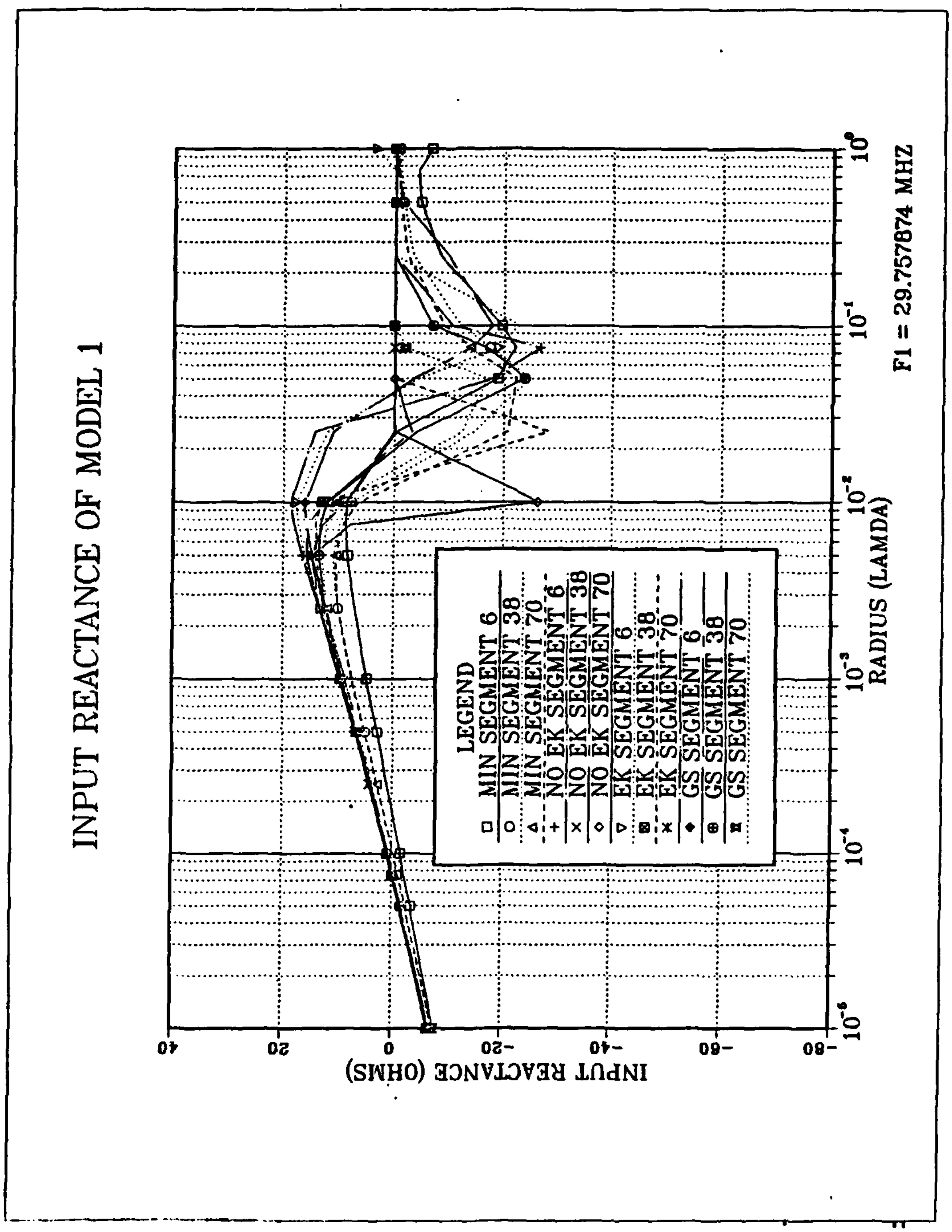

Figure 10. Model 1-1-F1, 1-2-F1, and 1-3-F1 Showing Input Reactance vs. Radius

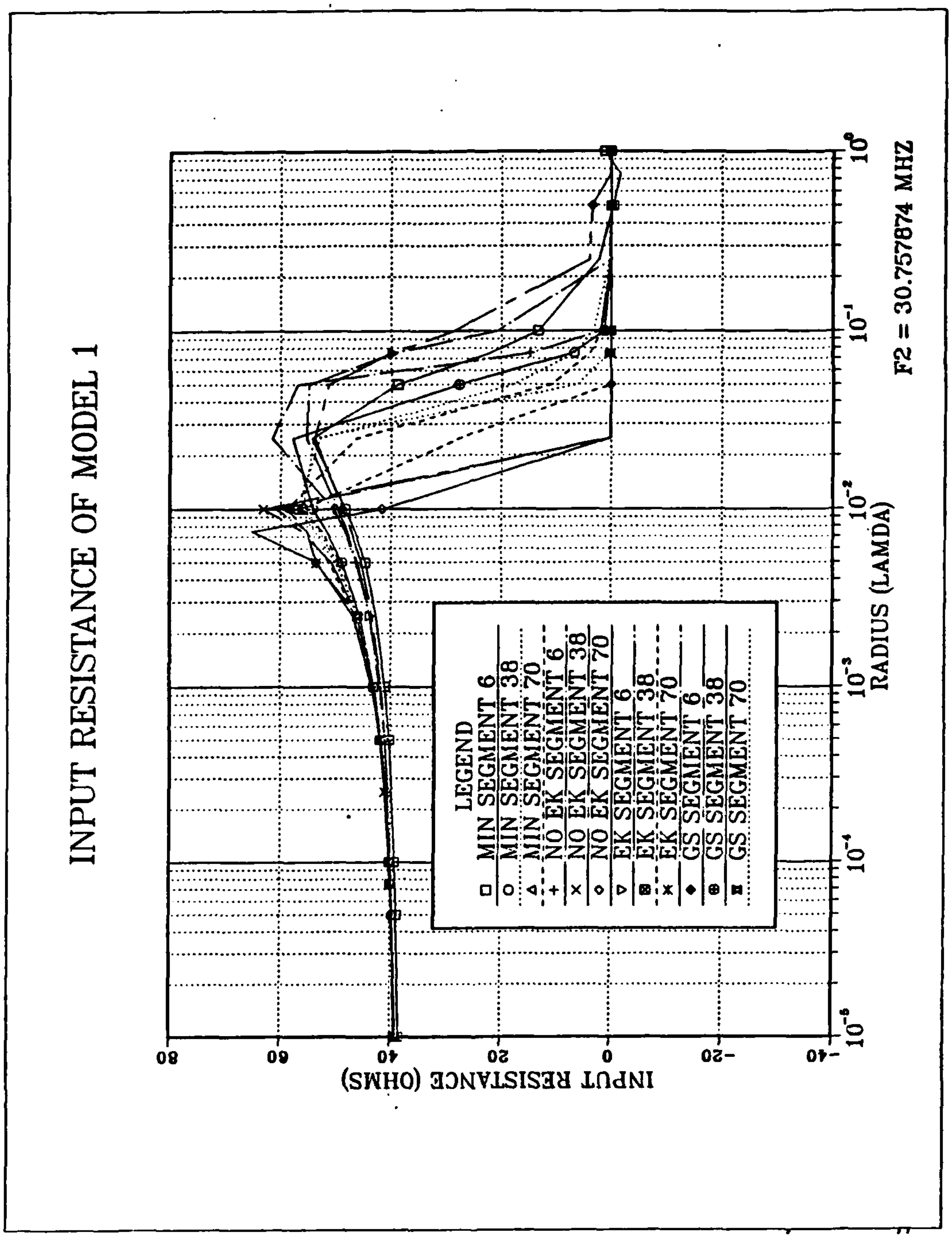

Figure 11. Model 1-1-F2, 1-2-F2, and 1-3-F2 Showing Input Resistance vs. Radius

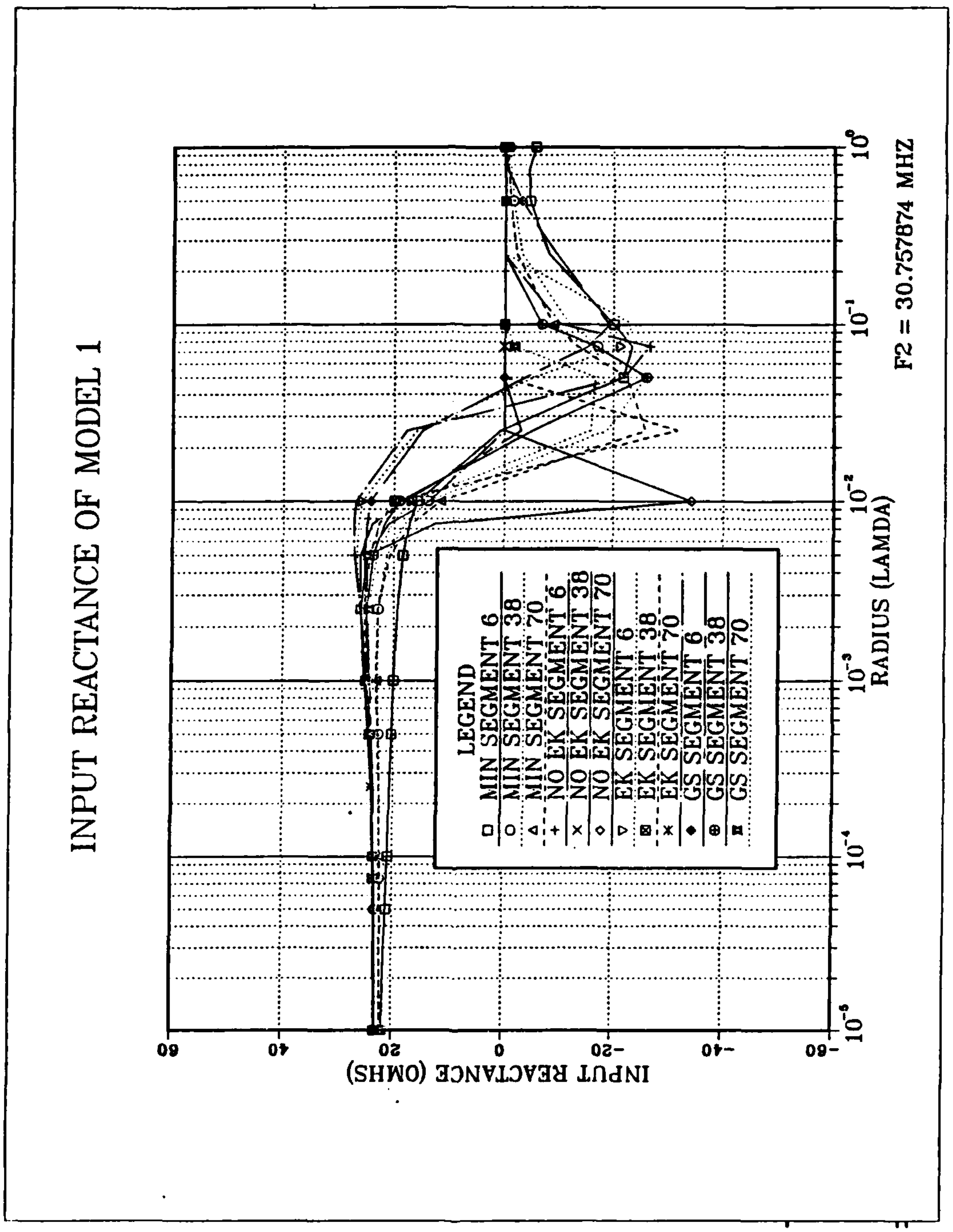

Figure 12. Model 1-1-F2, 1-2-F2, and 1-3-F2 Showing Input Reactance vs. Radius

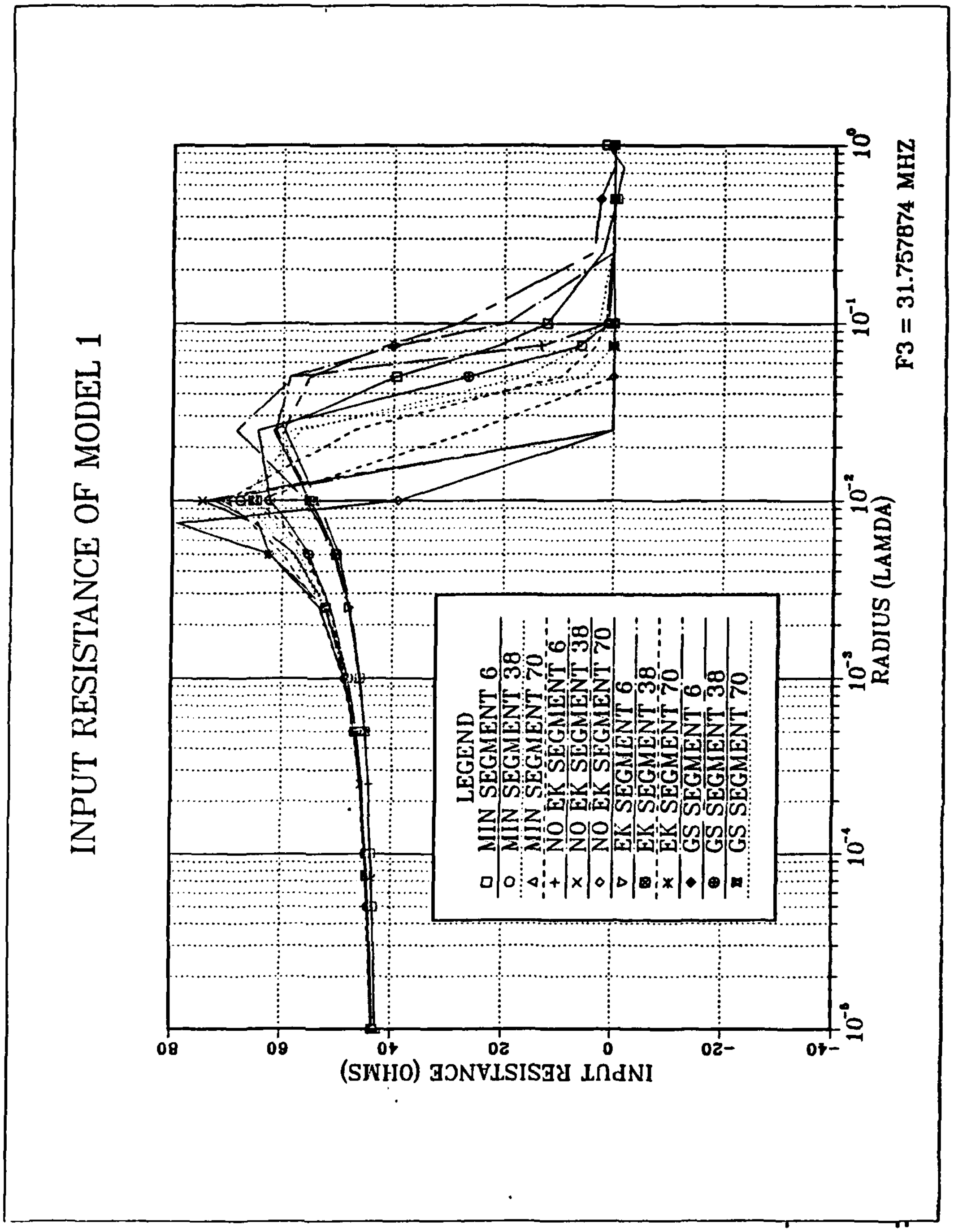

Figure 13. Model 1-1-F3, 1-2-F3, and 1-3-F3 Showing Input Resistance vs. Radius

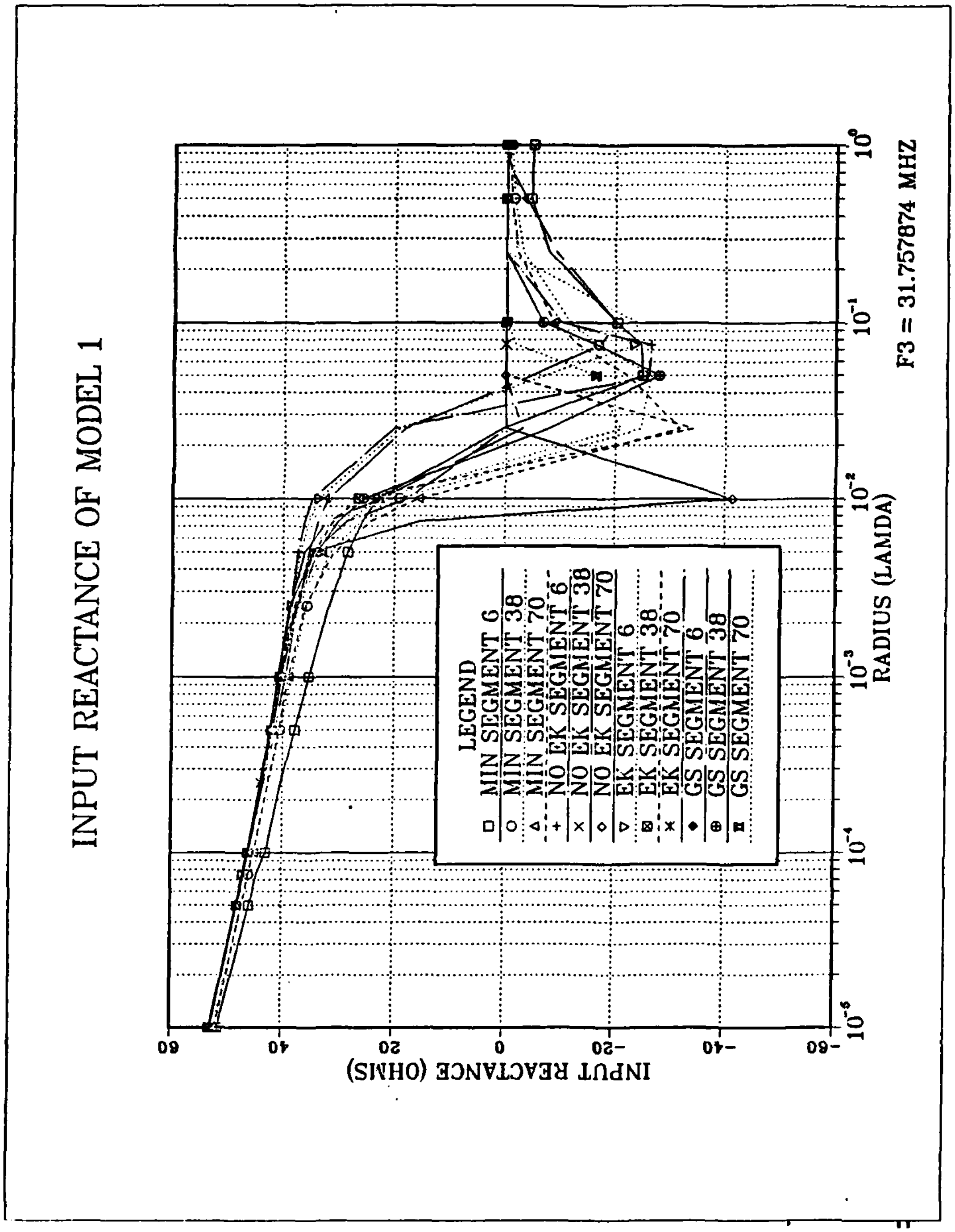

Figure 14. Model 1-1-F3, 1-2-F3, and 1-3-F3 Showing Input Reactance vs. Radius

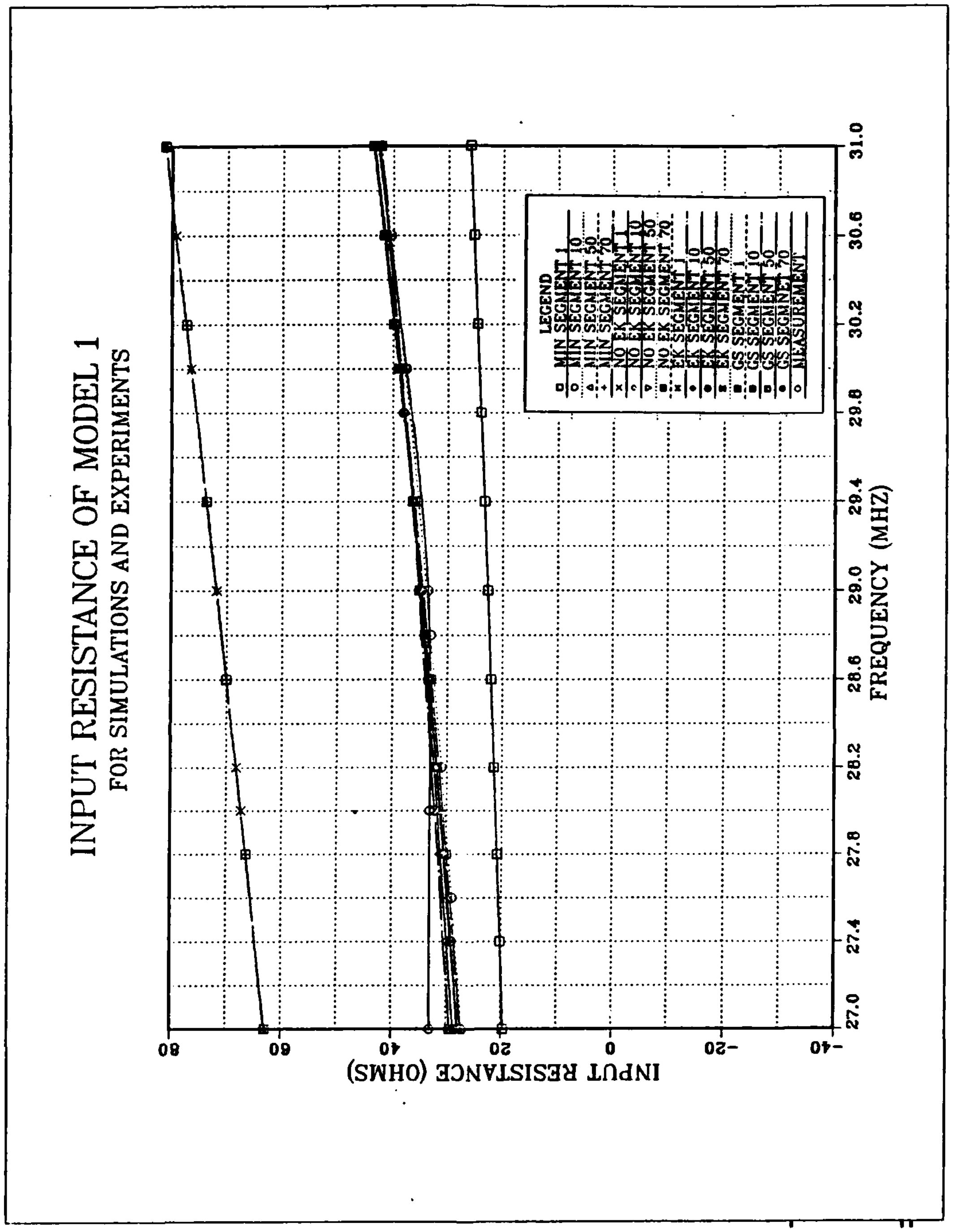

Figure 15. **Model 1 Input Resistance vs. Frequency (Constant Radius, 1/8 inch)**

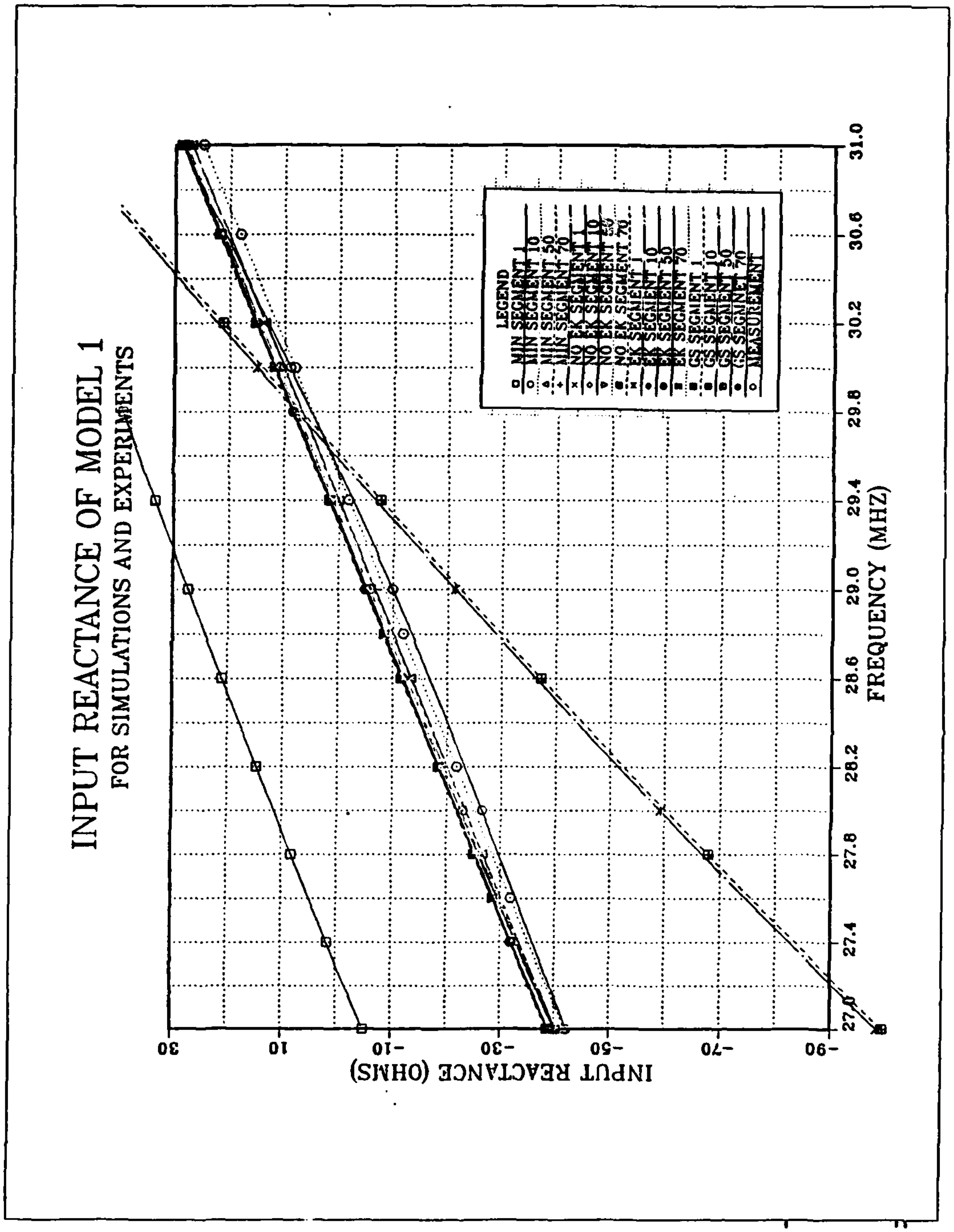

Figure 16. Model 1 Input Reactance vs. Frequency (Constant Radius, 1/8 inch)

B. MODEL 2 RESULTS

1. Model 2-1 results

The ratio of adjacent radii r_1/r_2 for this model is 2 and the radius step between the adjacent sections is 1/8 inch.

Figures 17 and 18 show the results of MININEC and experiments. The resistance and reactance for this model as calculated by MININEC are in close agreement with the results of the experiment.

Figures 19 and 20 show the results of NEC (without the EK card) and the experiment. The input resistance (the real part) of NEC (without the EK card) is in good agreement with that of the experiment but the reactance with apparently converged results using segmentations of 33,33 and 35,35 deviates some 20 ohms from the experiment.

Figures 21 and 22 show the results of NEC (with the EK card) and the experiment. The input resistance (the real part) of NEC (without the EK card) is in good agreement with that of the experiment but the reactance similarly deviates some 20 ohms as was the case with the EK card. Comparing Figures 19 - 22, the results of NEC (without the EK card) agree perfectly with those of NEC (with the EK card) for this model.

Figures 23 and 24 show the results of NECGS and the experiments. The input resistance (the real part) and the reactance are about 5 ohms higher than those of the experiments. The resistance and reactance are in very good agreement agreement for different models of NECGS. (In the figures, the following applies: no letters after the segment number indicates different radii modeling , (E) indicates equal radius modeling, (C) indicates different radii modeling with an end cap, and (CE) indicates equal radius modeling with an end). For the imaginary part of the input impedance, the model of equal radii with the end cap is slightly different from the others.

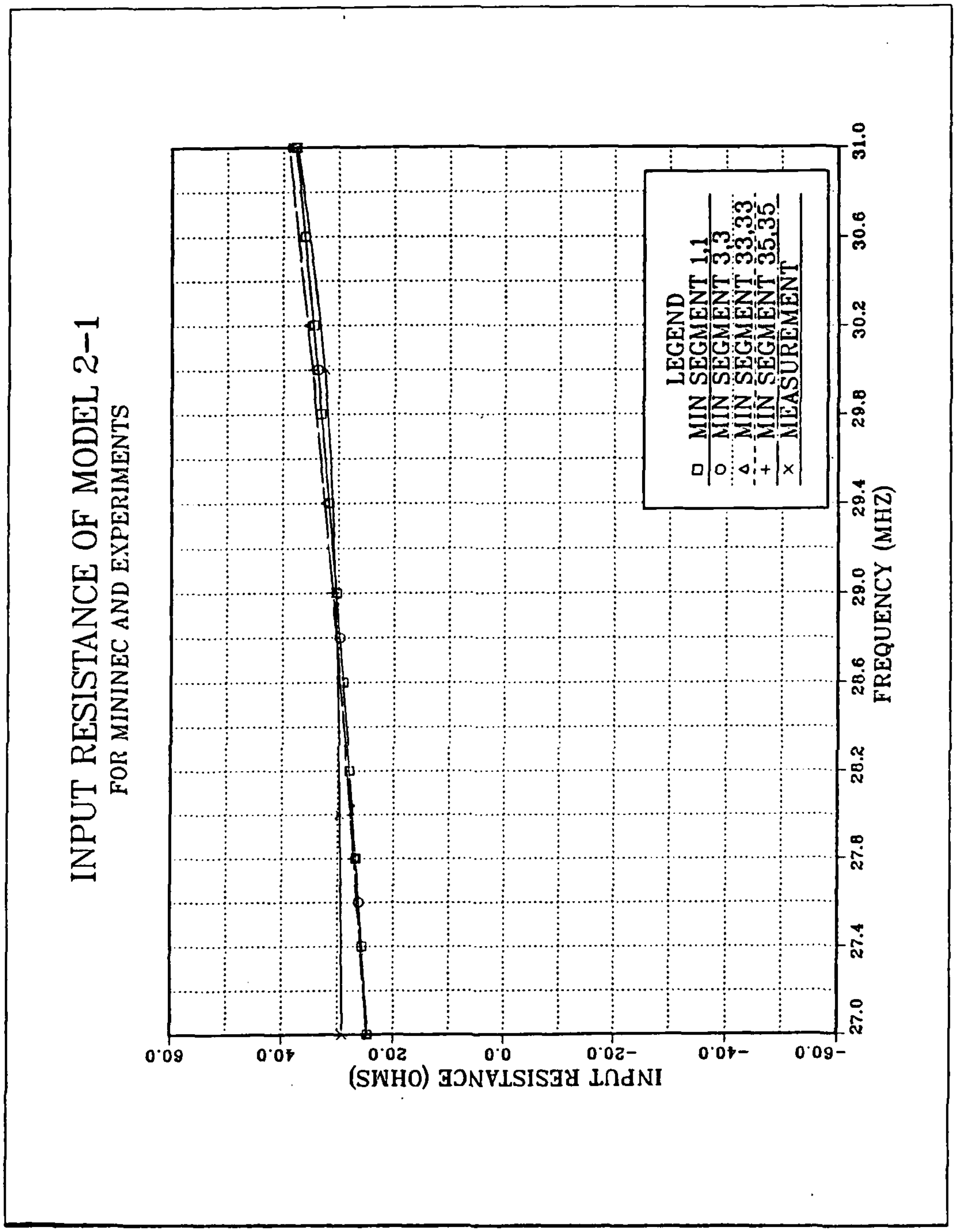

Figure 17. Model 2-1 Input Resistance vs. Frequency (27-31 MHz) for MININEC and the Experiment

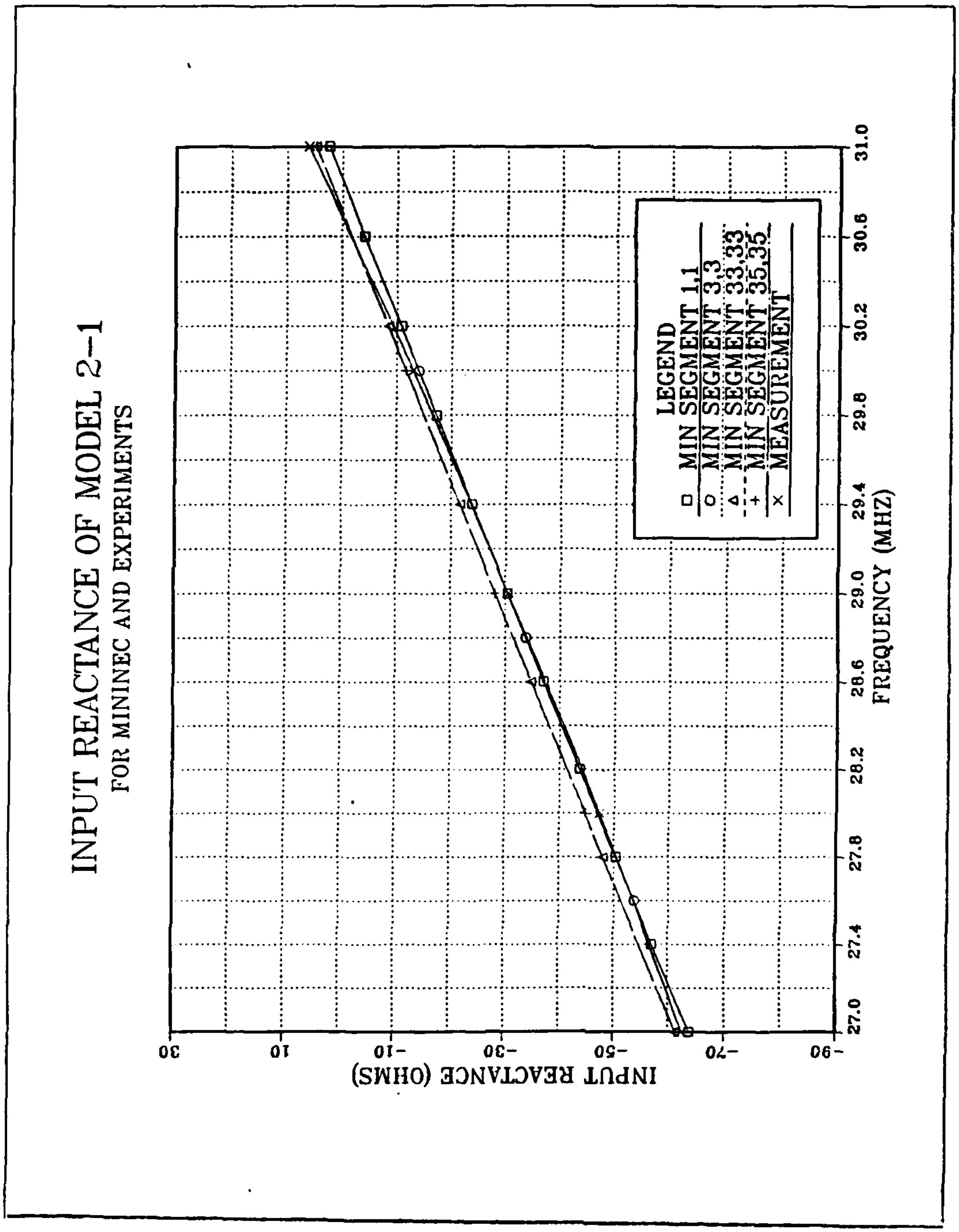

Figure 18. Model 2-1 Input Reactance vs. Frequency (27-31 MHz) for MININEC and the Experiment

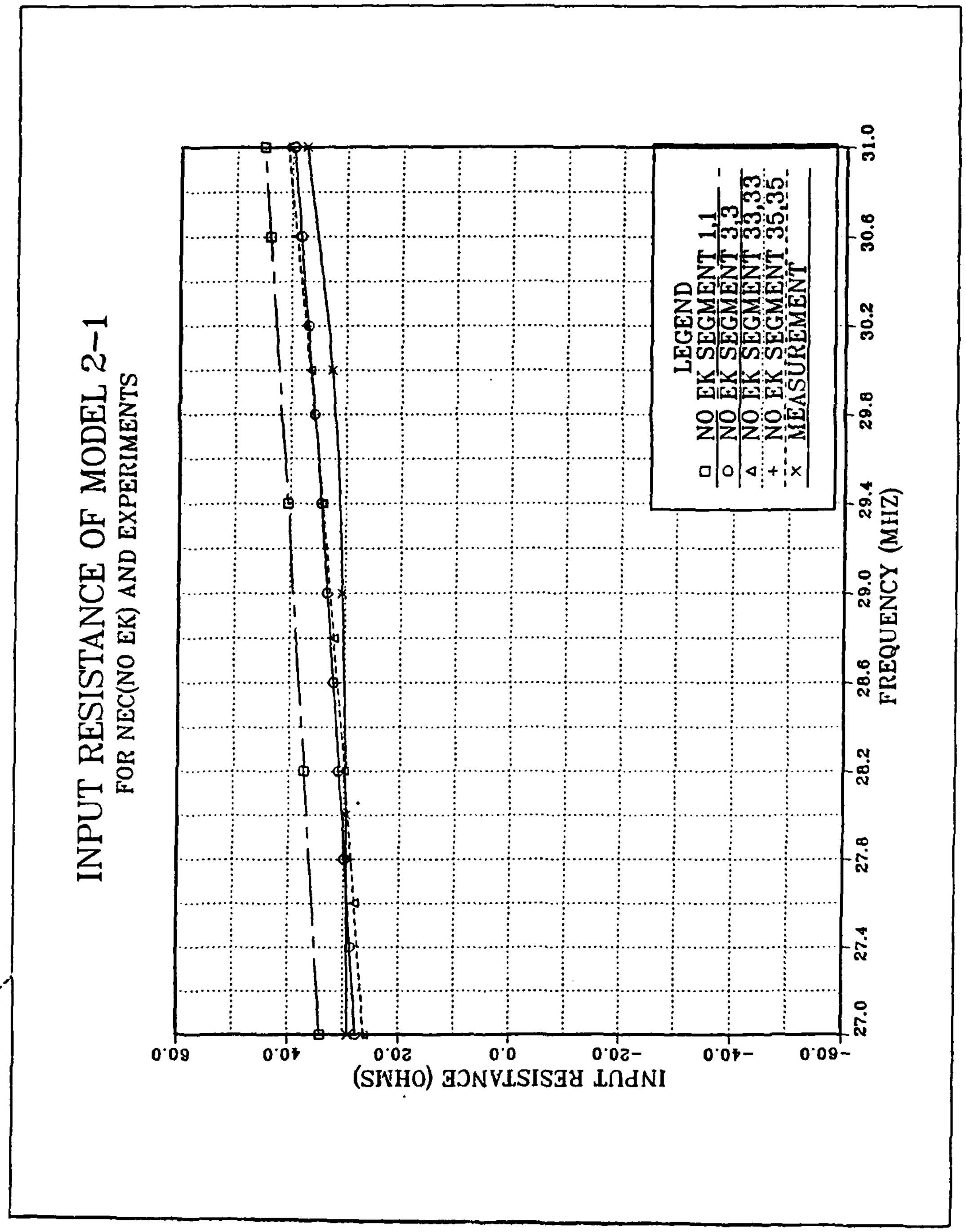

Figure 19. Model 2-1 Input Resistance vs. Frequency (27-31 MHz) for NEC (no EK card) and the Experiment

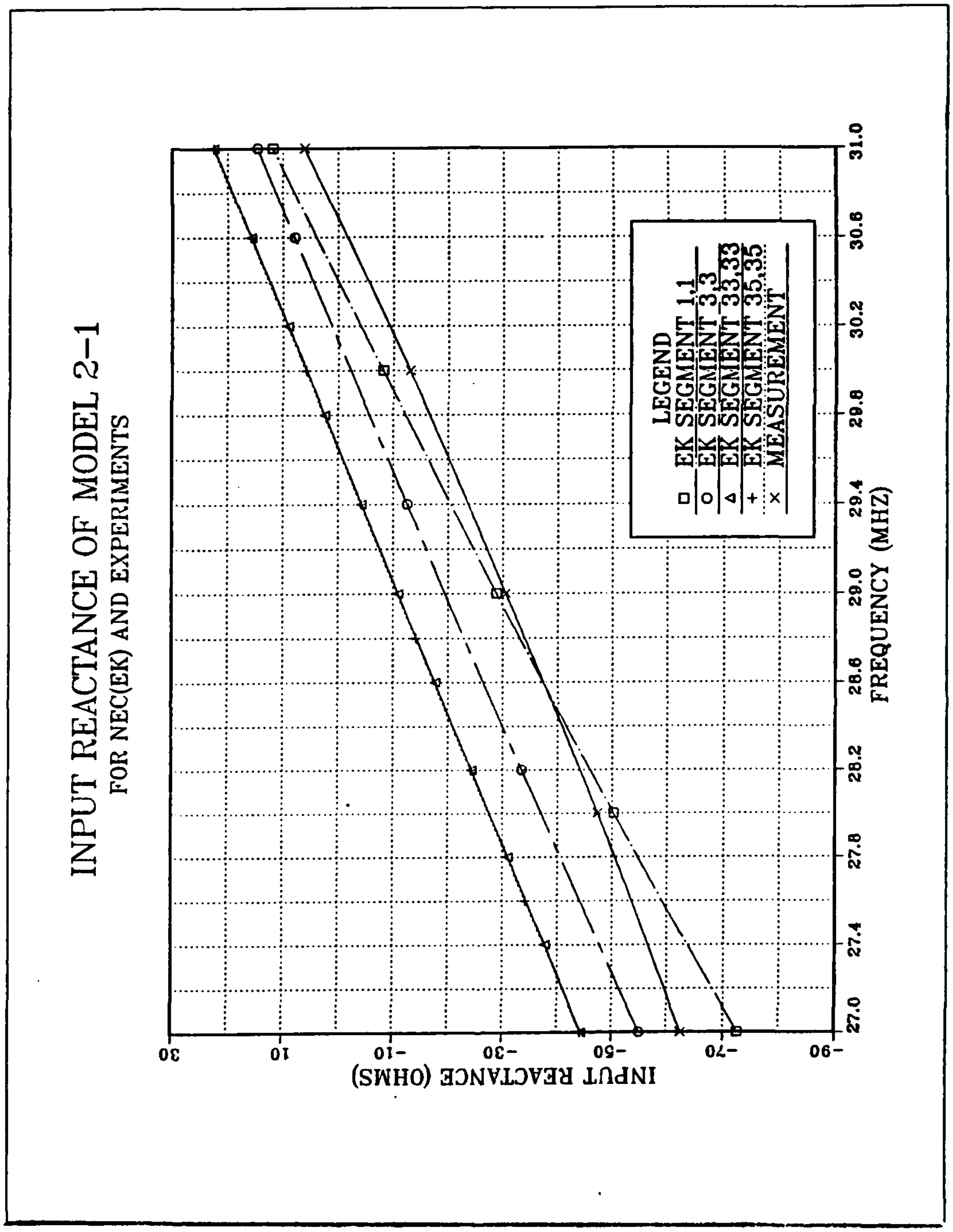

Figure 20. Model 2-1 Input Reactance vs. Frequency (27-31 MHz) for NEC (no EK card) and the Experiment

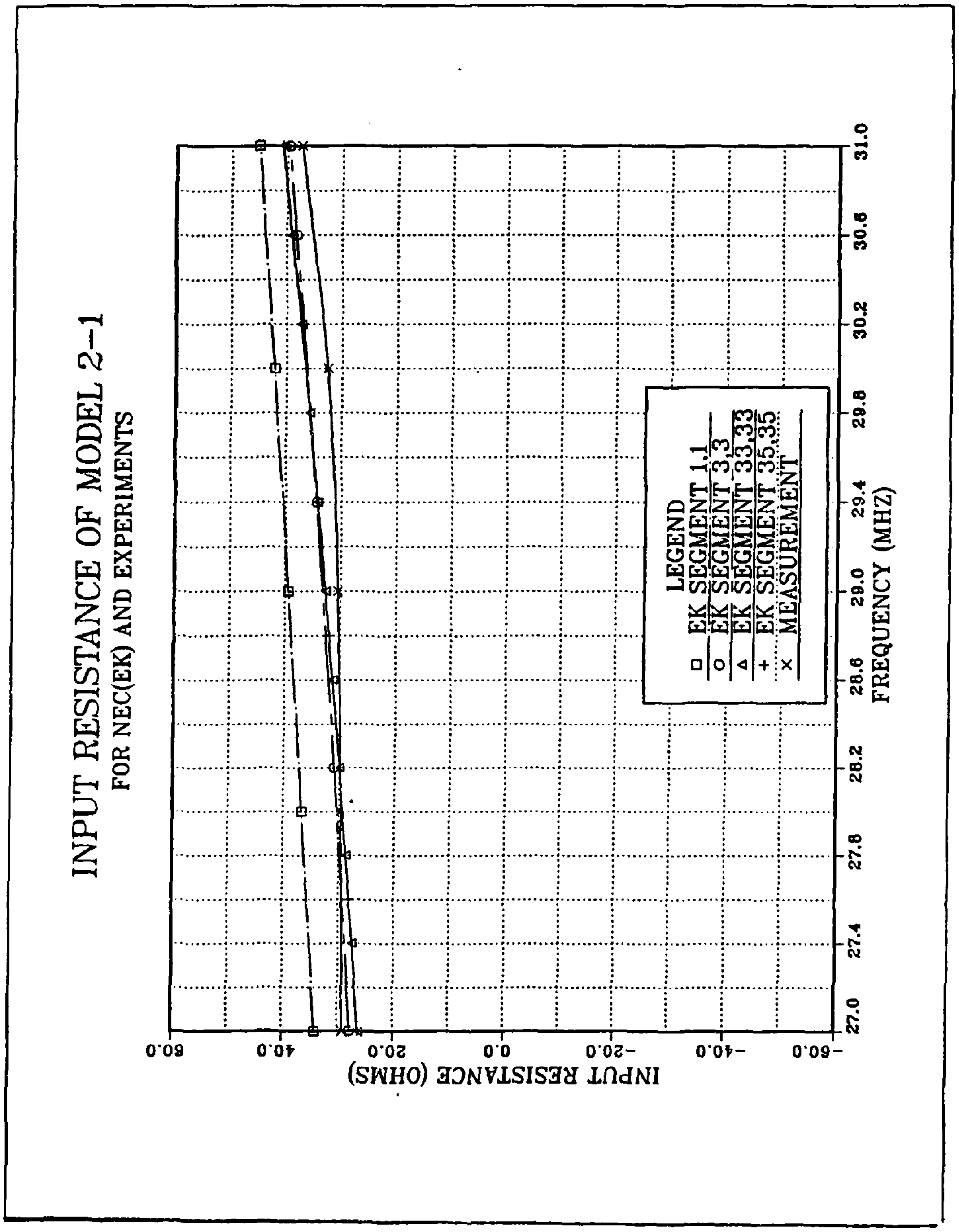

Figure 21. Model 2-1 Input Resistance vs. Frequency (27-31 MHz) for NEC (EK card) and the Experiment

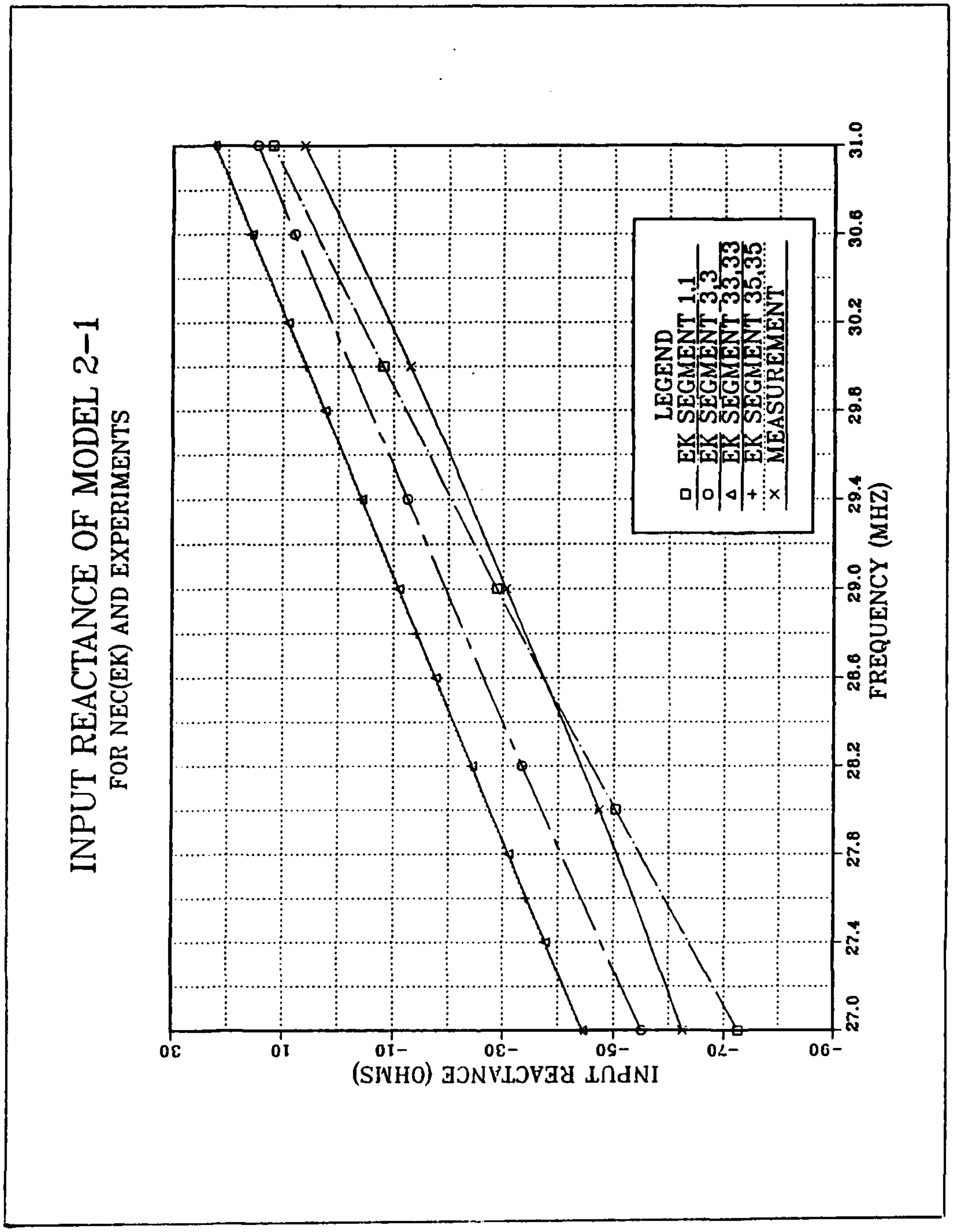

Figure 22. **Model 2-1 Input Reactance vs. Frequency (27-31 MHz) for NEC (EK card) and the Experiment**

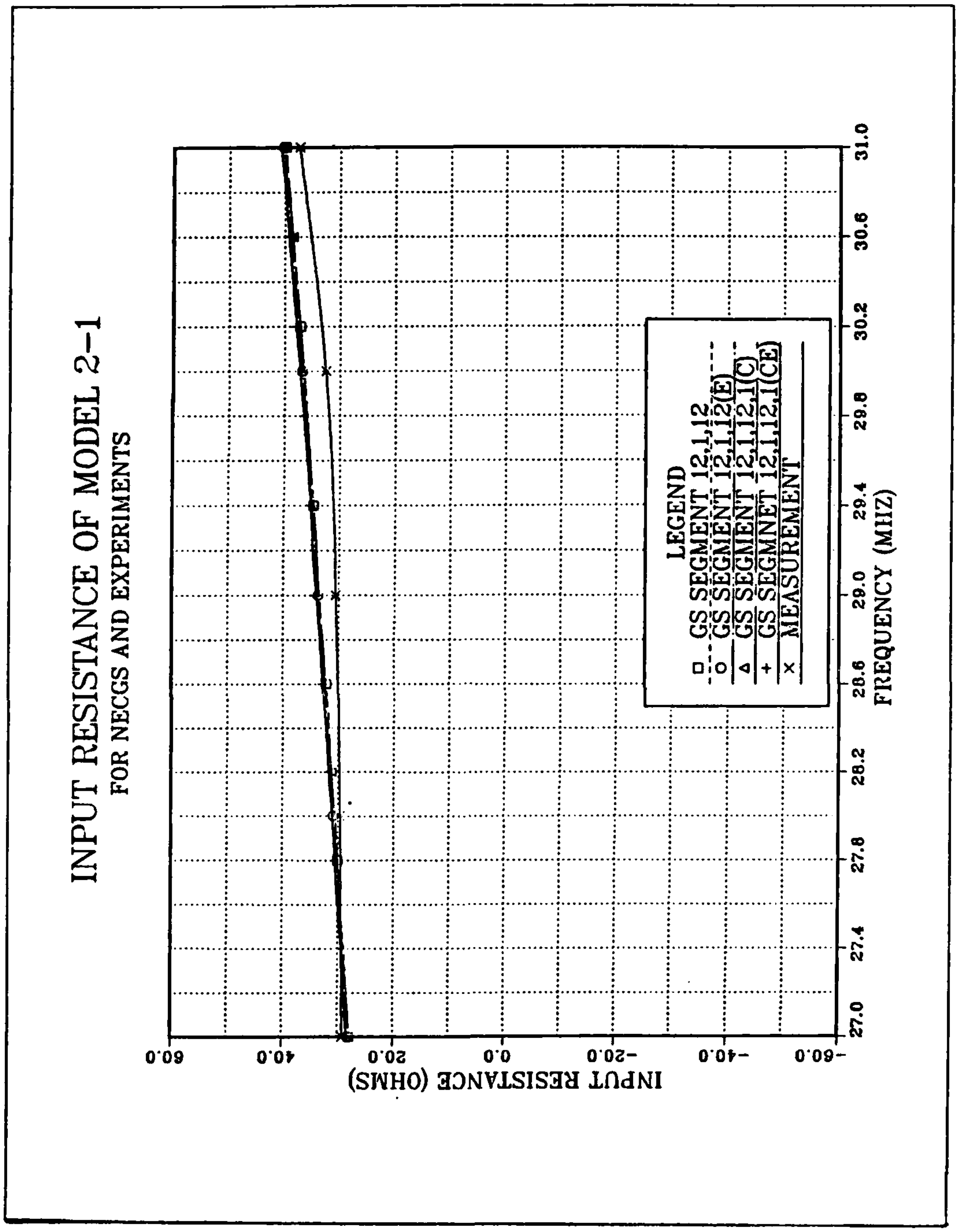

Figure 23. Model 2-1 Input Resistance vs. Frequency (27-31 MHz) for NECGS and the Experiment

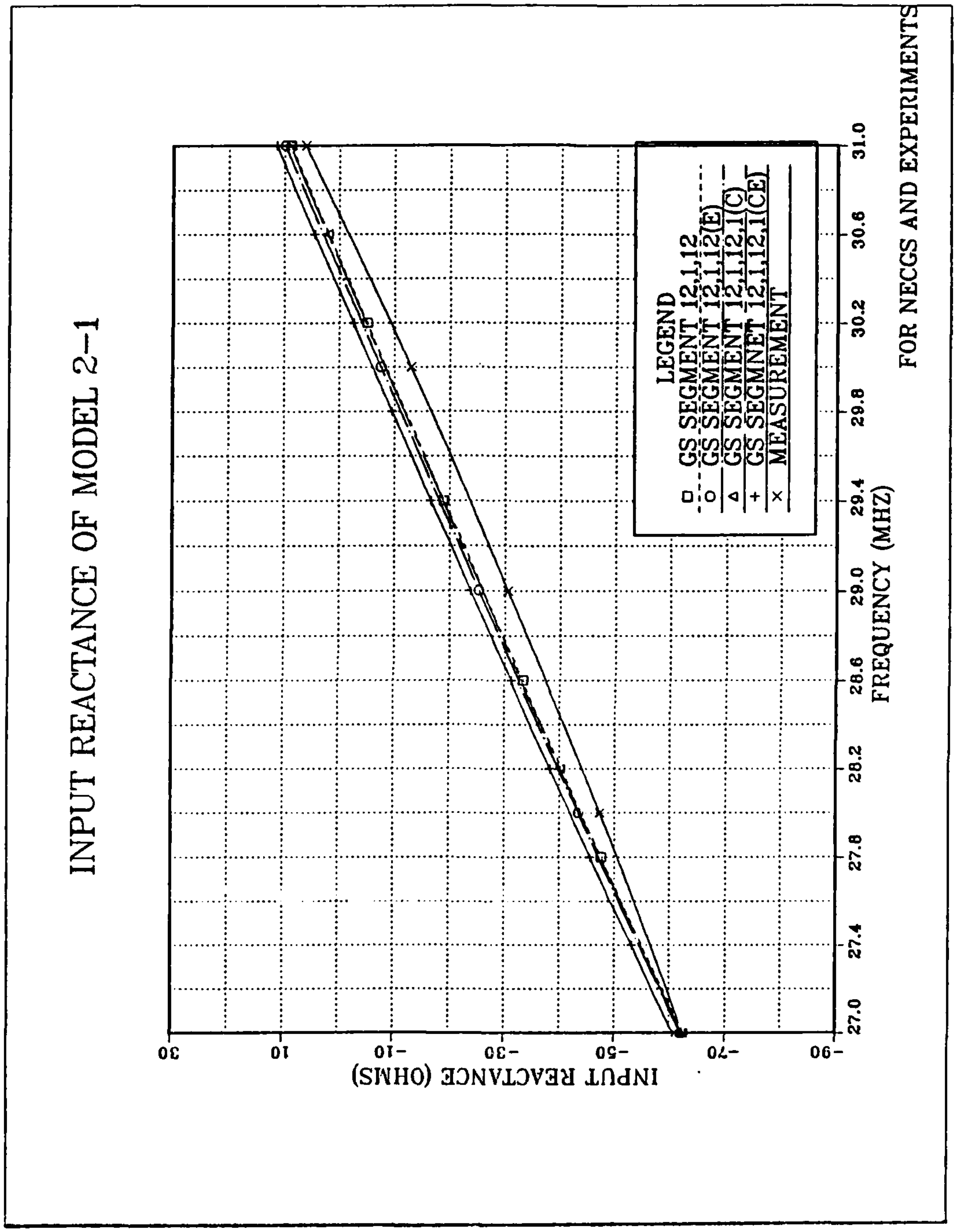

Figure 24. Model 2-1 Input Reactance vs. Frequency (27-31 MHz) for NECGS and the Experiment

2. Model 2-2 results

The ratio of adjacent radii r_1/r_2 for this model is 2 and the radius step between the adjacent sections is 1/4 inch. The ratio is the same as Model 2-1, but the radii of the sections are doubled.

Figures 25 and 26 show the results of MININEC and the experiment. The input resistance values (the real part) from MININEC are a maximum of 5 ohms differen. from those of the experiment. The input reactances (the imaginary part) of MININEC for segmentations of 1,1 and 3,3 are the closest to those of the experiment.

Figures 27 and 28 show the results of NEC (without the EK card) and the experiment. The input resistance values (the real part) from NEC (without the EK card) have a maximum deviation of 6 ohms, which is slightly worse than the MININEC results. The apparently converged reactance (the imaginary part) of NEC (with the EK card) has a maximum deviation of 20 ohms from those of the experiment.

Figures 29 and 30 show the results of NEC (with the EK card) and the experiment. The input resistance values (the real part) from NEC (with the EK card) have a maximum deviation of 6 ohms from those of the experiment. But the apparently converged input reactance values (the imaginary part) from NEC (with the EK card) have a maximum deviation of 30 ohms from those of the experiment. The input resistance of NEC (with the EK card) shows little difference from that of NEC (without the EK card). The input reactance (with and without the EK card), however, is different.

Figures 31 and 32 show the results of NECGS and the experiment. The input resistances of NECGS without the end cap are closer to the results of the experiment than those of NECGS with the end cap. The input reactance of NECGS does not match exactly with the experimental results for this model.

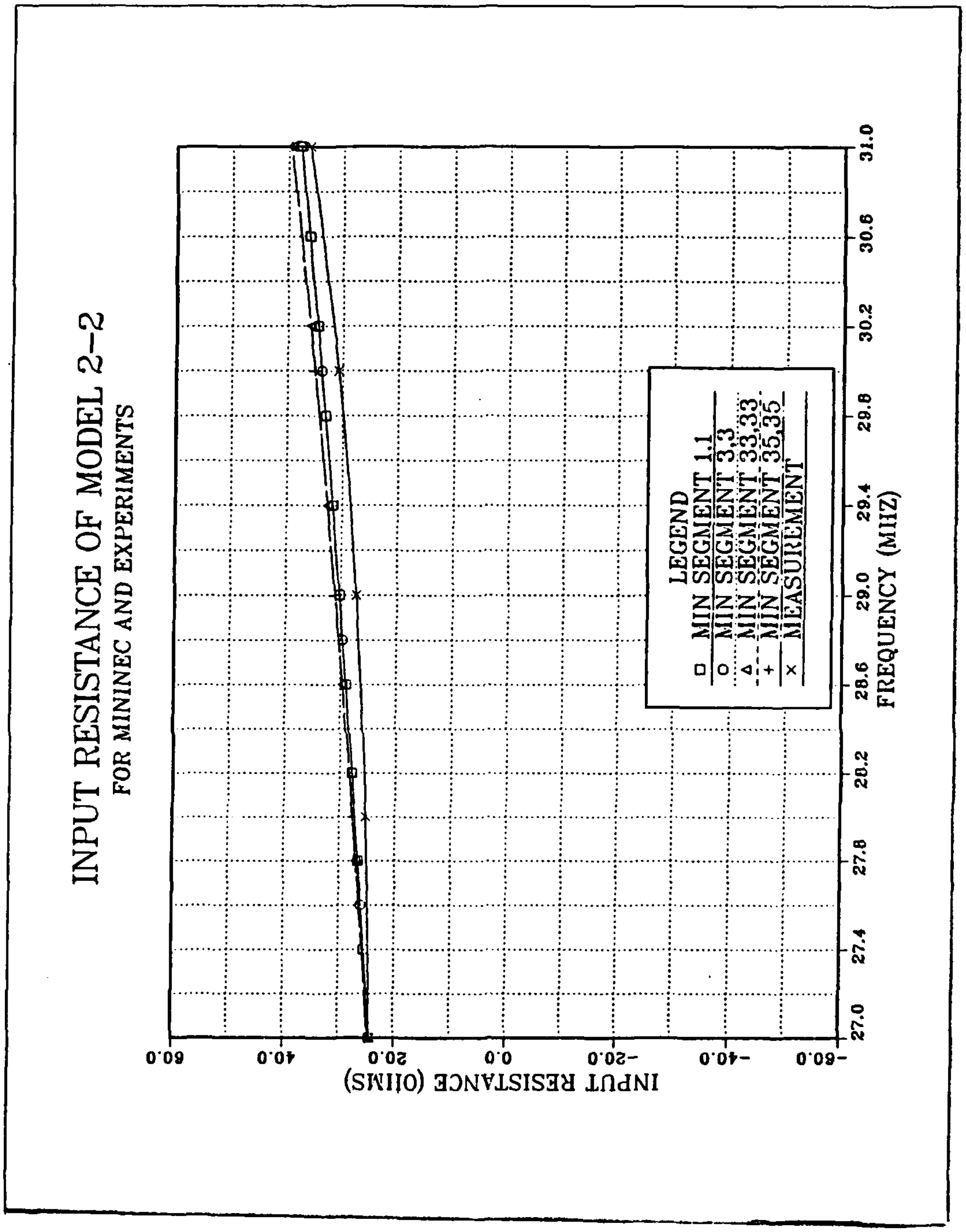

Figure 25. Model 2-2 Input Resistance vs. Frequency (27-31 MHz) for MININEC and the Experiment

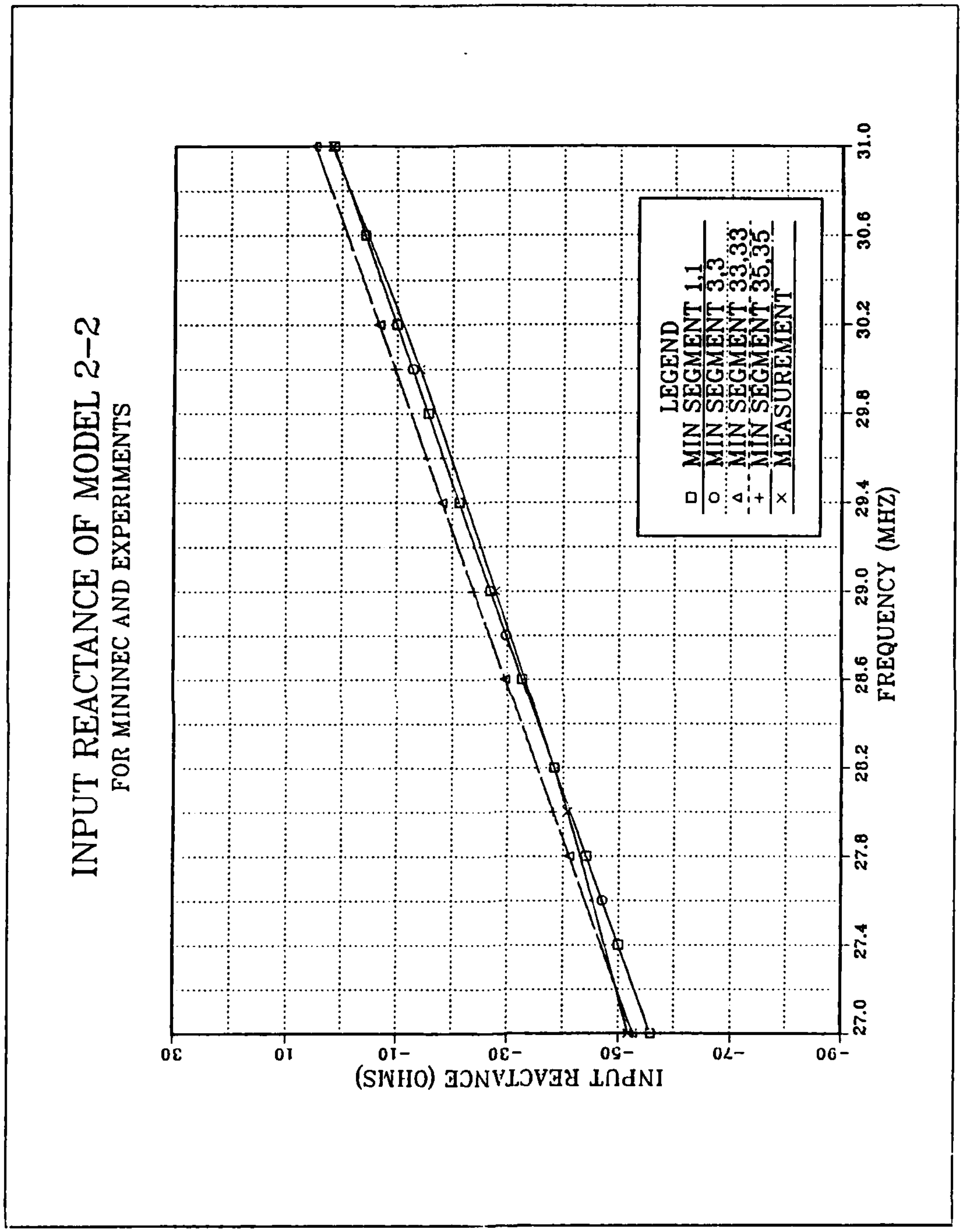

Figure 26. Model 2-2 Input Reactance vs. Frequency (27-31 MHz) for MININEC and the Experiment

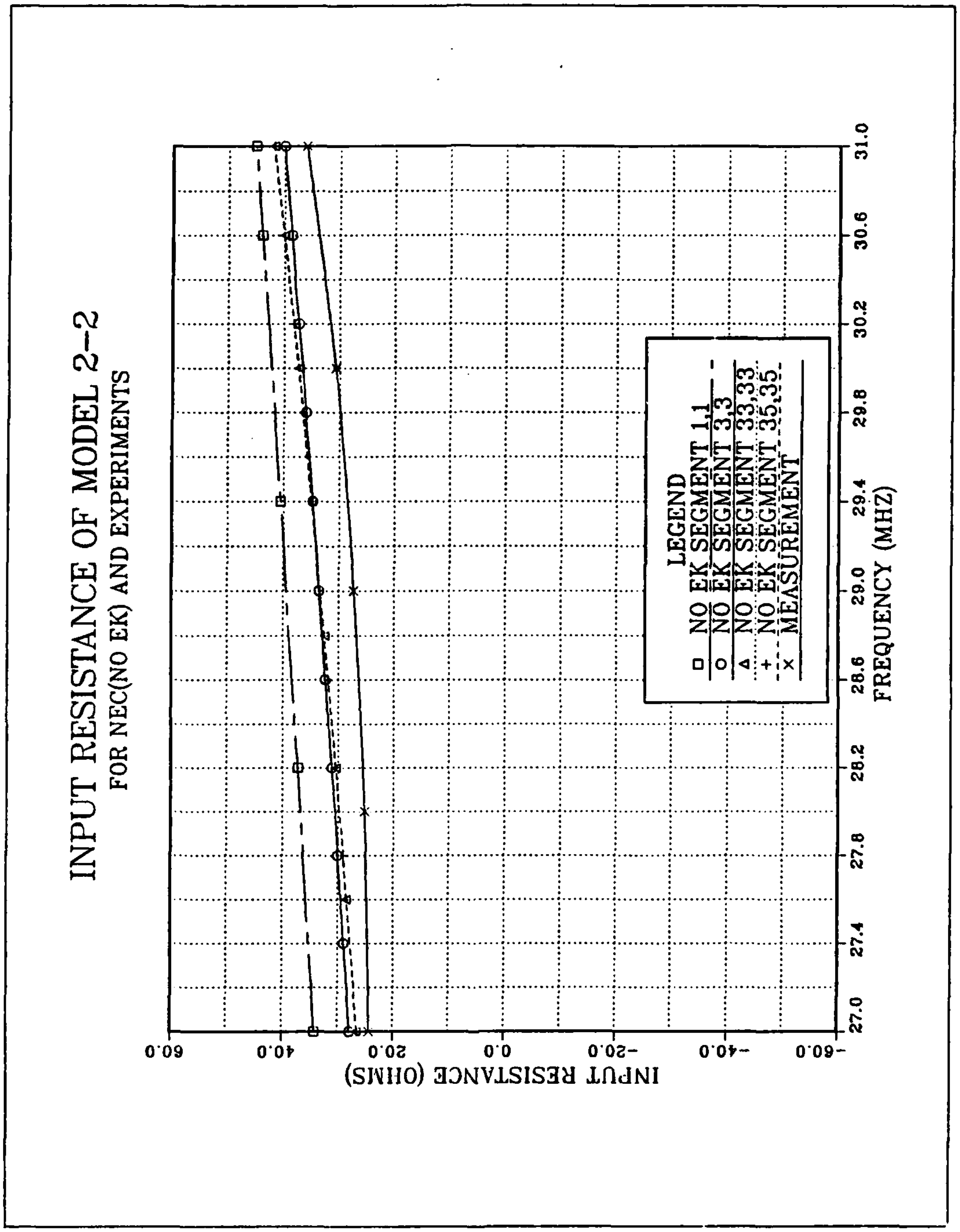

Figure 27. Model 2-2 Input Resistance vs. Frequency (27-31 MHz) for NEC (no EK card) and the Experiment

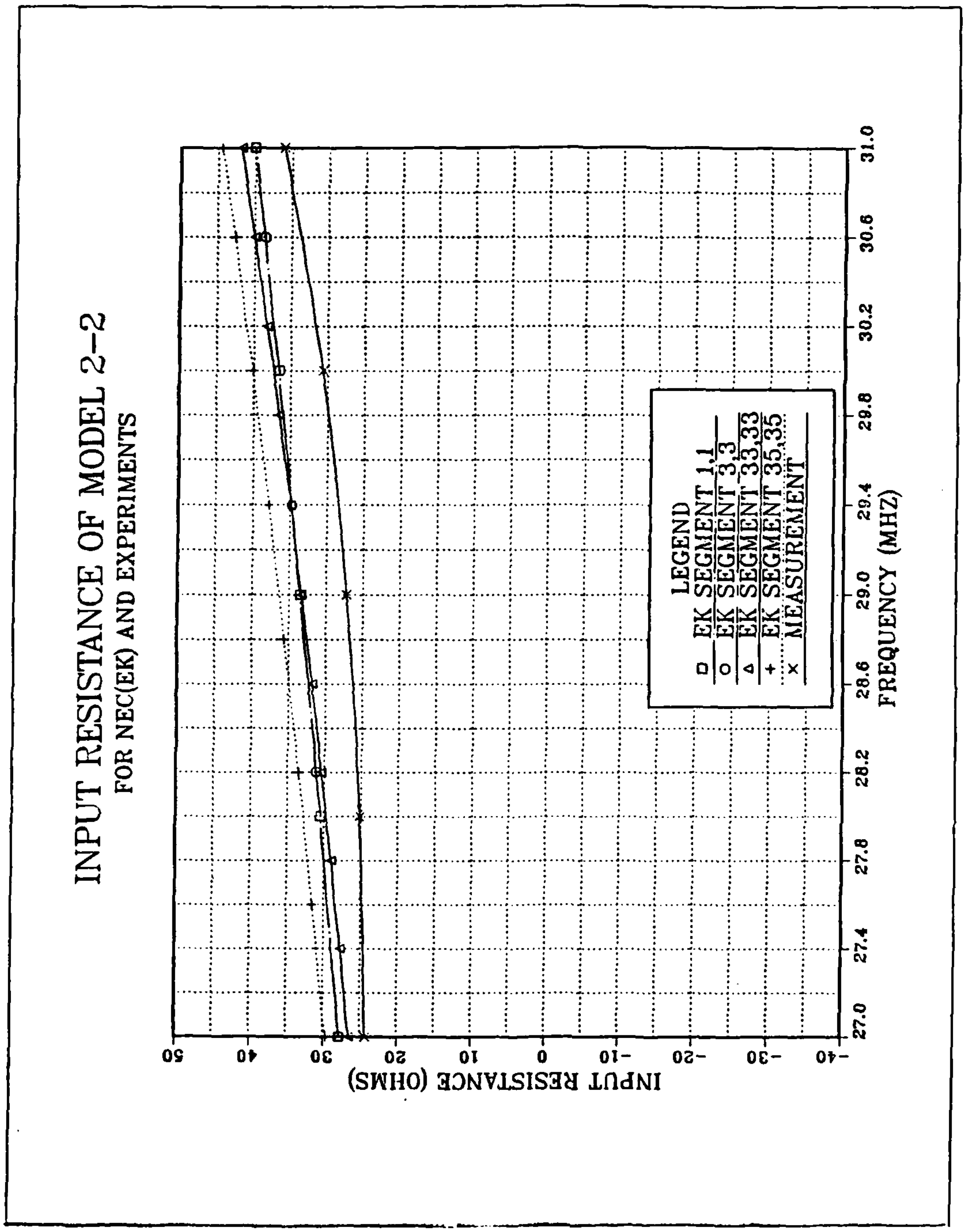

Figure 29. Model 2-2 Input Resistance vs. Frequency (27-31 MHz) for NEC (EK card) and the Experiment

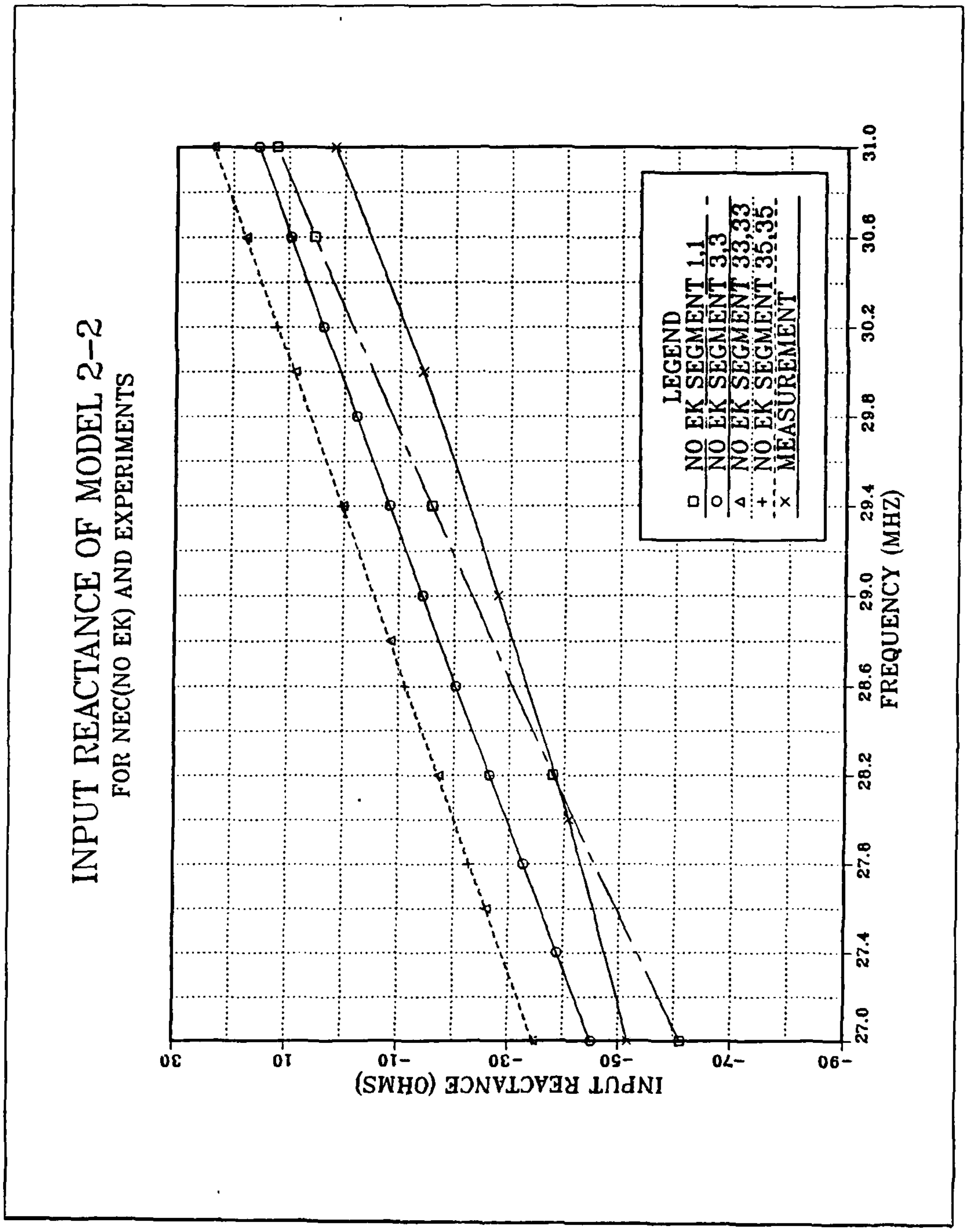

Figure 28. **Model 2-2 Input Reactance vs. Frequency (27-31 MHz) for NEC (no EK card) and the Experiment**

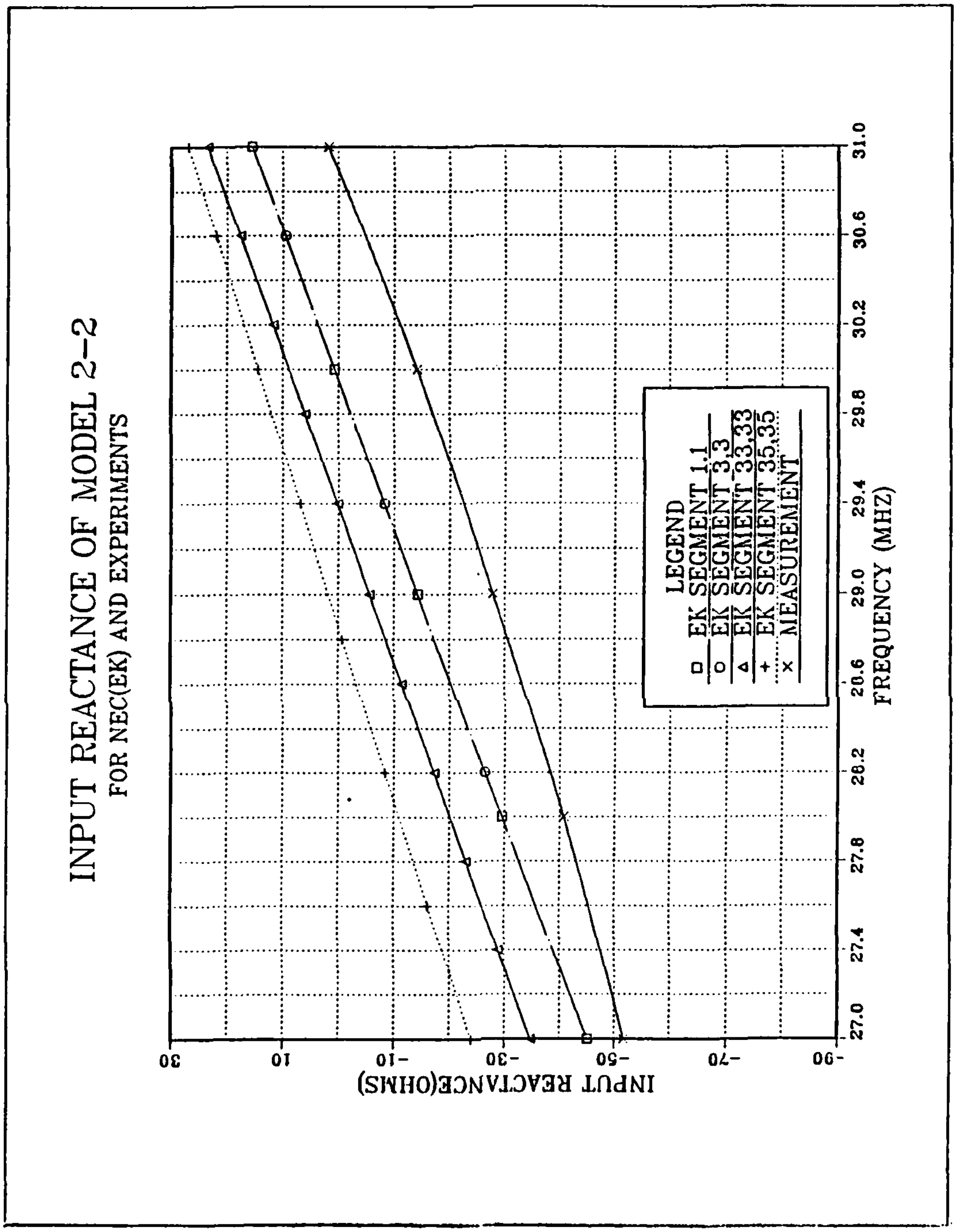

Figure 30. Model 2-2 Input Reactance vs. Frequency (27-31 MHz) for NEC (EK card) and the Experiment.

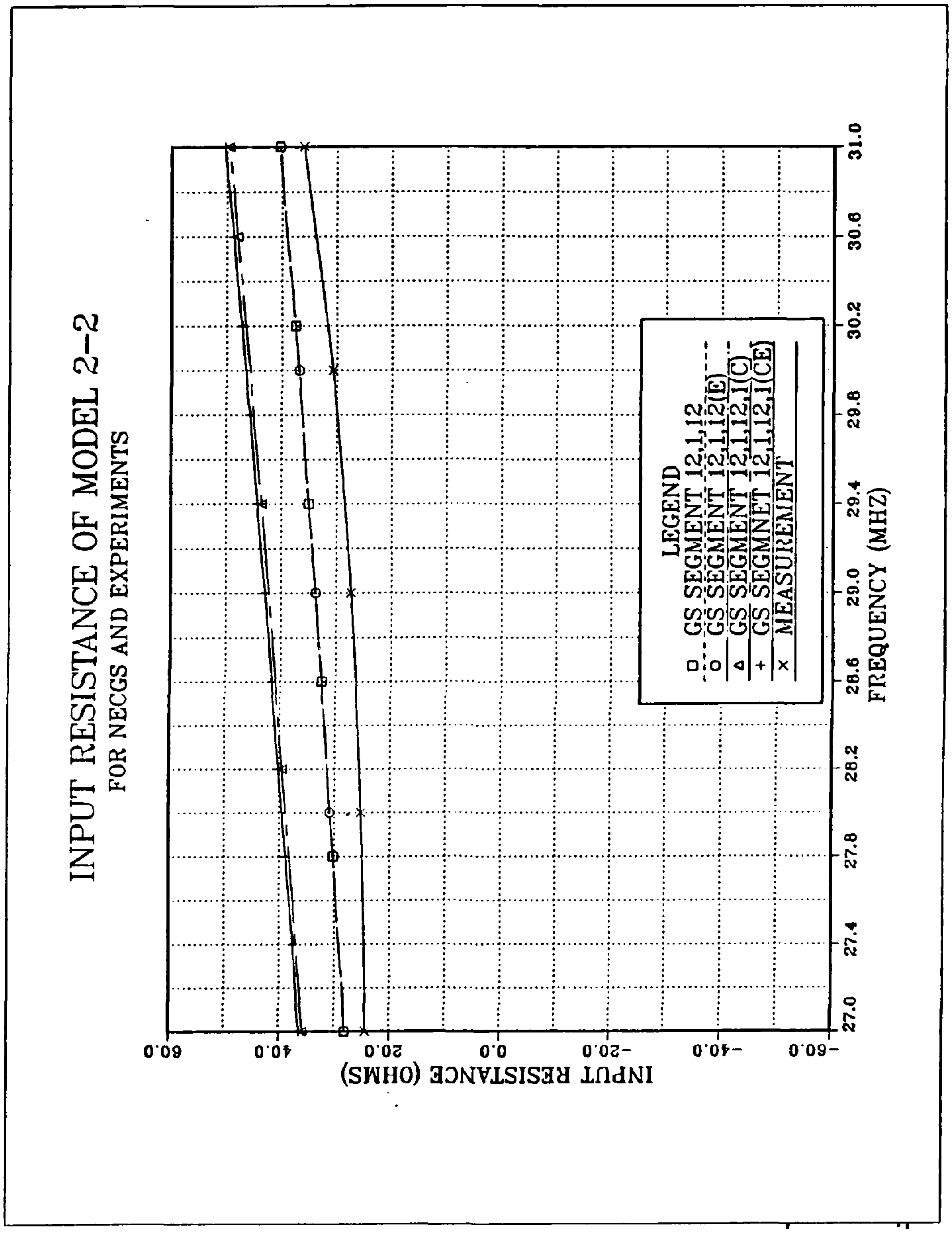

Figure 31. Model 2-2 Input Resistance vs. Frequency (27-31 MHz) for NECGS and the Experiment.

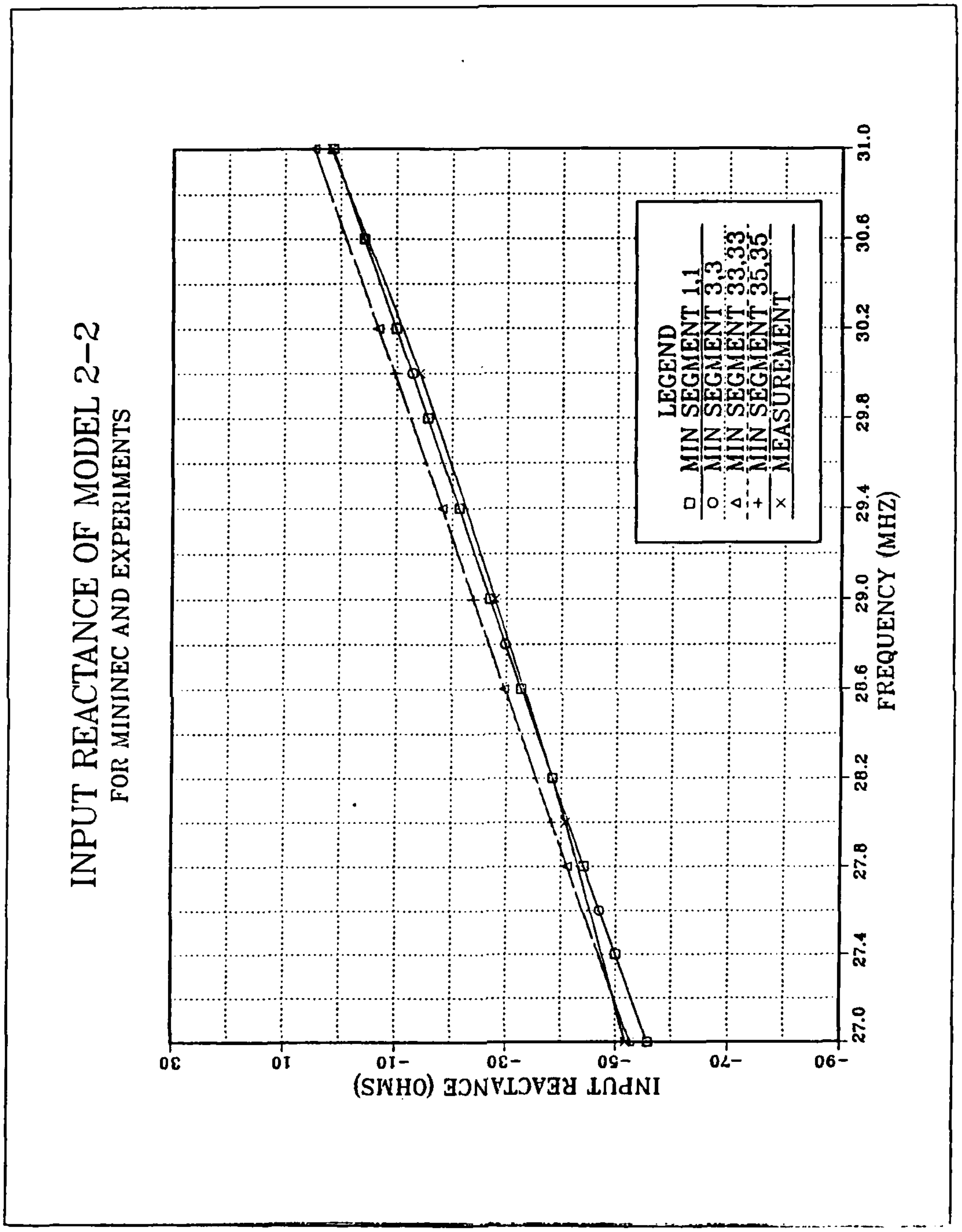

Figure 32. Model 2-2 Input Reactance vs. Frequency (27-31 MHz) for NECGS and the Experiment.

3. Model 2-1-E results

Model 2-1-E has an equivalent average radius of 3/16 inch for Model 2-1. Figures 33 and 34 show the results of all computer codes and the experiments with segmentations of 6, 66, and 70 segments. The input resistance results from the computer code is in good agreement with the experimental results except for those of 2 segments. The reactance of the computer code results is very different from the experimental results (about 20 ohms).

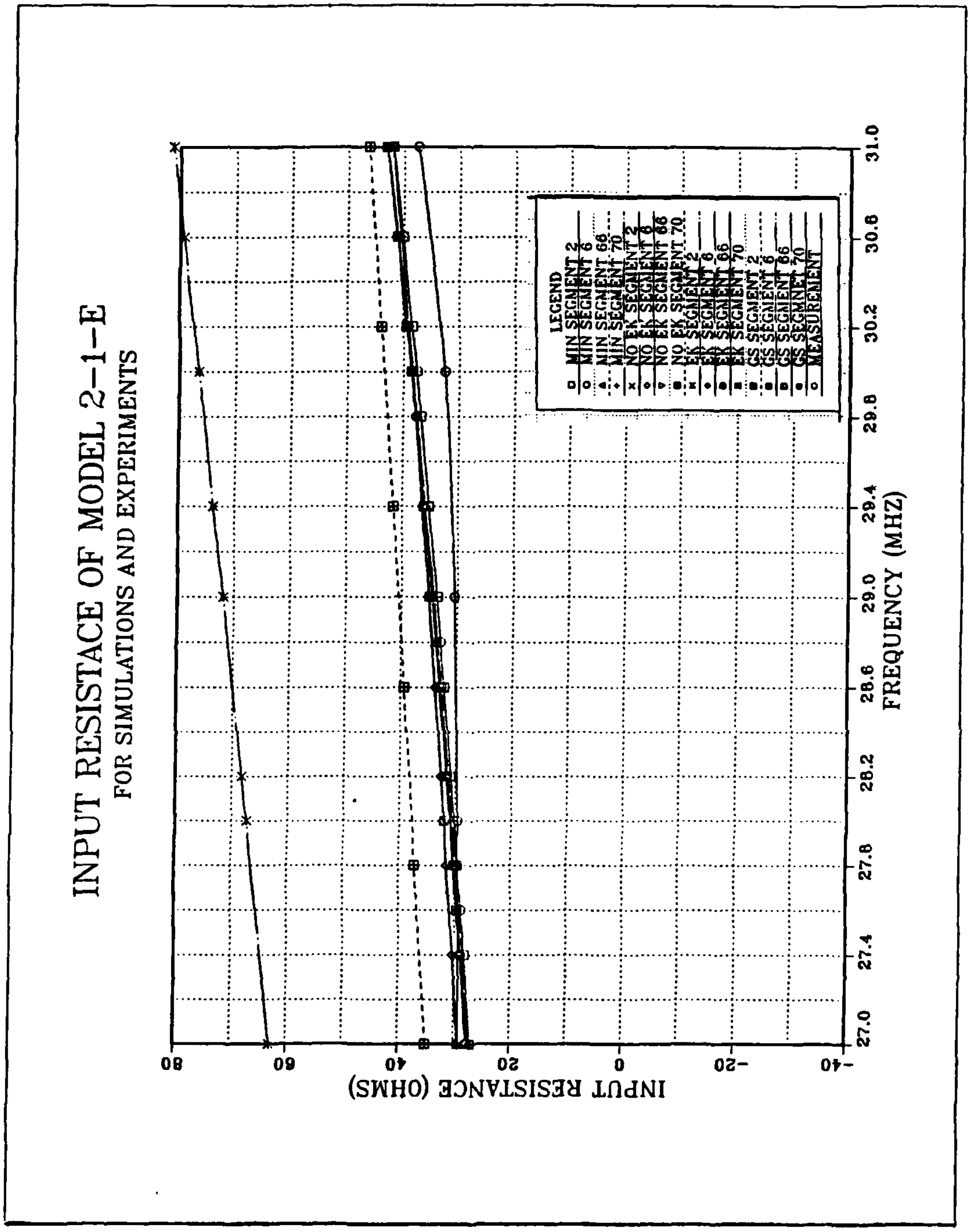

Figure 33. **Model 2-1-E Input Resistance vs. Frequency (27-31 MHz) for all Computer Simulations and the Experiment**

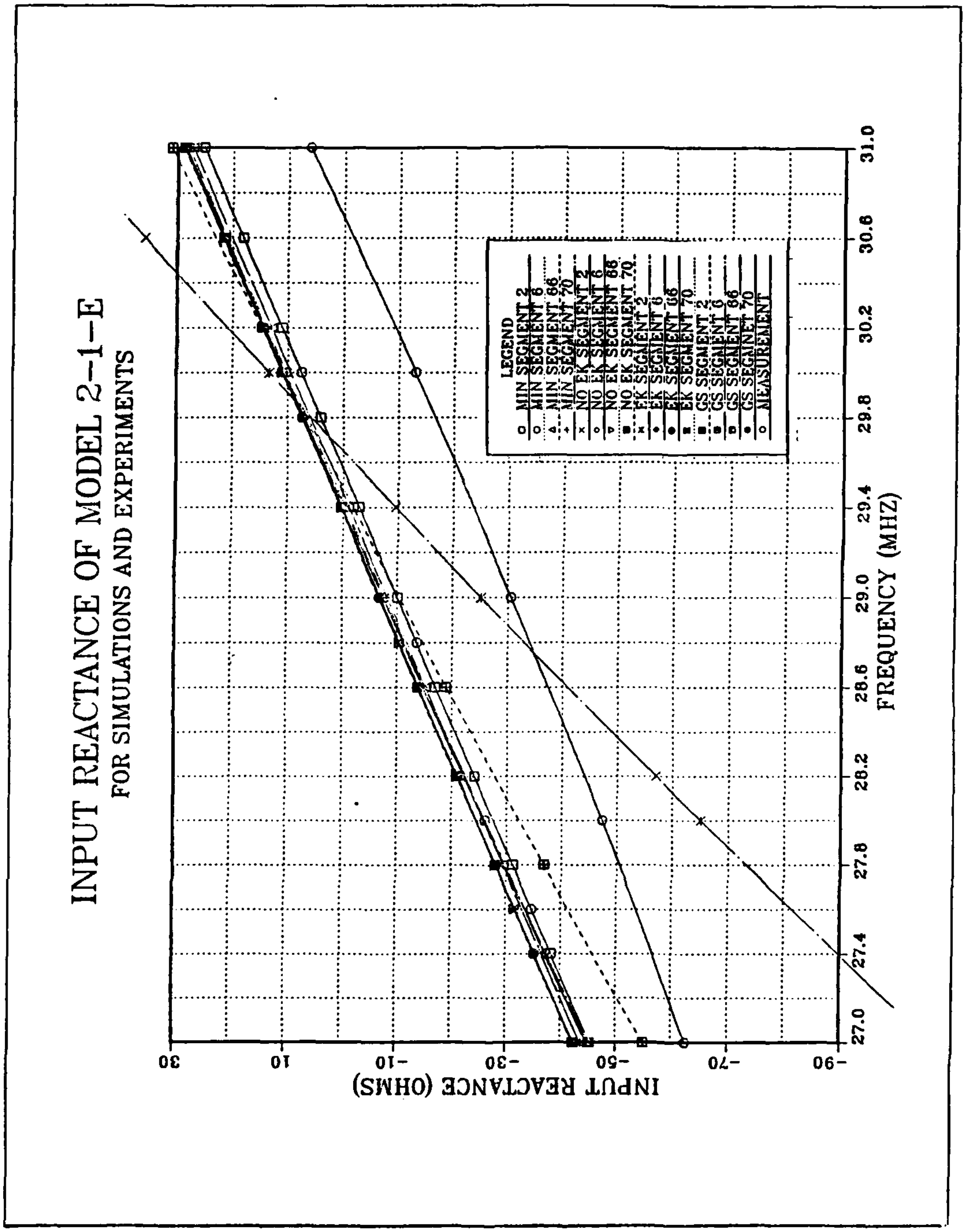

Figure 34. Model 2-1-E Input Reactance vs. Frequency (27-31 MHz) for all Computer Simulations and the Experiment

4. Model 2-2-E results

Model 2-2-E has an equivalent average radius of 3/8 inch for Model 2-2. Figures 35 and 36 show the results of all computer codes and the experiments with segmentations of 6, 66, and 70 segments. The input resistance results from the computer codes are different from those of the experiment for the Model 2-1-E. The input reactance of the computer code results is very different than that of the experiment. Comparing with Model 2-1-E, the results of using a thicker equivalent average radius for a large difference between adjacent radii are worse than those of a thinner equivalent average radius.

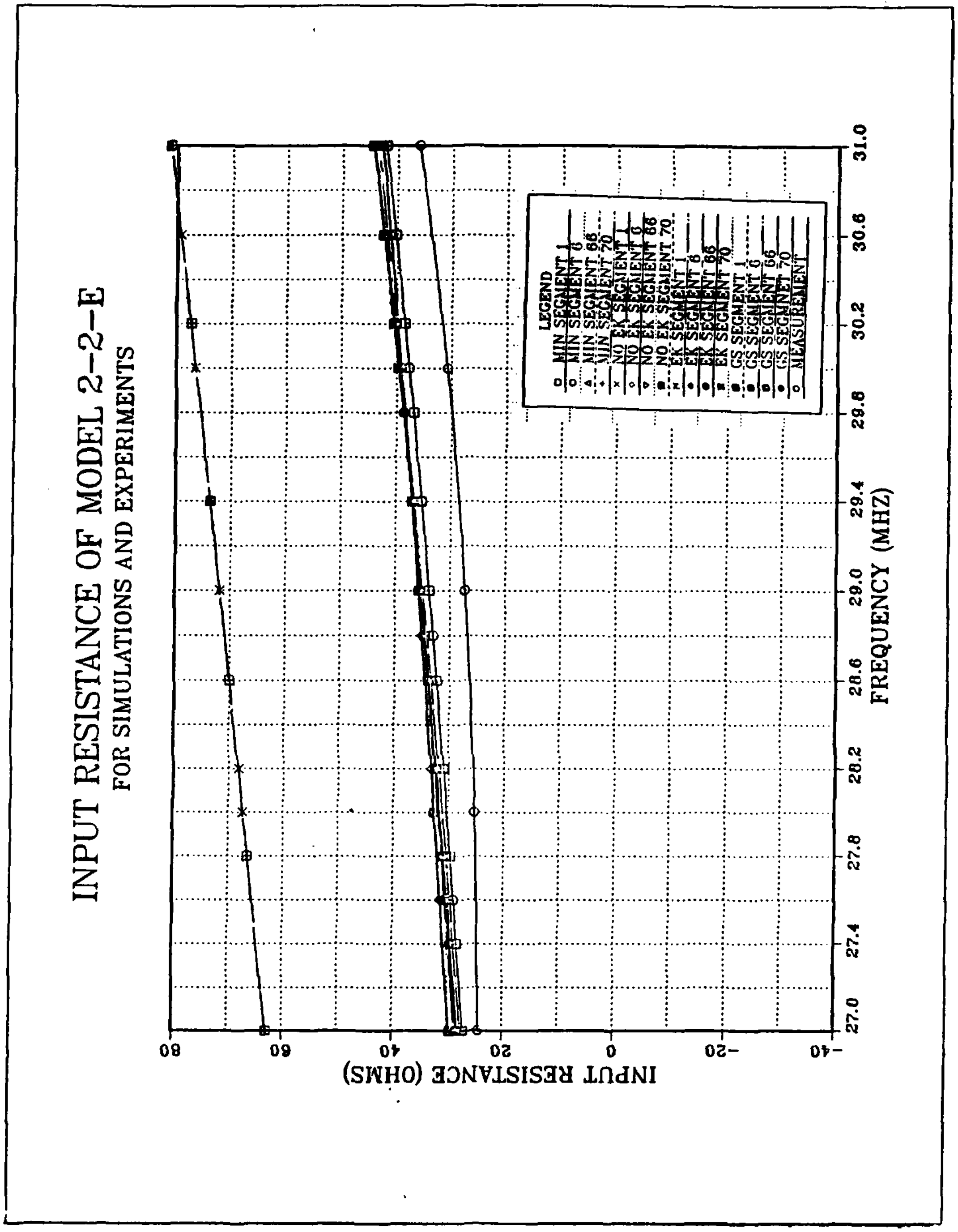

Figure 35. Model 2-2-E Input Resistance vs. Frequency (27-31 MHz) for all Computer Simulations and the Experiment

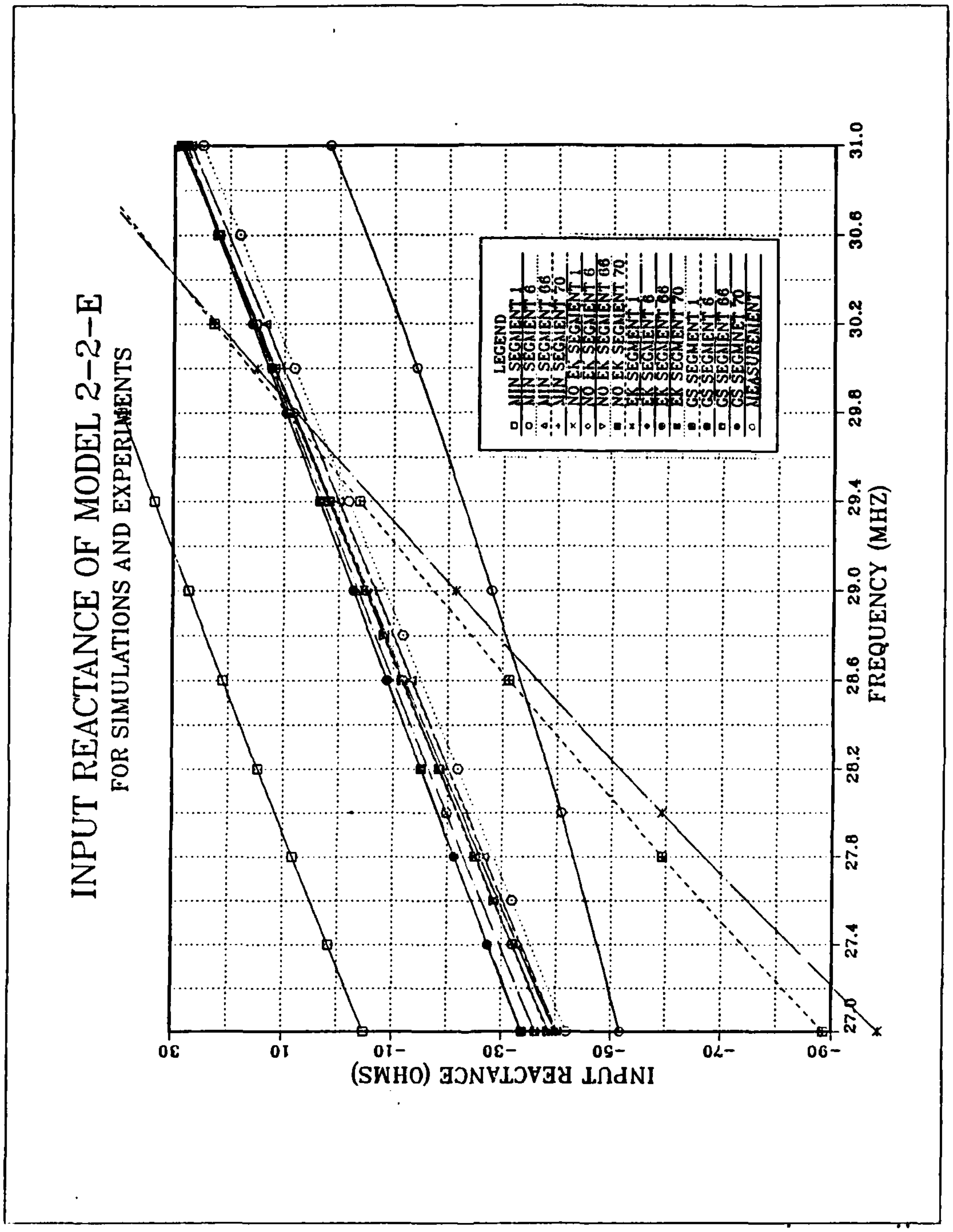

Figure 36. Model 2-2-E Input Reactance vs. Frequency (27-31 MHz) for all Computer Simulations and the Experiment

C. MODEL 3 RESULTS

1. Model 3-1 results.

Model 3-1 has 3 different radii with a step change of 4/3 between adjacent sections which is a smaller step than that of Model 2-1 and 2-2. Figure 37 shows the input resistance for computer code results. They are in good agreement with those of the experiment except for NECGS with an end cap. Figure 38 shows the input reactance for MININEC and the experiment. Both results are in good agreement. Figures 39 and 40 show that the results for NEC (without the EK and with the EK card) are not in good agreement with the results of the experiment. Figure 41 shows the results of NECGS which are in good agreement with the results of the experiment.

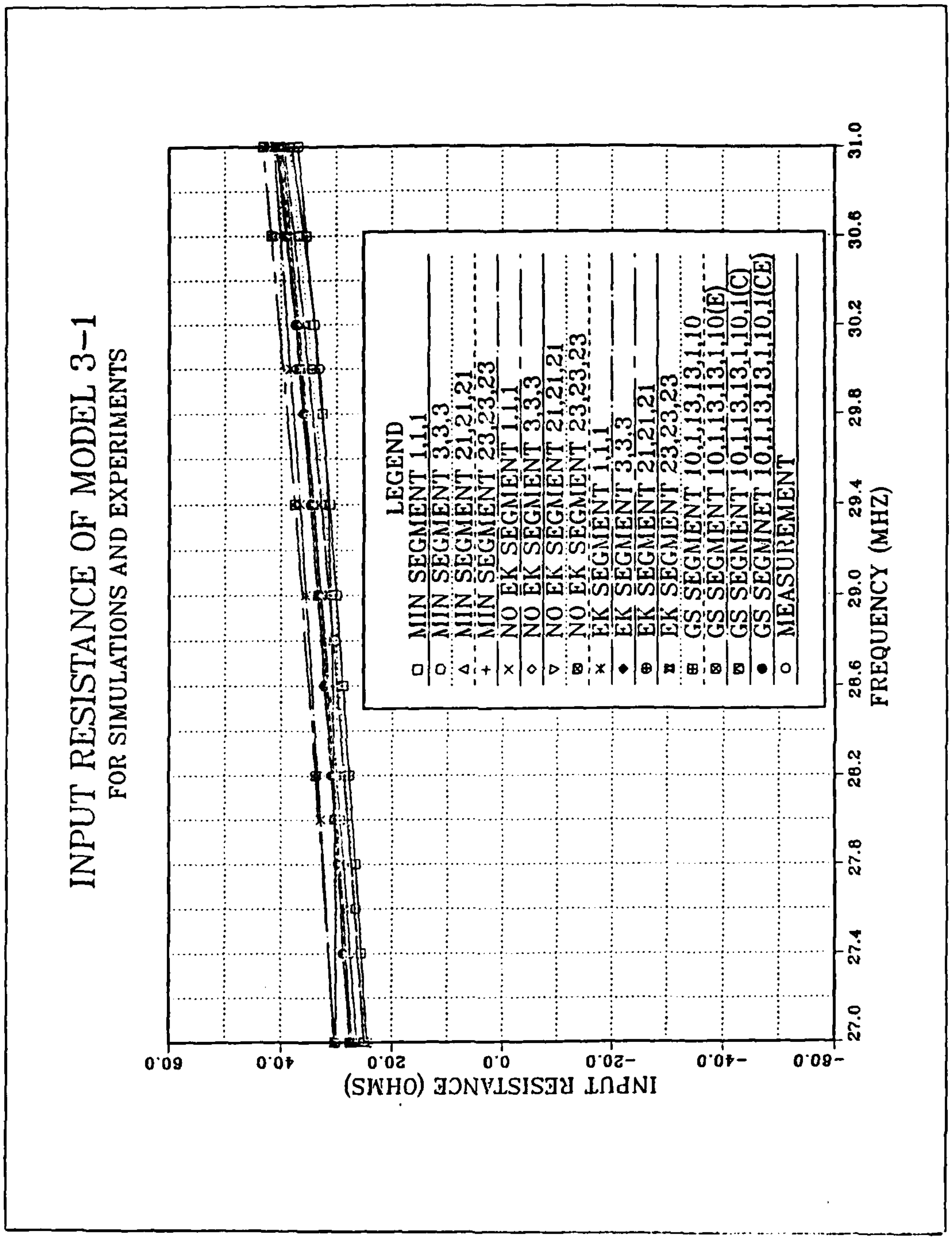

Figure 37. Model 3-1 Input Resistance vs. Frequency (27-31 MHz) for all Computer Simulations and the Experiment

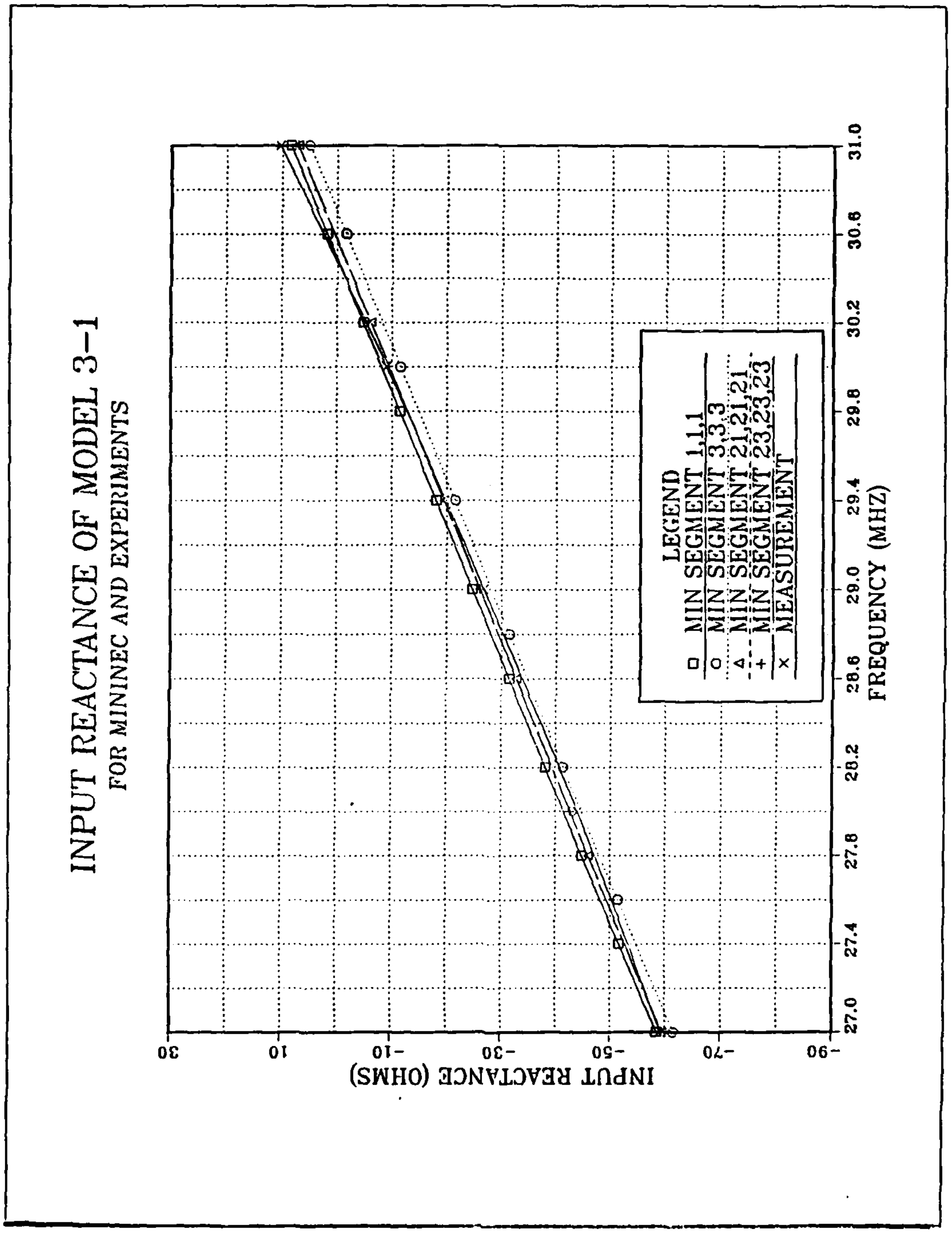

Figure 38. Model 3-1 Input Reactance vs. Frequency (27-31 MHz) for MININEC and the Experiment

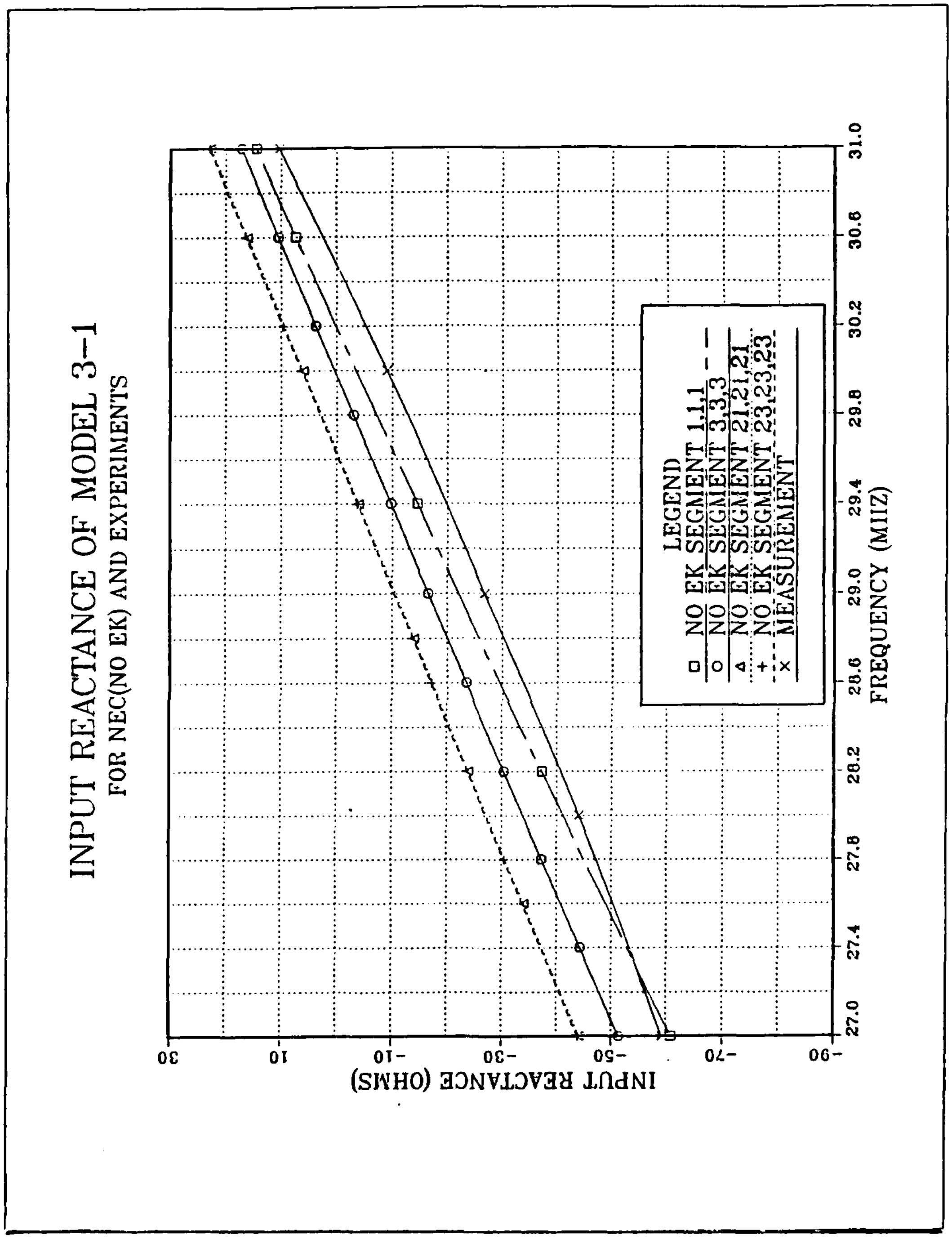

Figure 39. Model 3-1 Input Reactance vs. Frequency (27-31 MHz) for NEC (no EK card) and the Experiment

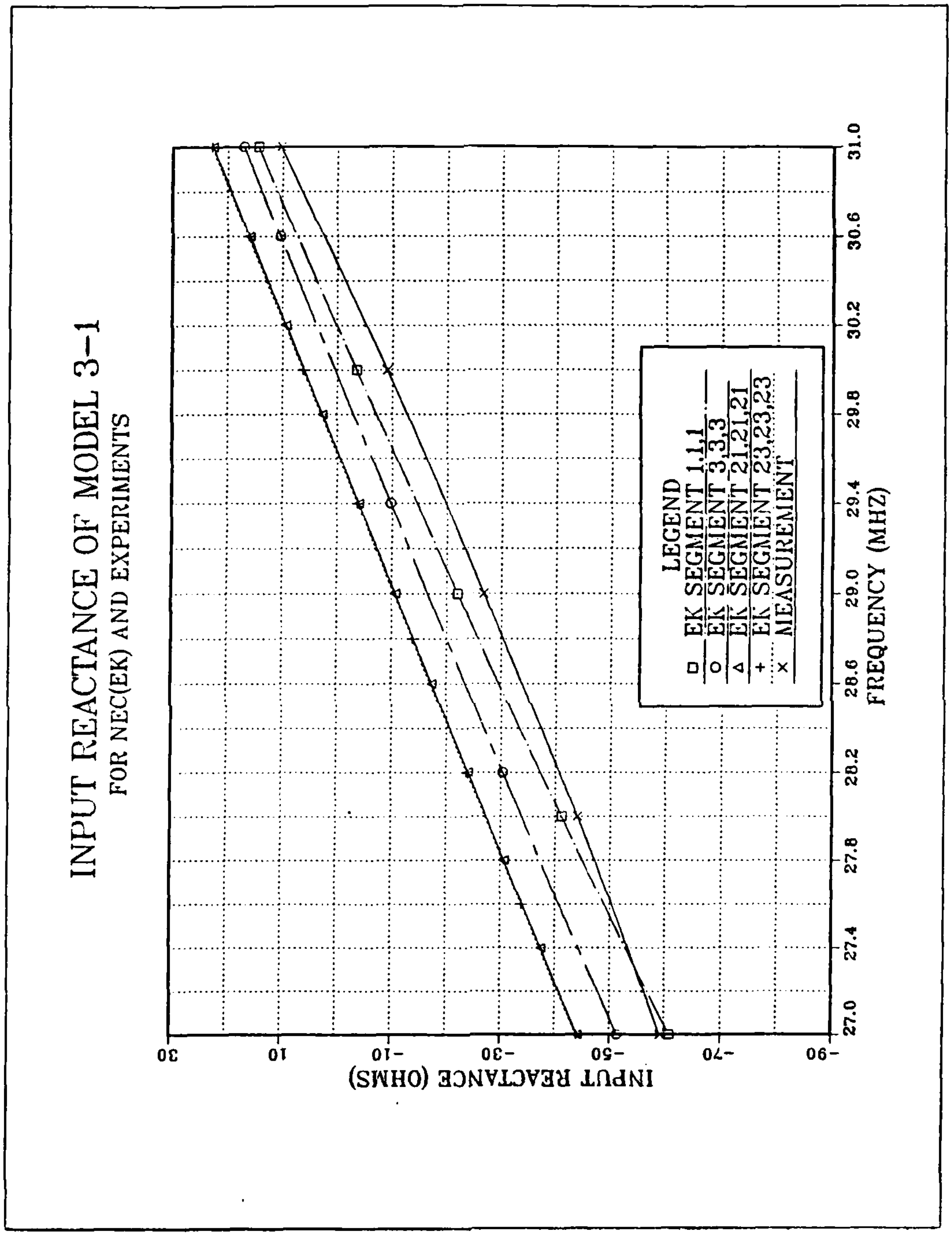

Figure 40. Model 3-1 Input Reactance vs. Frequency (27-31 MHz) for NEC (EK card) and the Experiment

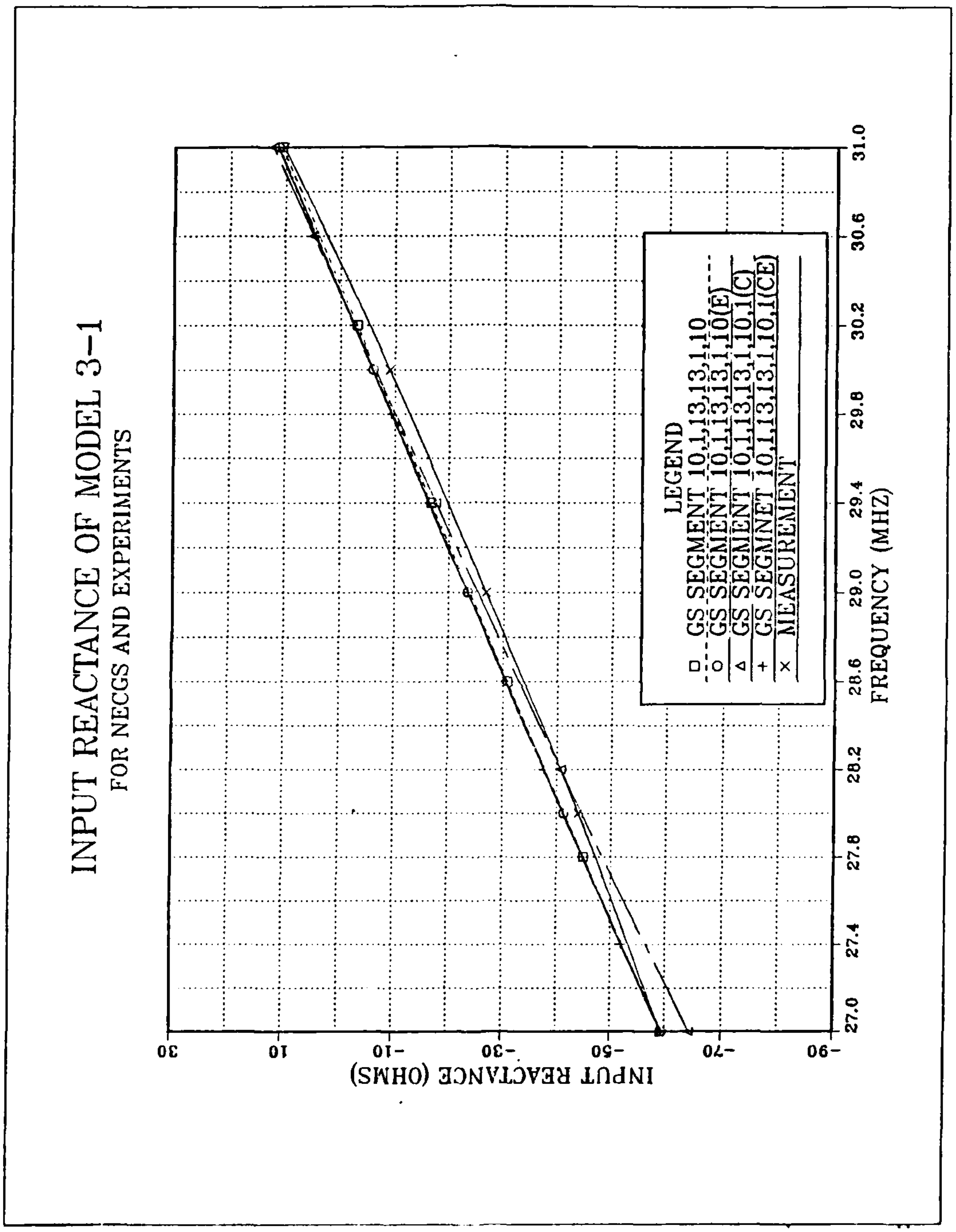

Figure 41. Model 3-1 Input Reactance vs. Frequency (27-31 MHz) for NECGS and the Experiment

2. Model 3-2 results

Model 3-2 has 3 different radii with a maximum step ratio of 15/14 between adjacent sections which is a smaller step than that of Model 3-1. The step difference between adjacent radii is 1/16 inch. Figure 42 shows good agreement between the resistance of computer code results and those of the experiment. Figure 43 shows that input reactance for MININEC is in good agreement with the results of the experiment. Figure 44 shows that the input reactance values for NEC (without EK card) deviate some 15 ohms from the measured input reactance. Figure 45 shows that the input reactance values for NEC (with EK card) deviate some 14 ohms from the measured reactance. Figure 46 shows that the input reactance values for NECGS agree better than both of the NEC results.

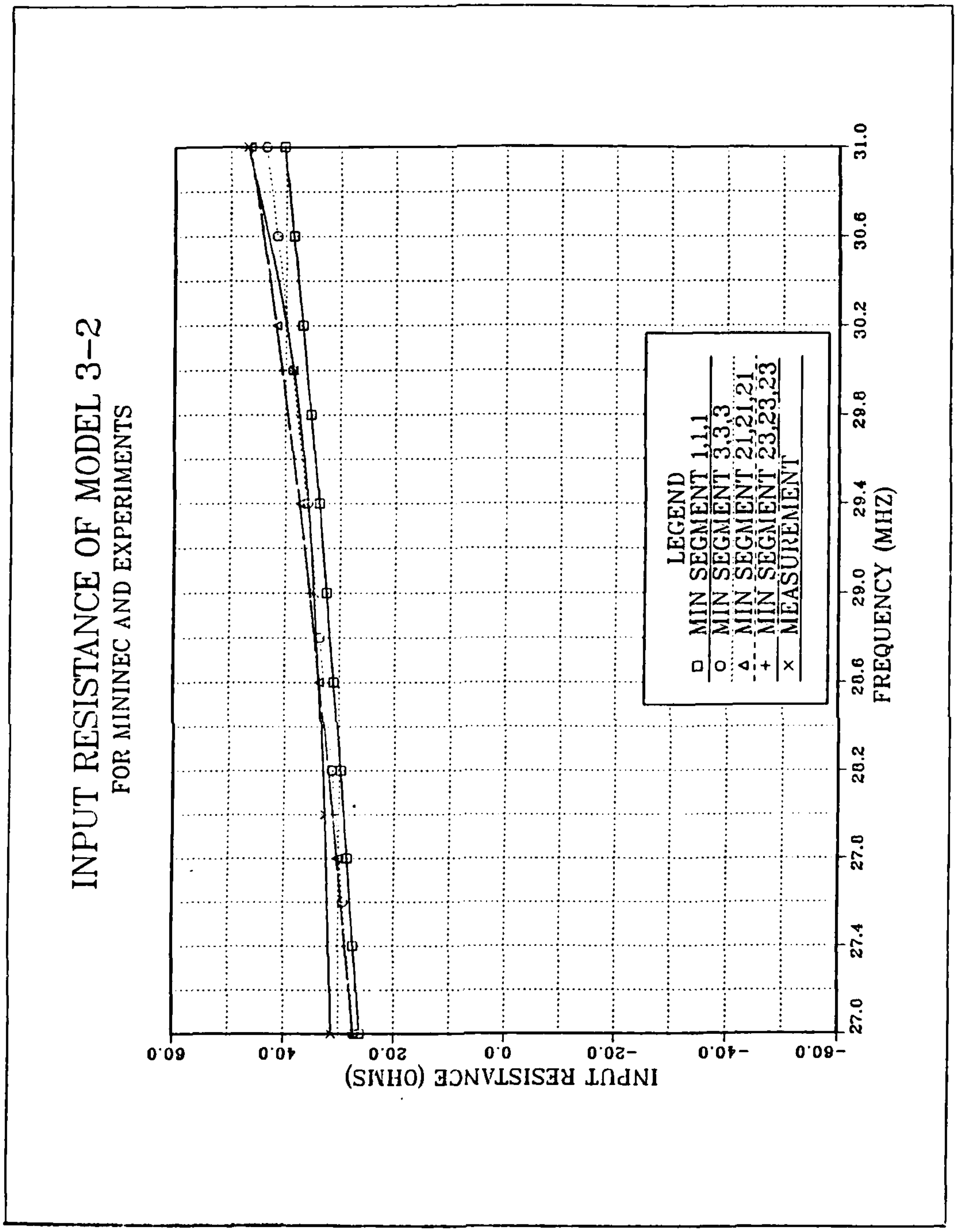

Figure 42. Model 3-2 Input Resistance vs. Frequency (27-31 MHz) for all Computer Simulations and the Experiment

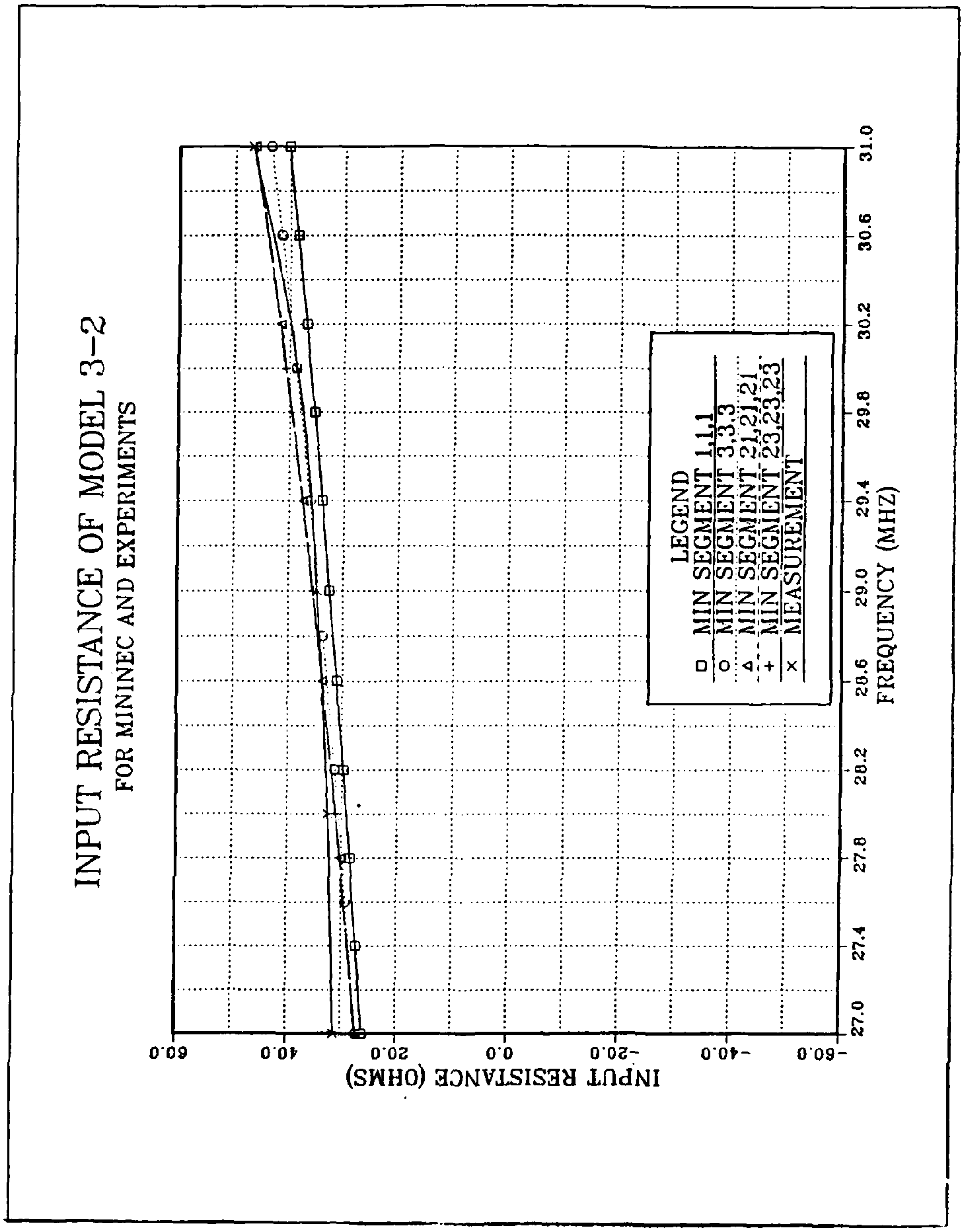

Figure 43. Model 3-2 Input Reactance vs. Frequency (27-31 MHz) for MININEC and the Experiment

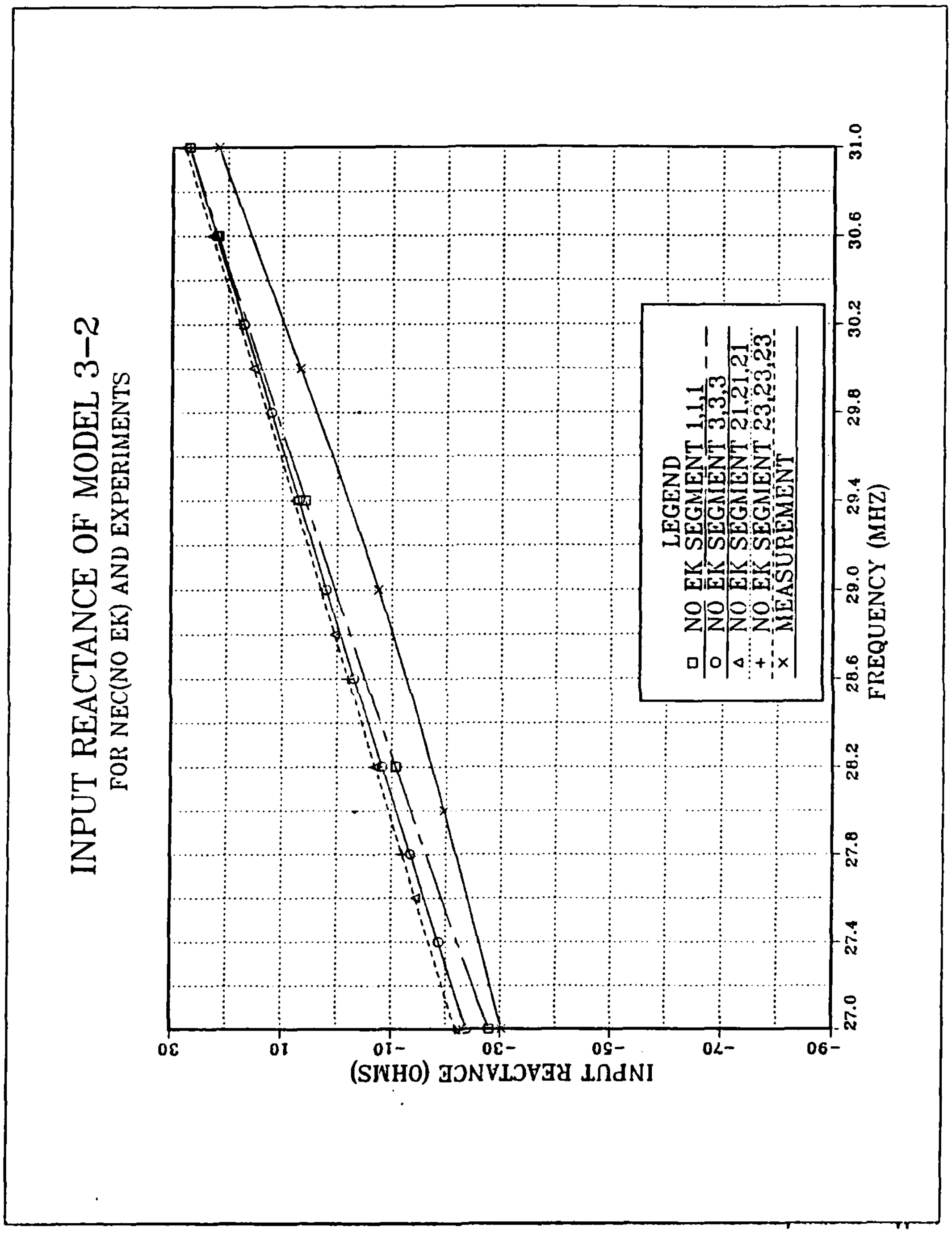

Figure 44. Model 3-2 Input Reactance vs. Frequency (27-31 MHz) for NEC (no EK card) and the Experiment

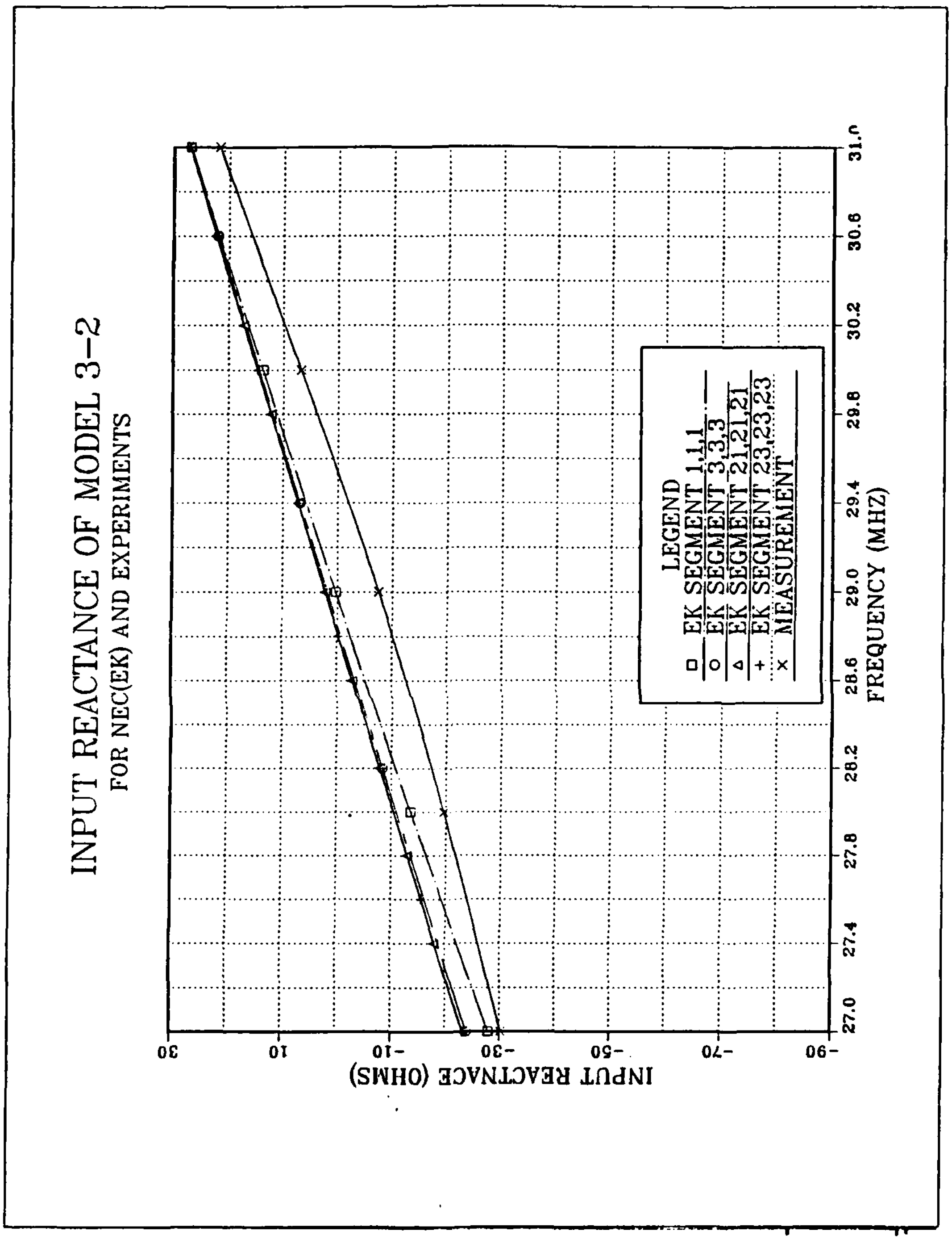

Figure 45. Model 3-2 Input Reactance vs. Frequency (27-31 MHz) for NEC (EK card) and the Experiment

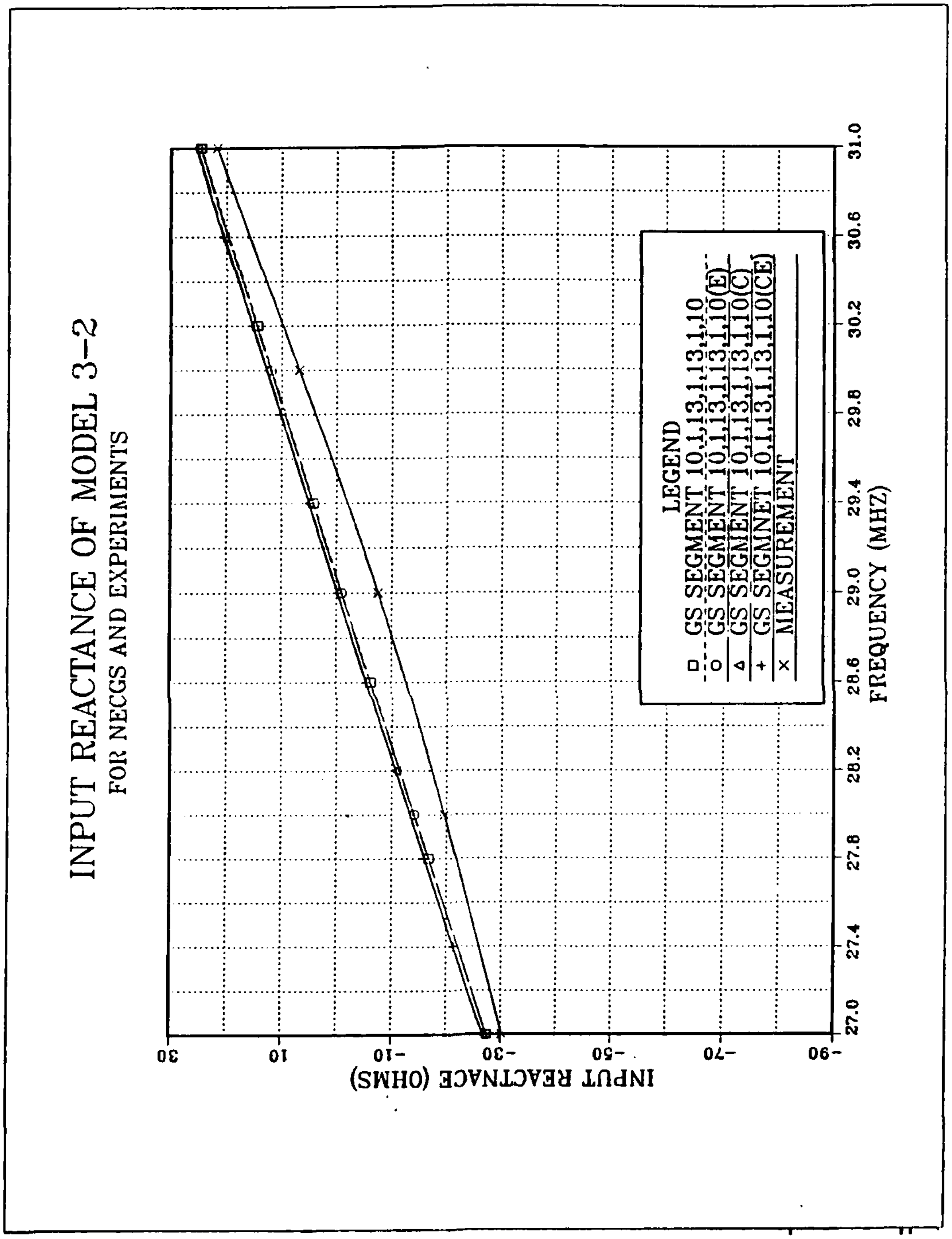

Figure 46. Model 3-2 Input Reactance vs. Frequency (27-31 MHz) for NECGS and the Experiment

3. Model 3-1-E results

Model 3-1-E is an equivalent average constant radius version of Model 3-1. Figure 47 shows that the input resistance values for the computer results are reasonably good compared to the experimental results except for NECGS with an end cap. Figure 48 shows that the input reactance values for the computer results do not agree well with the experimental results.

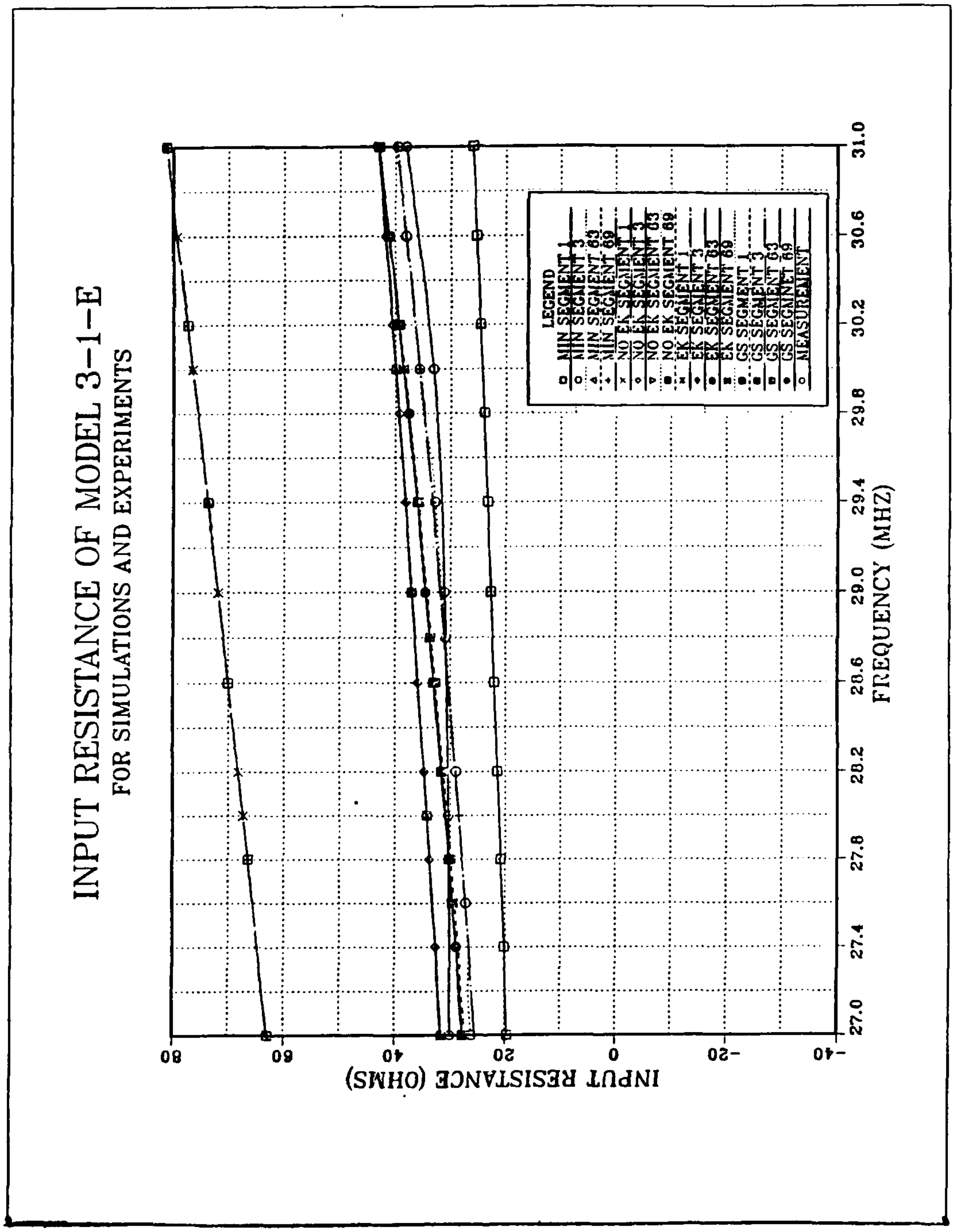

Figure 47. Model 3-1-E Input Resistance vs. Frequency (27-31 MHz) for all Computer Simulations and the Experiment

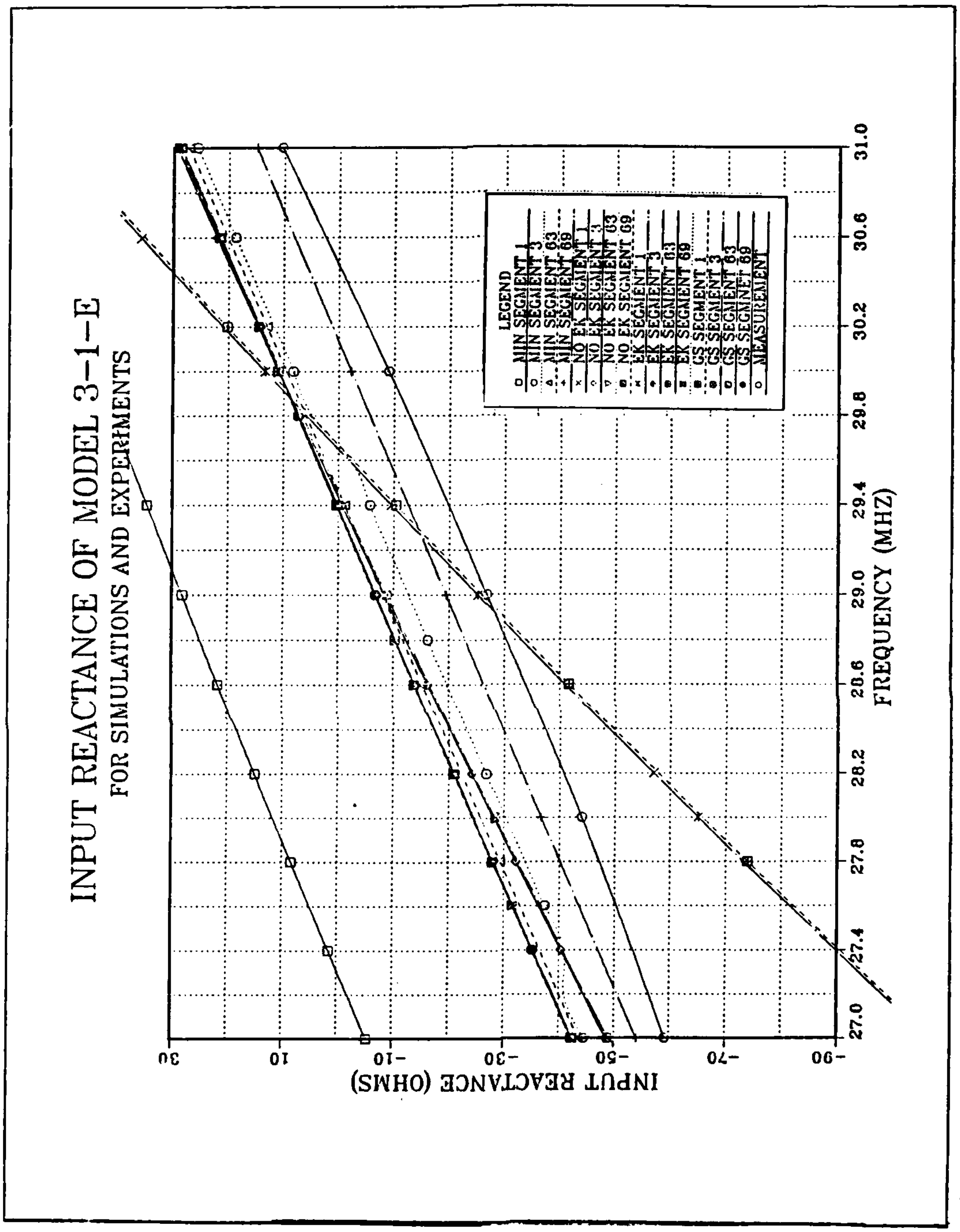

Figure 48. **Model 3-1-E Input Reactance vs. Frequency (27-31 MHz) for all Computer Simulations and the Experiment**

4. Model 3-2-E results

Model 3-2-E is the equivalent average constant radius version of Model 3-2. Figure 49 shows the input resistance values for the computer results do not agree as well as case of Model 3-1-E. Figure 50 shows similar results for the reactance comparisons.

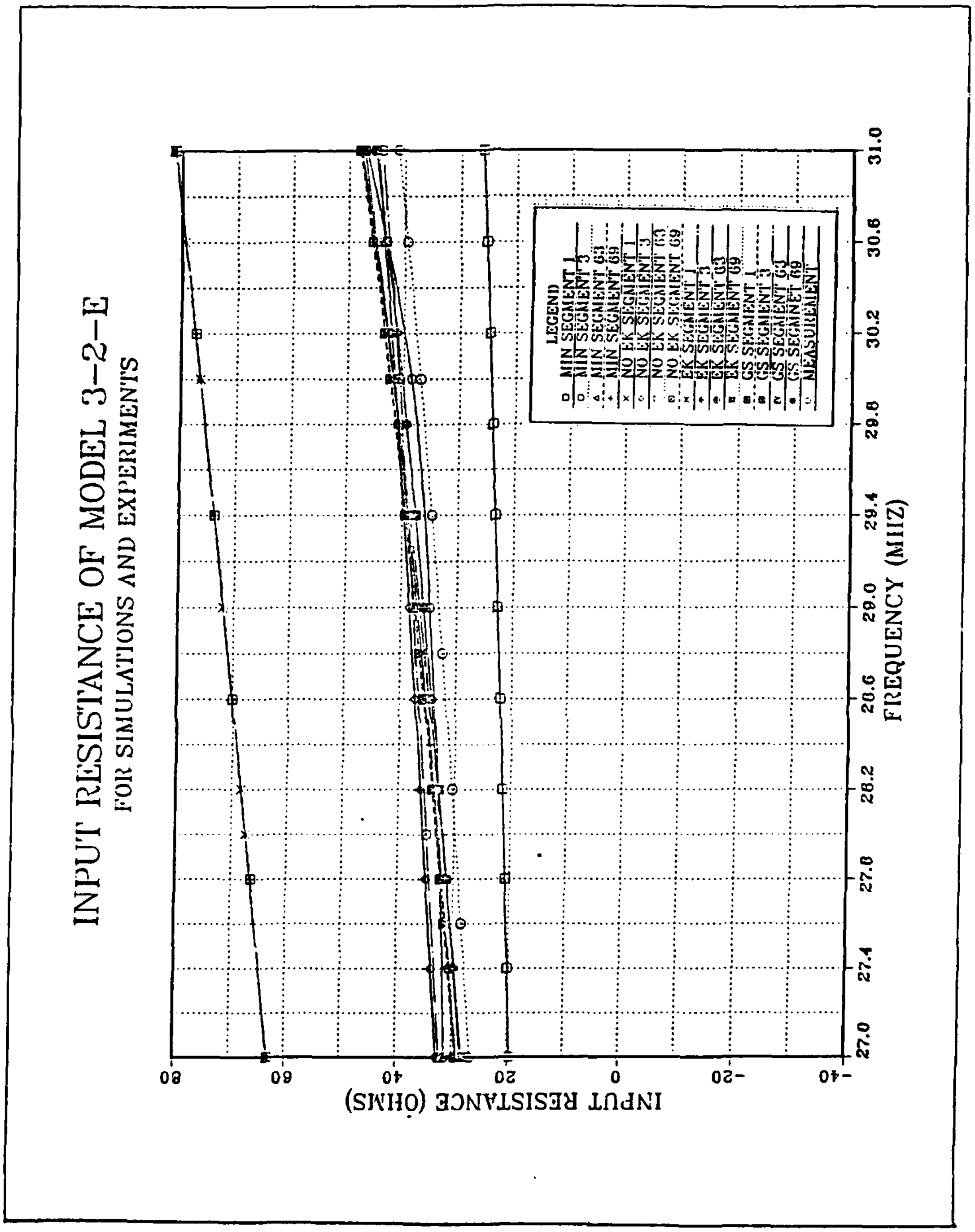

Figure 49. Model 3-2-E Input Resistance vs. Frequency (27-31 MHz) for all Computer Simulations and the Experiment

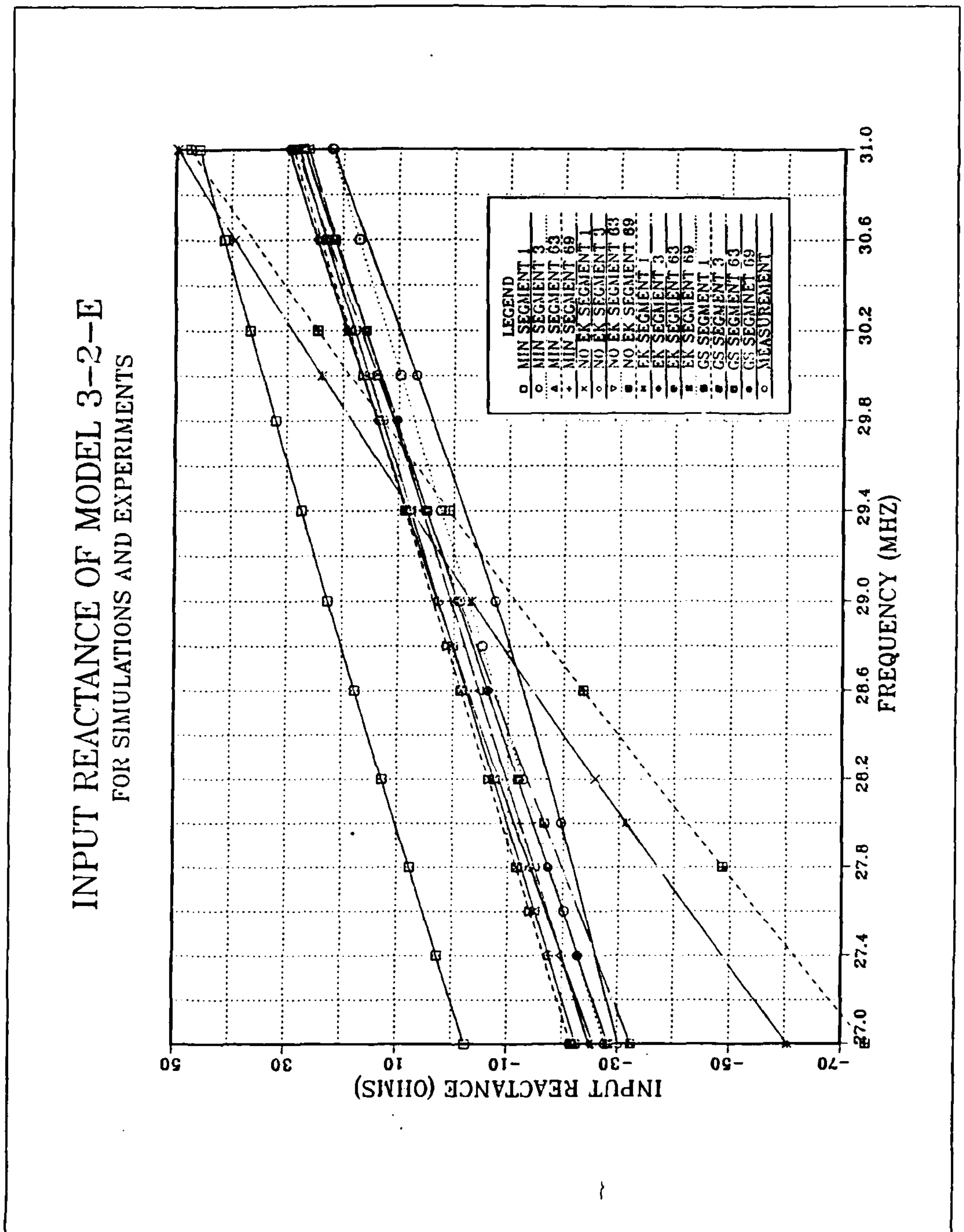

Figure 50. Model 3-2-E Input Reactance vs. Frequency (27-31 MHz) for all Computer Simulations and the Experiment

D. MODEL 4 RESULTS

1. Model 4-1 results

Model 4-1 has 5 different radii with a maximum step ratio change of 3/2 between the adjacent sections. The step difference between adjacent radii is 1/16 inch. Figures 51, 53, 55, and 57 show good agreement between resistance values of the computer results and those of the experiment. Figure 52 shows good agreement between reactance values of the computer results (MININEC and NECGS) and those of the experiment. But Figures 52, 54 and 56 show bad agreement between reactance values of the computer results (MININEC and NECGS) and those of the experiment.

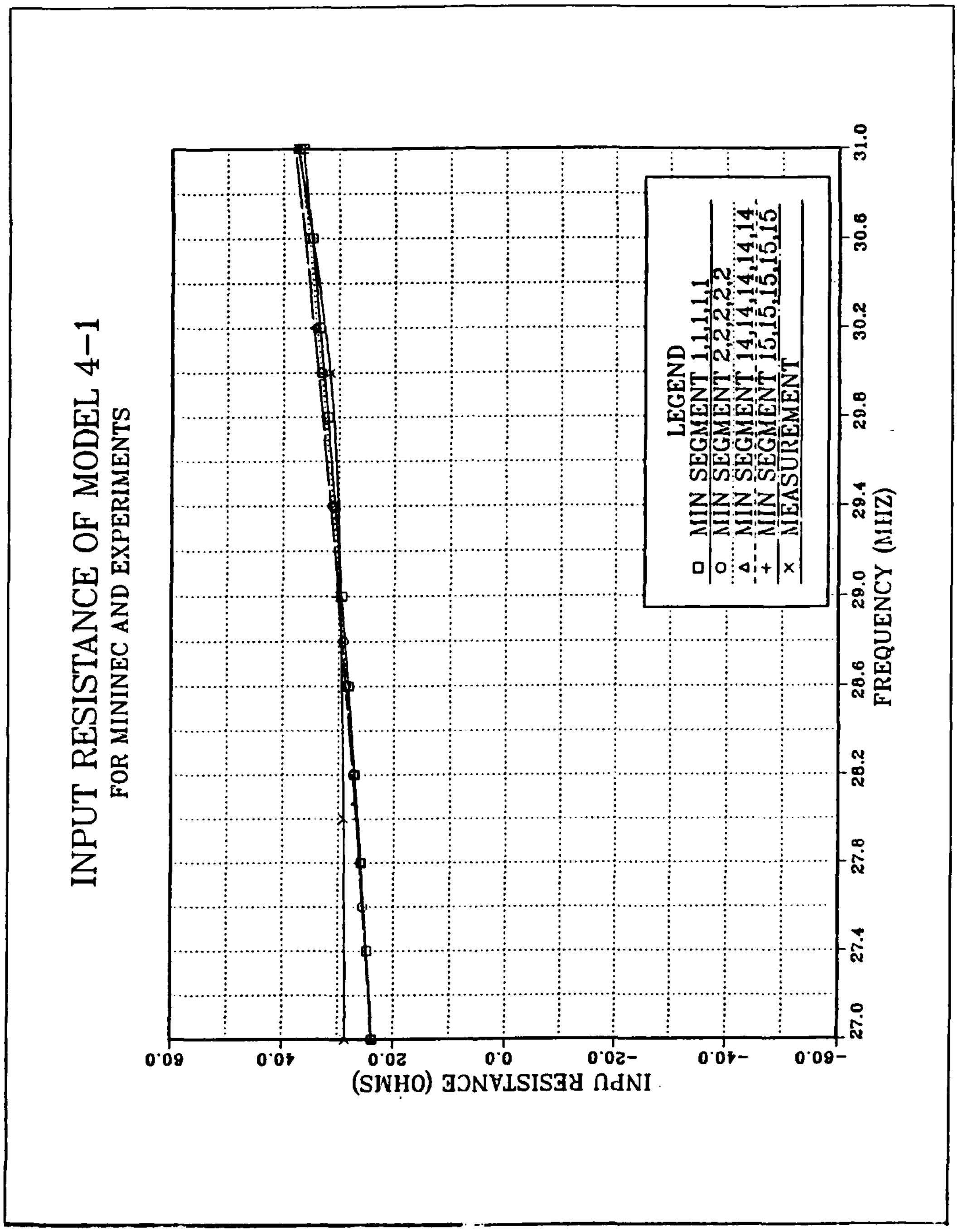

Figure 51. Model 4-1 Input Resistance vs. Frequency (27-31 MHz) for MININEC and the Experiment

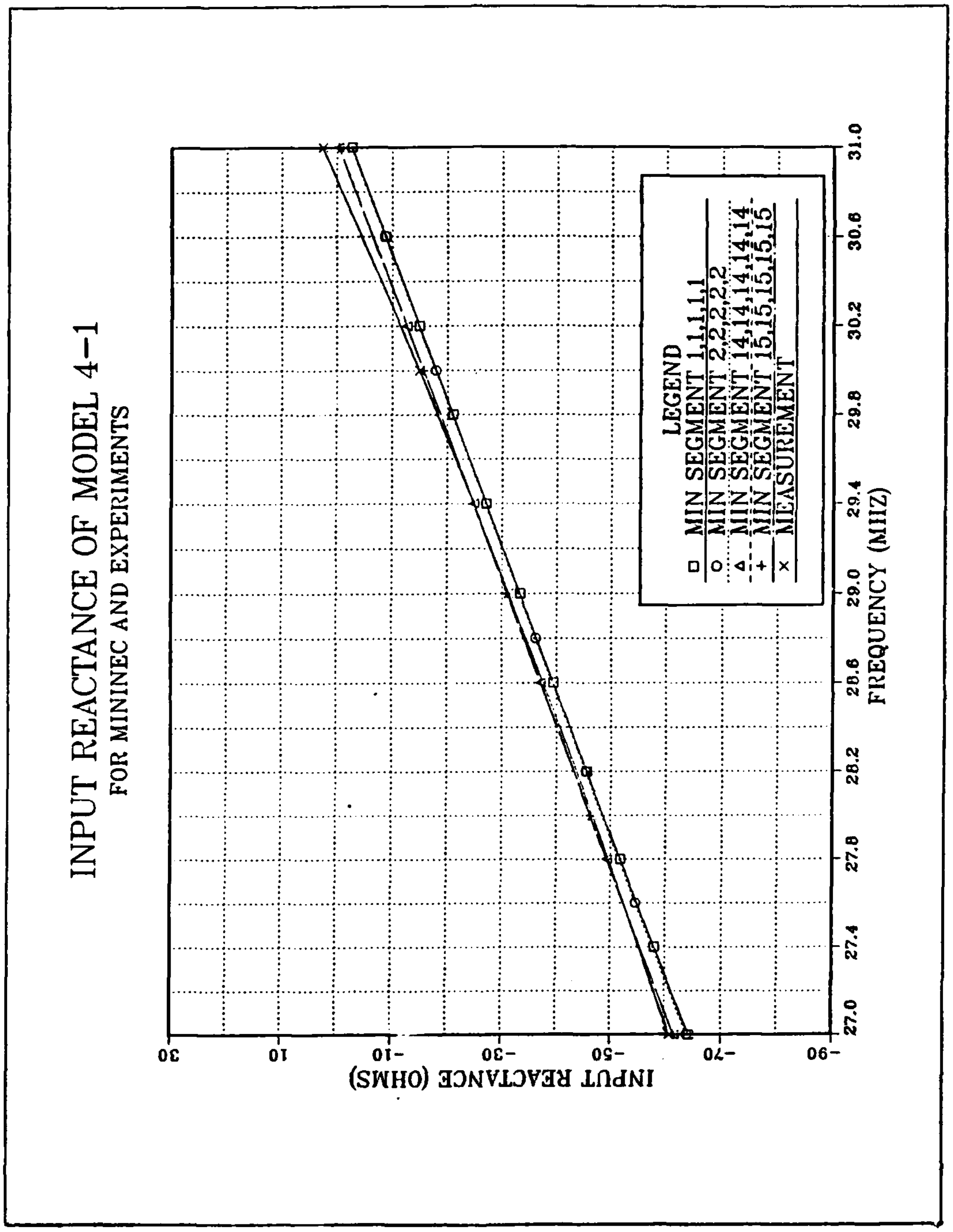

Figure 52. **Model 4-1 Input Reactance vs. Frequency (27-31 MHz) for MININEC and the Experiment**

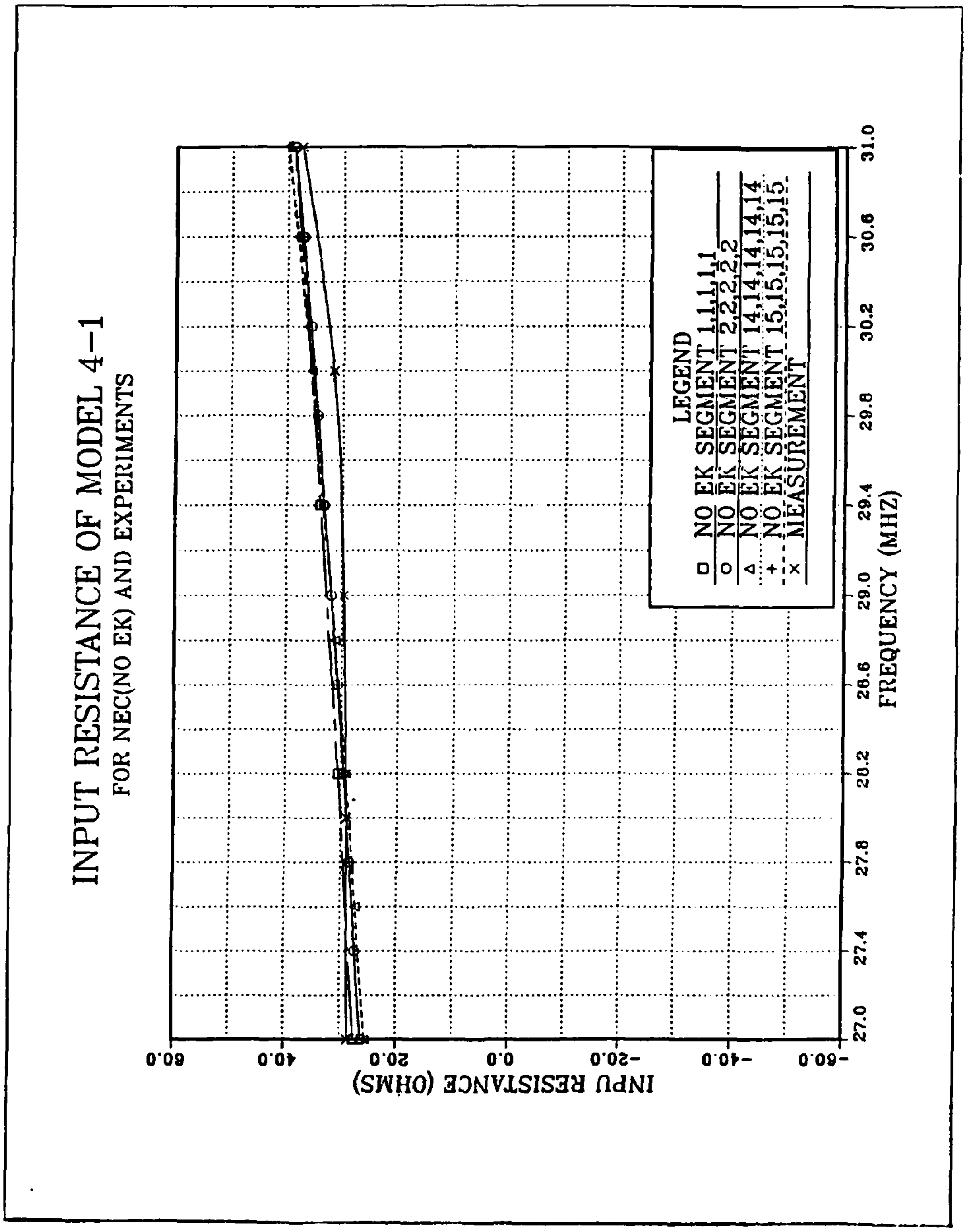

Figure 53. Model 4-1 Input Resistance vs. Frequency (27-31 MHz) for NEC (no EK card) and the Experiment

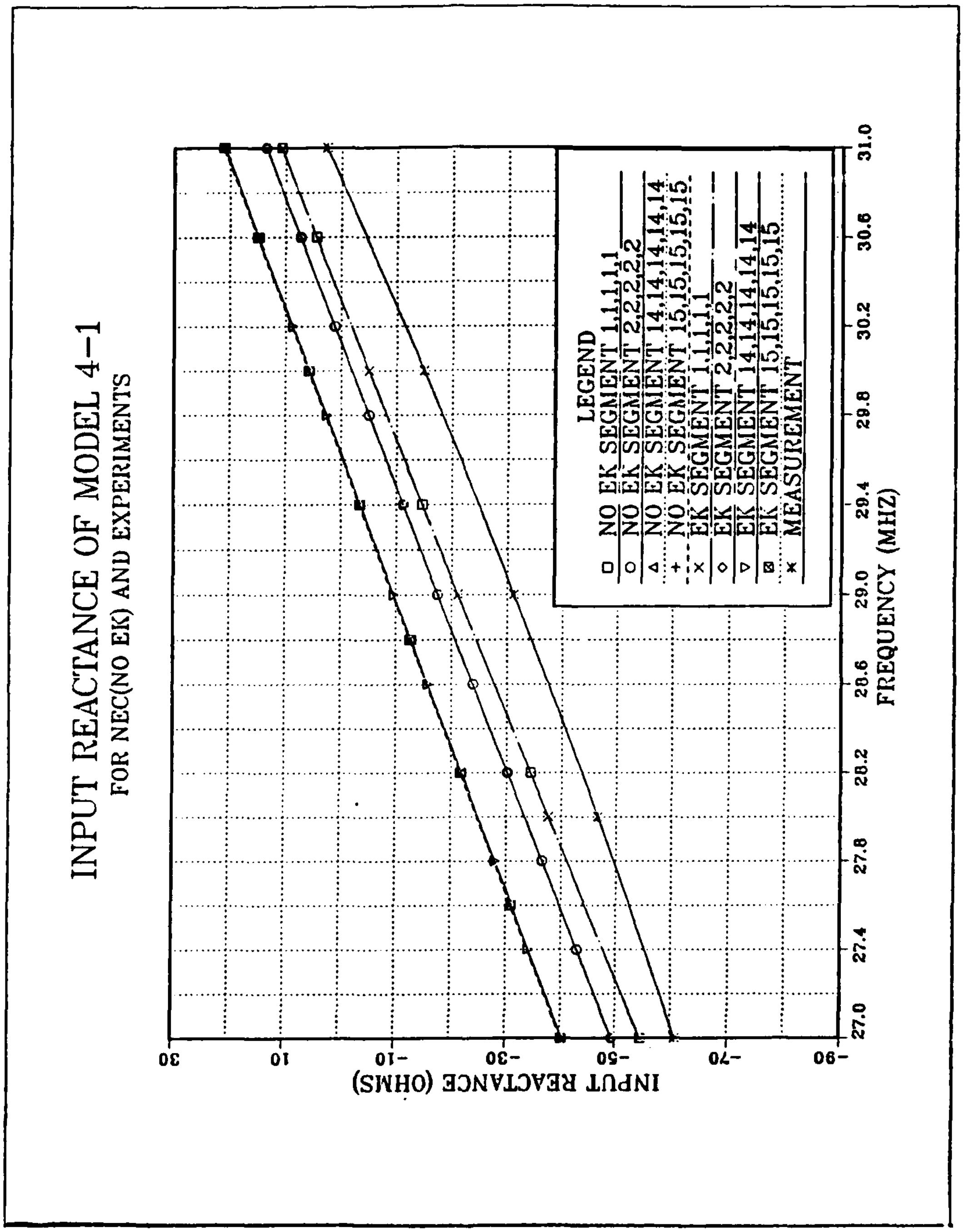

Figure 54. Model 4-1 Input Reactance vs. Frequency (27-31 MHz) for NEC (no EK card) and the Experiment

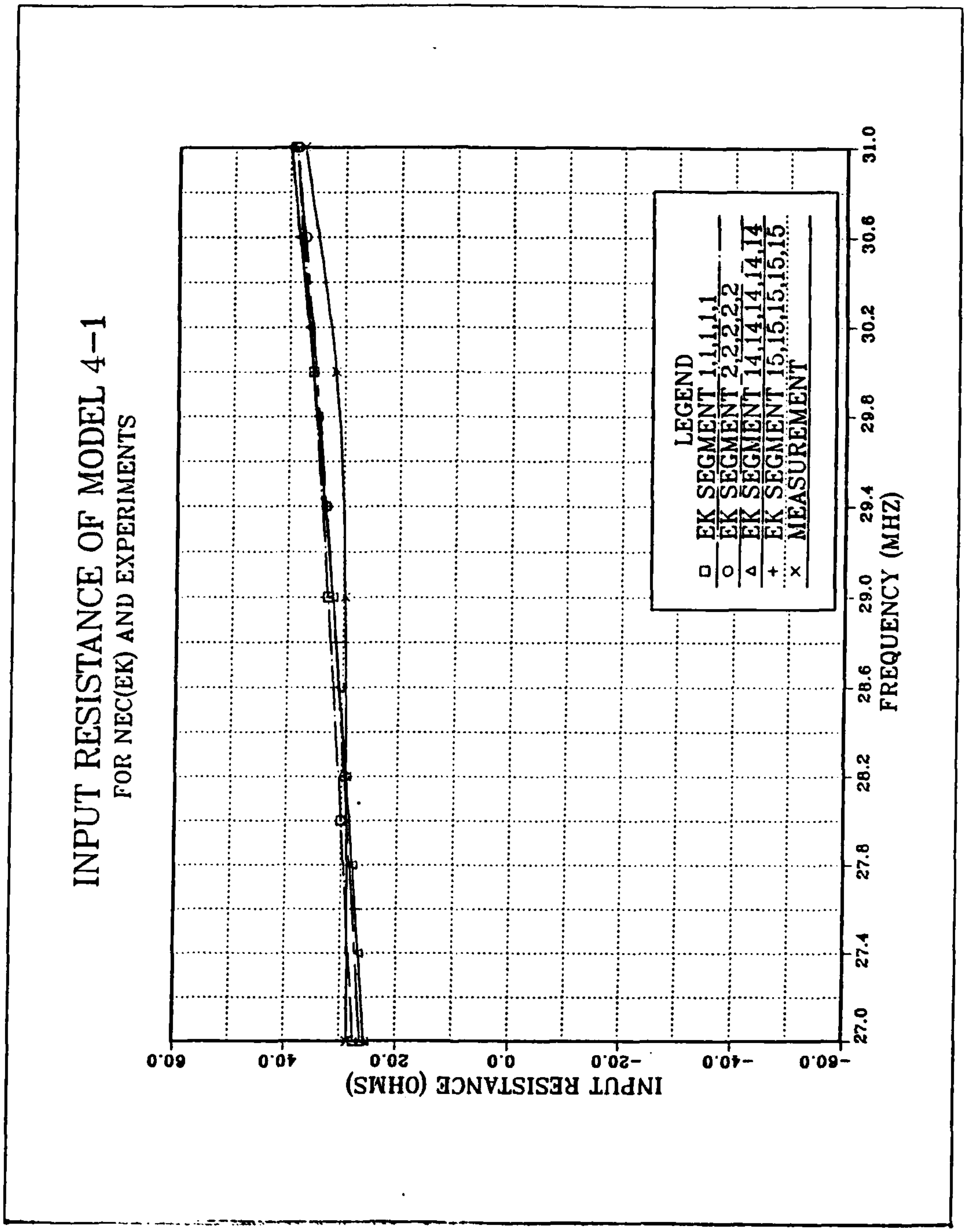

Figure 55. Model 4-1 Input Resistance vs. Frequency (27-31 MHz) for NEC (EK card) and the Experiment

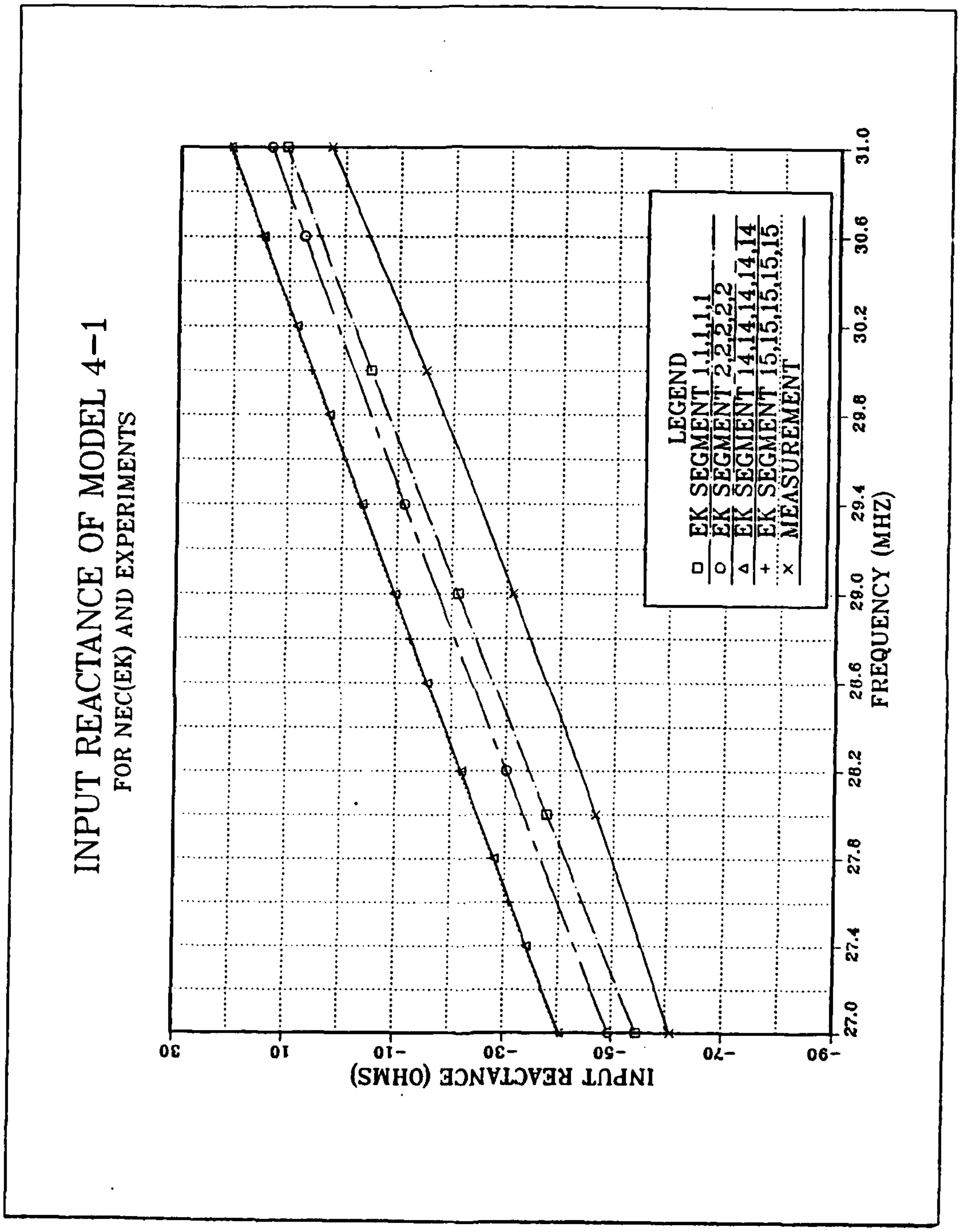

Figure 56. Model 4-1 Input Reactance vs. Frequency (27-31 MHz) for NEC (EK card) and the Experiment

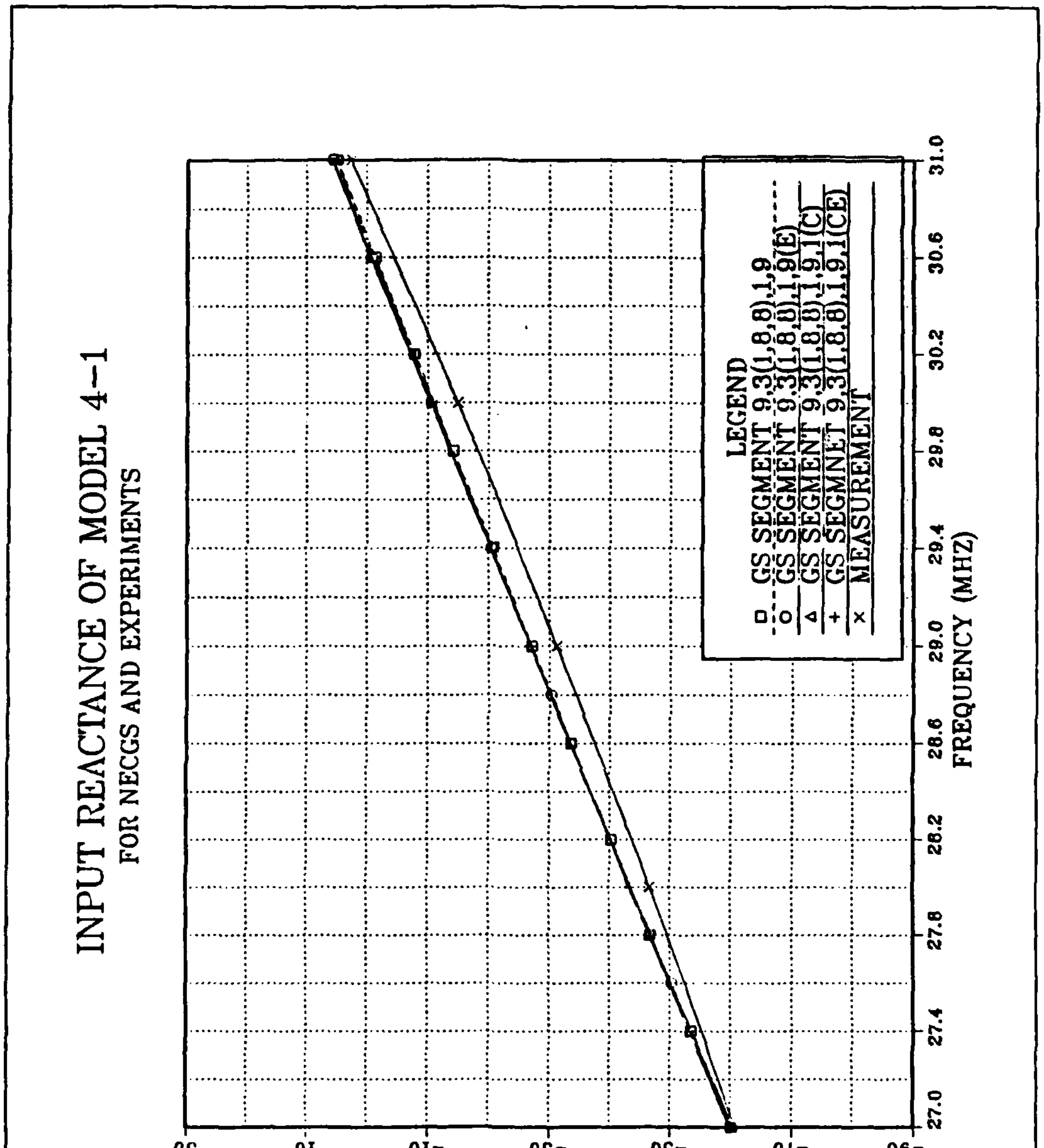

Figure 57. Model 4-1 Input Resistance vs. Frequency (27-31 MHz) for NECGS and the Experiment

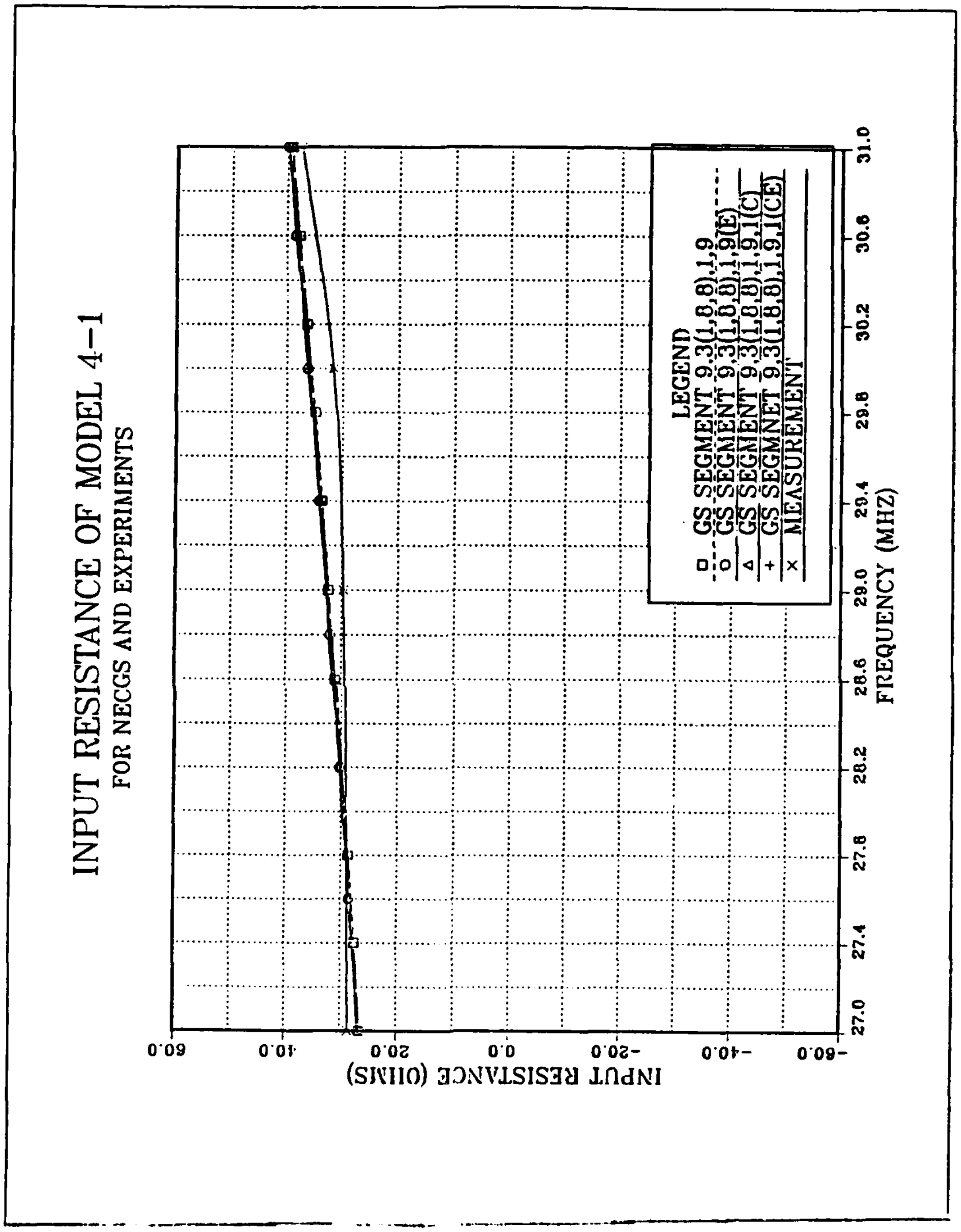

Figure 58. **Model 4-1 Input Reactance vs. Frequency (27-31 MHz) for NECGS and the Experiment**

2. Model 4-2 results

Model 4-2 has five different radii with a maximum step ratio of 13:12 between adjacent sections. The step difference between adjacent radii is also 1/16 inch. Figures 59, 61, 63, and 65 show that resistance values for all computer code results are in good agreement with those of the experiment. Figure 60 (MININEC) shows that input reactance results are in very good agreement with the experimental results. Figures 62 and 64 (NEC) show input reactance values deviate some 10 ohms from the experimental results. The results for NEC (with the EK card and without the EK card) are identical for this model. Figure 66 shows that reactance values for NECGS are close to the experimental results.

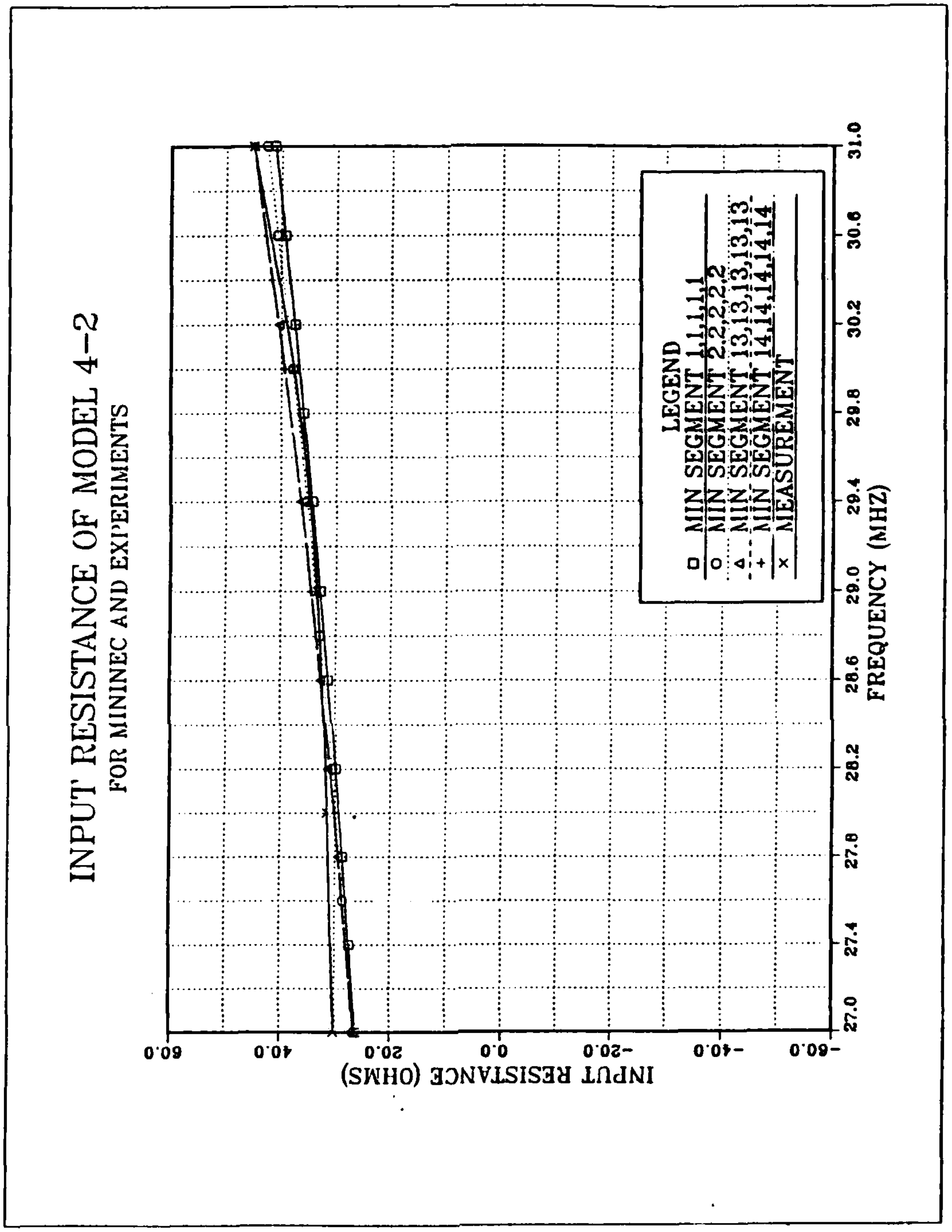

Figure 59. **Model 4-2 Input Resistance vs. Frequency (27-31 MHz) for MININEC and the Experiment**

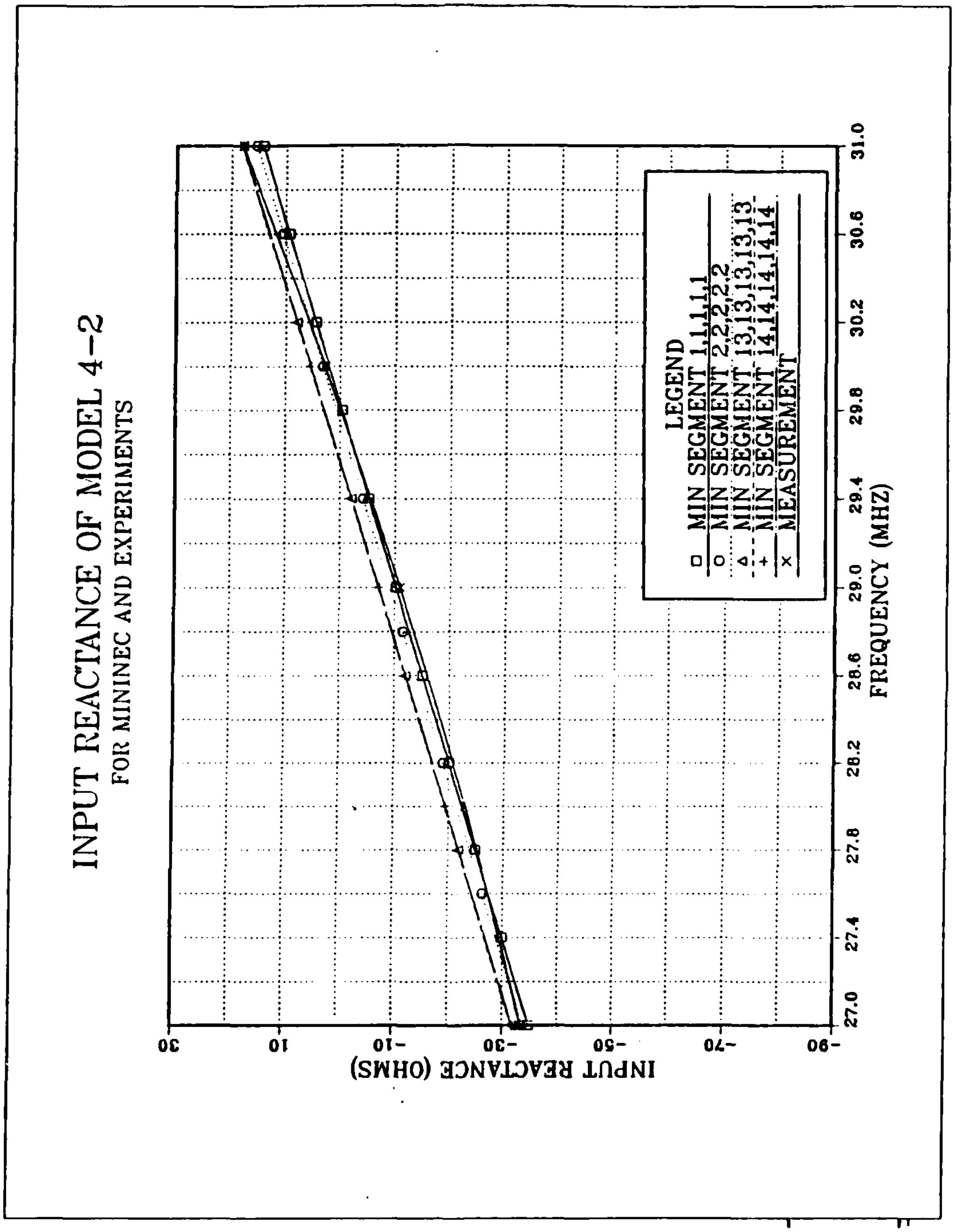

Figure 60. **Model 4-2 Input Reactance vs. Frequency (27-31 MHz) for MININEC and the Experiment**

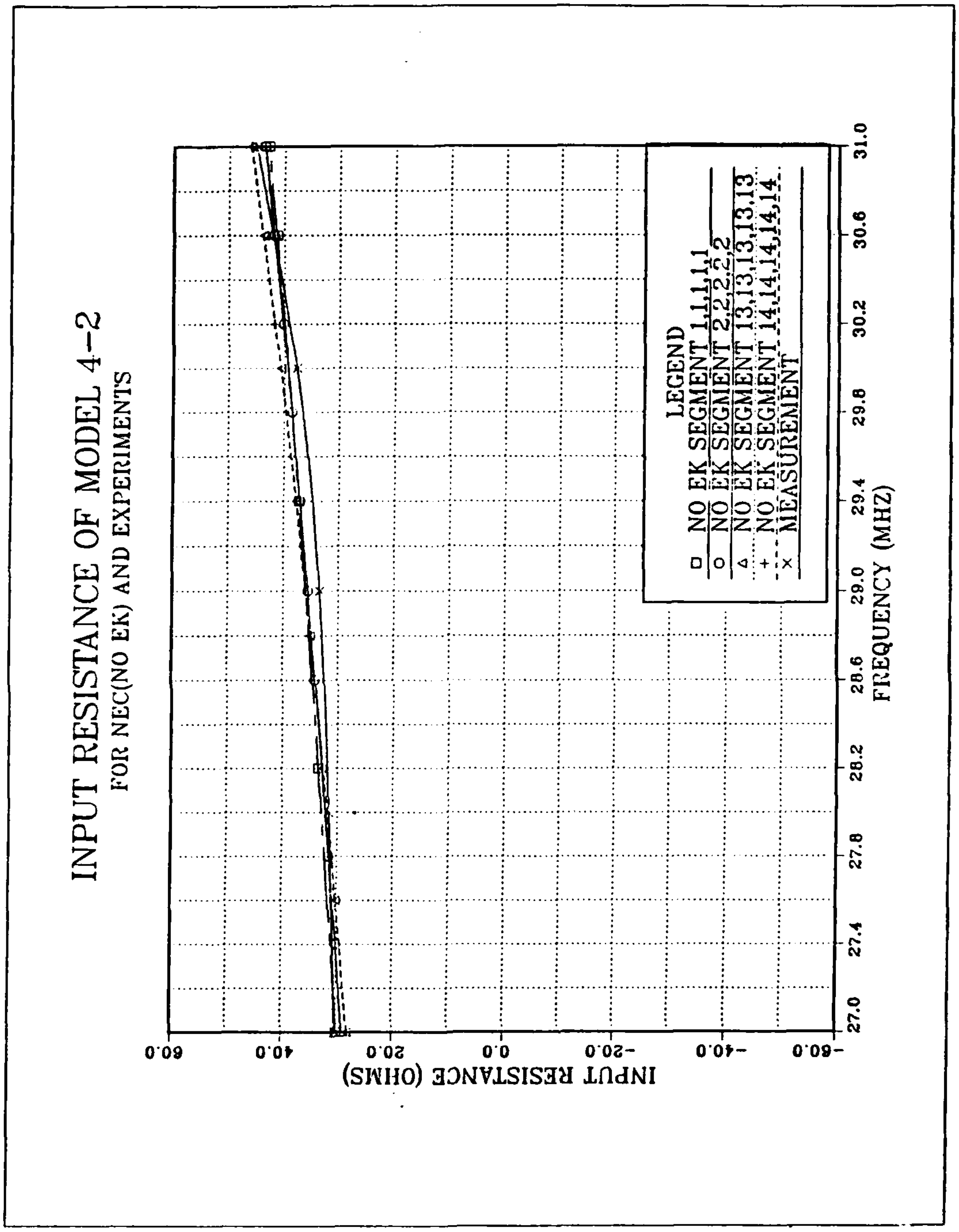

Figure 61. Model 4-2 Input Resistance vs. Frequency (27-31 MHz) for NEC (no EK card) and the Experiment

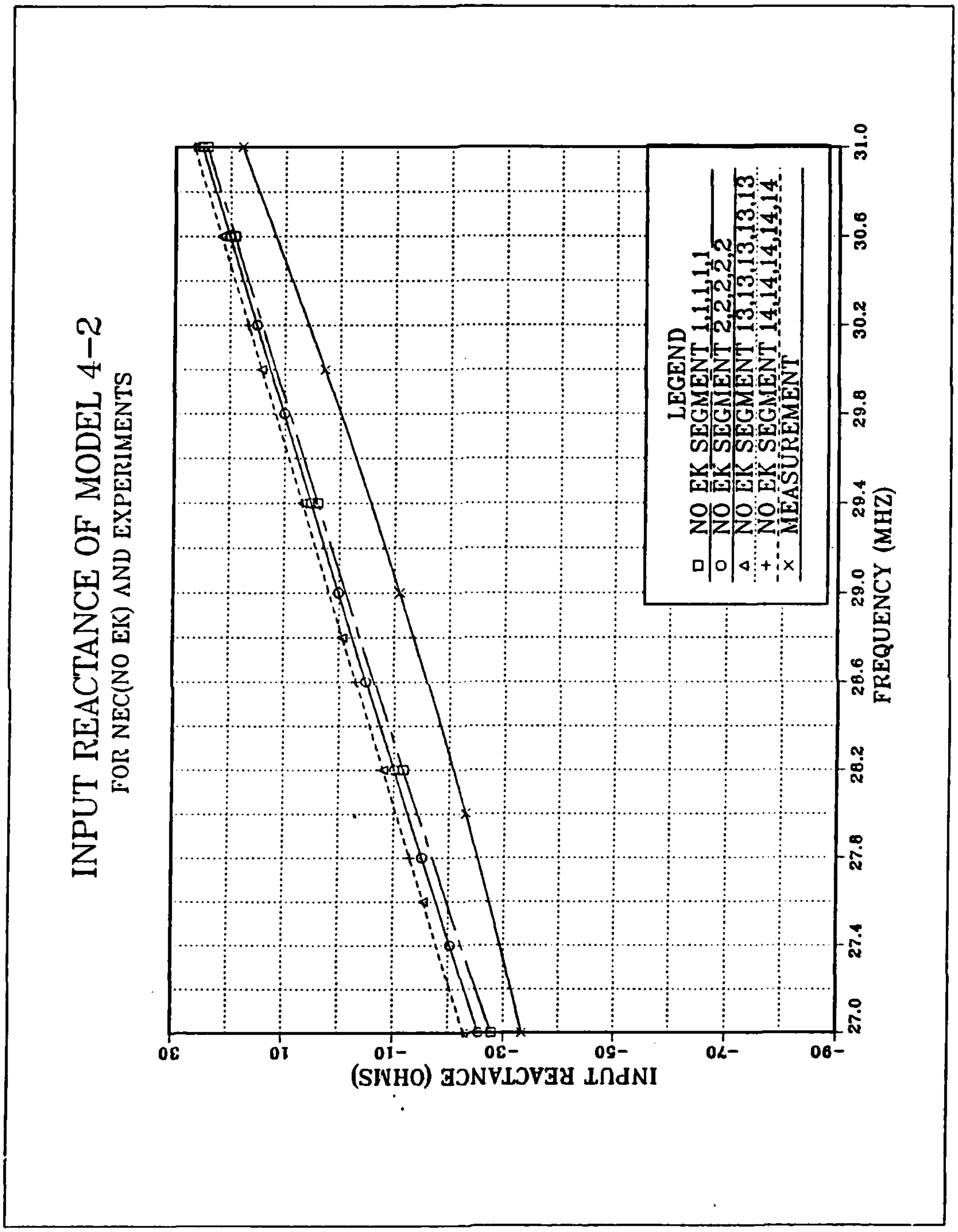

Figure 62. Model 4-2 Input Reactance vs. Frequency (27-31 MHz) for NEC (no EK card) and the Experiment

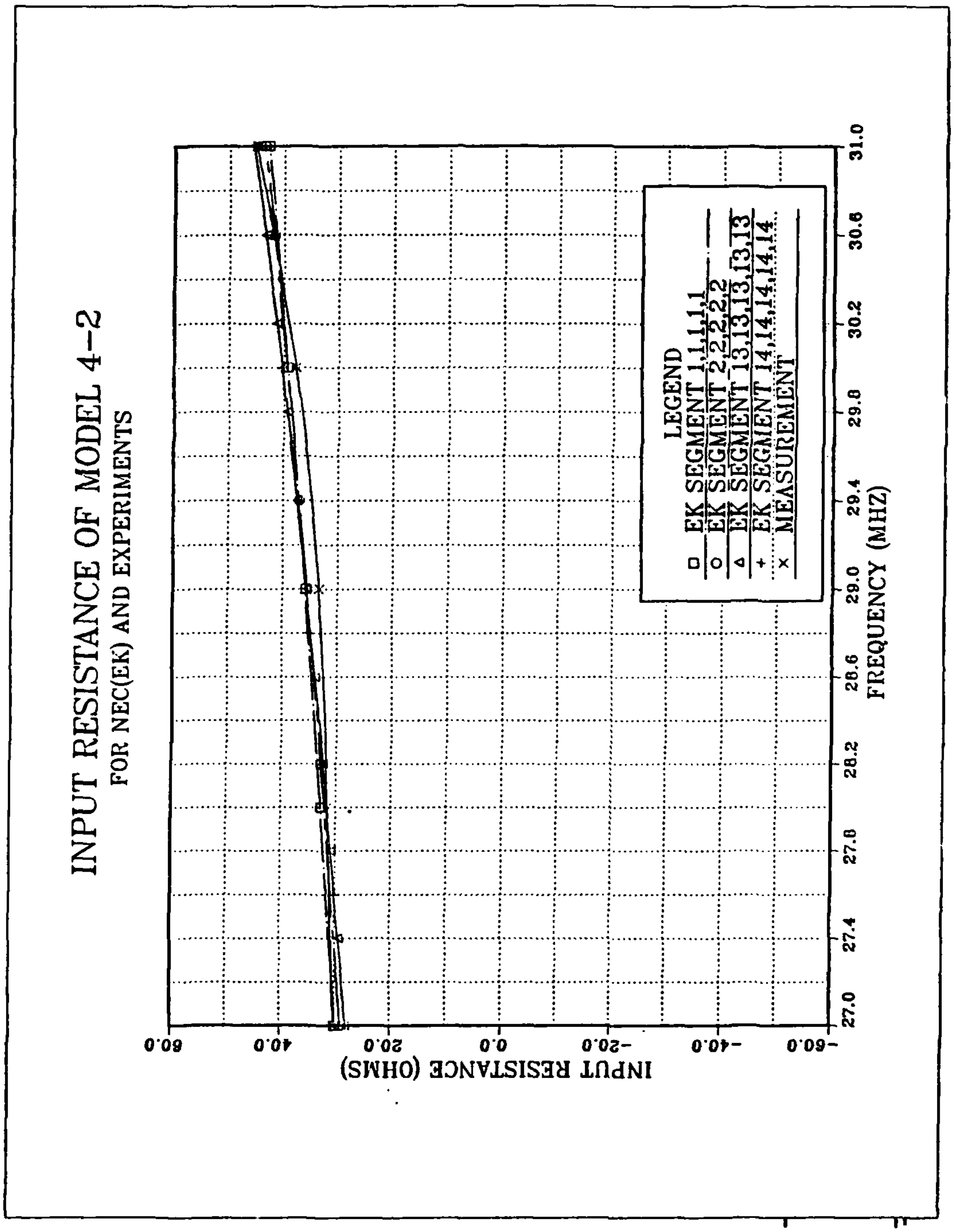

Figure 63. Model 4-2 Input Resistance vs. Frequency (27-31 MHz) for NEC (EK card) and the Experiment

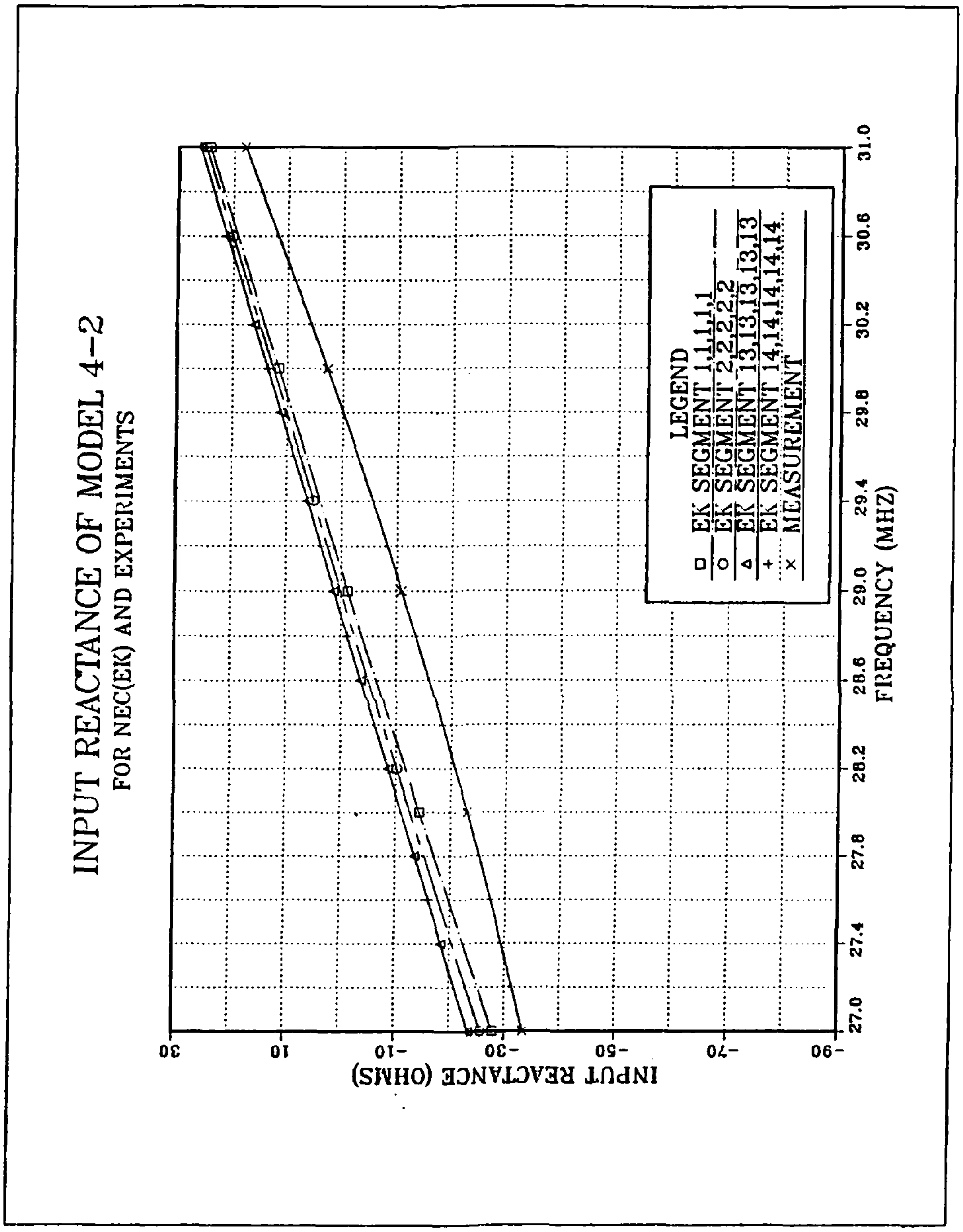

Figure 64. Model 4-2 Input Reactance vs. Frequency (27-31 MHz) for NEC (EK card) and the Experiment

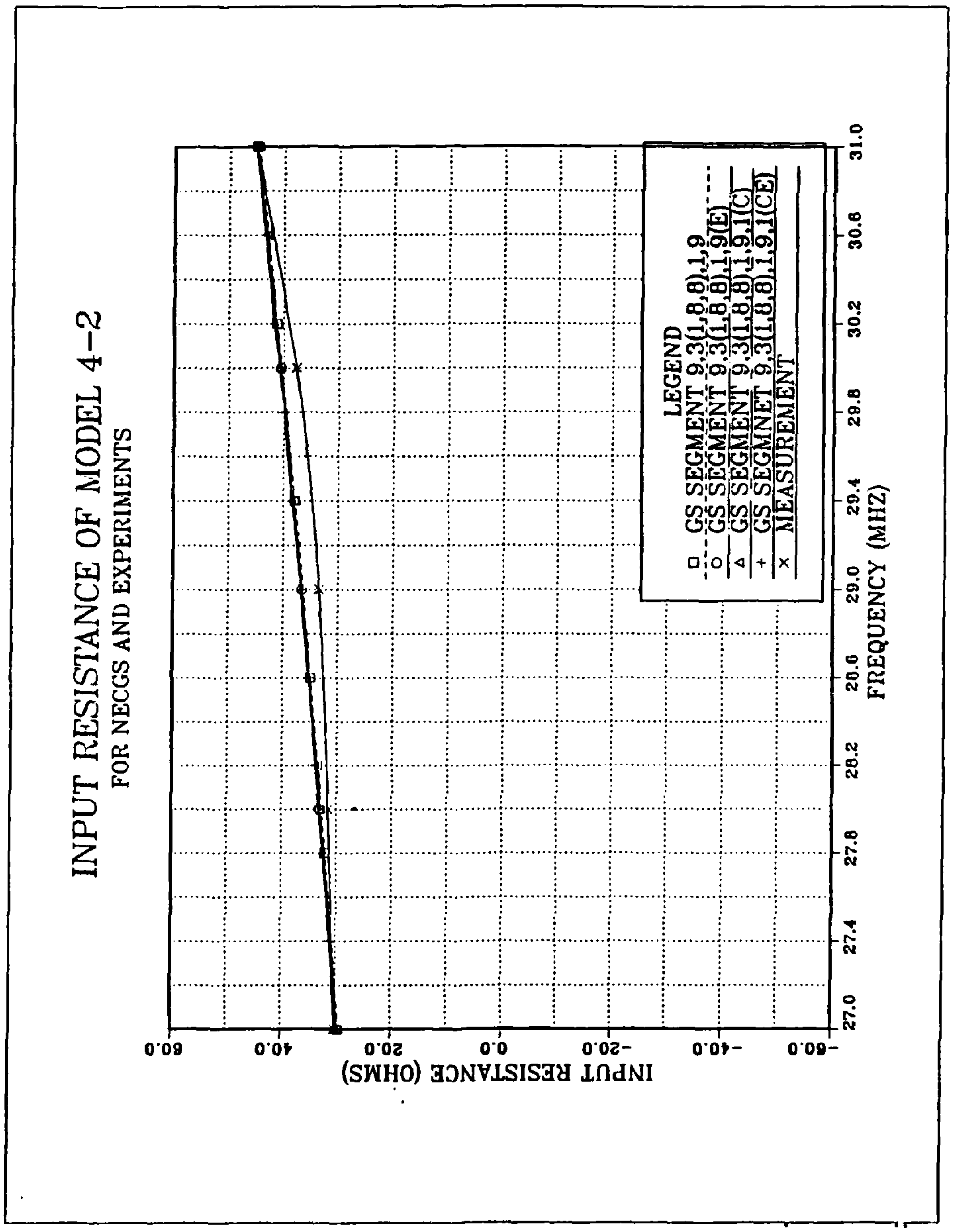

Figure 65. Model 4-2 Input Resistance vs. Frequency (27-31 MHz) for NECGS EK card and the Experiment

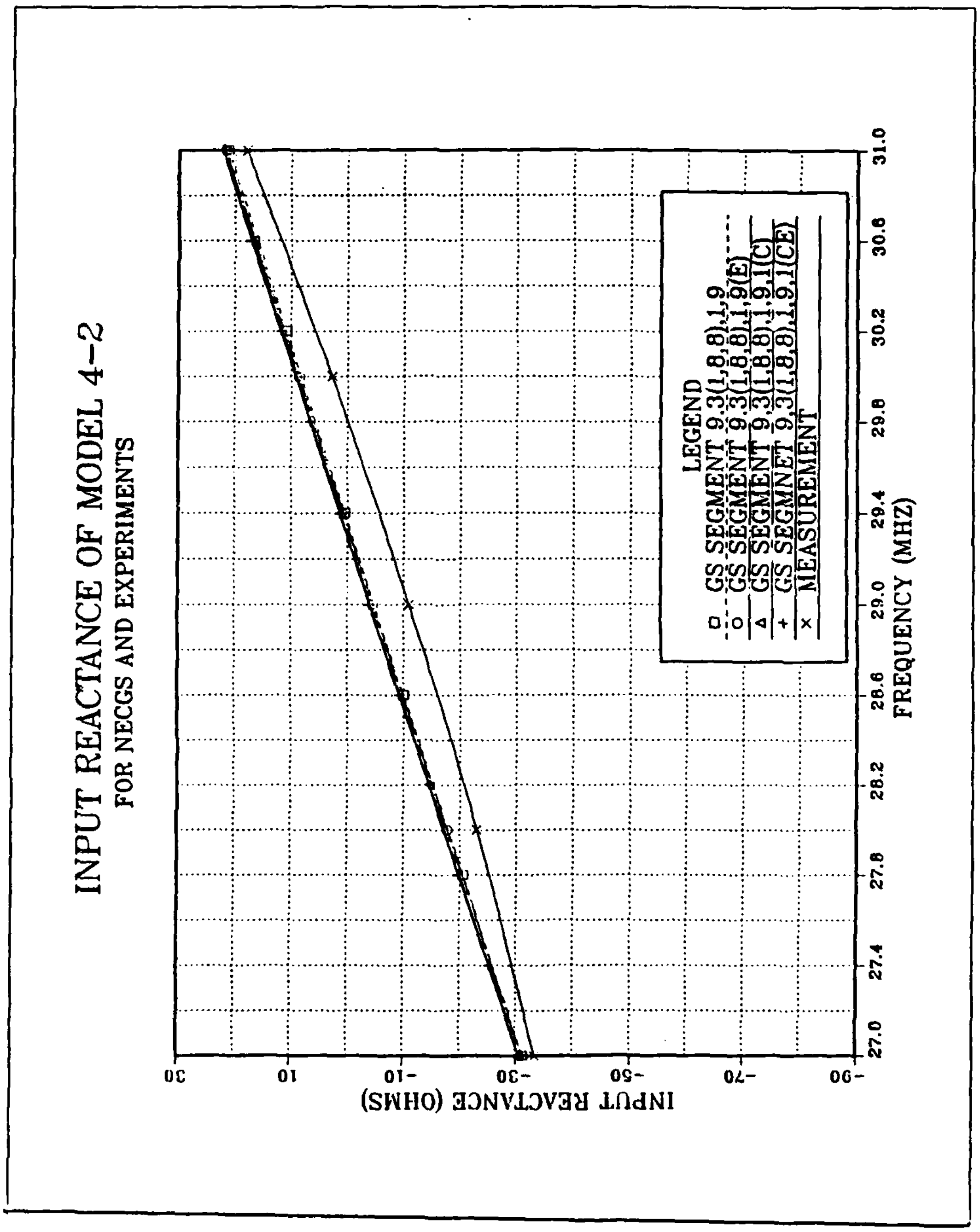

Figure 66. Model 4-2 Input Reactance vs. Frequency (27-31 MHz) for NECGS the Experiment.

3. Model 4-1-E results

Model 4-1-E is an equivalent average constant radius version of Model 4-1. Figure 67 shows that input resistance values are in fairly good agreement with those of the experiment. Figure 68 shows that input reactance values are very different from those of the experiment.

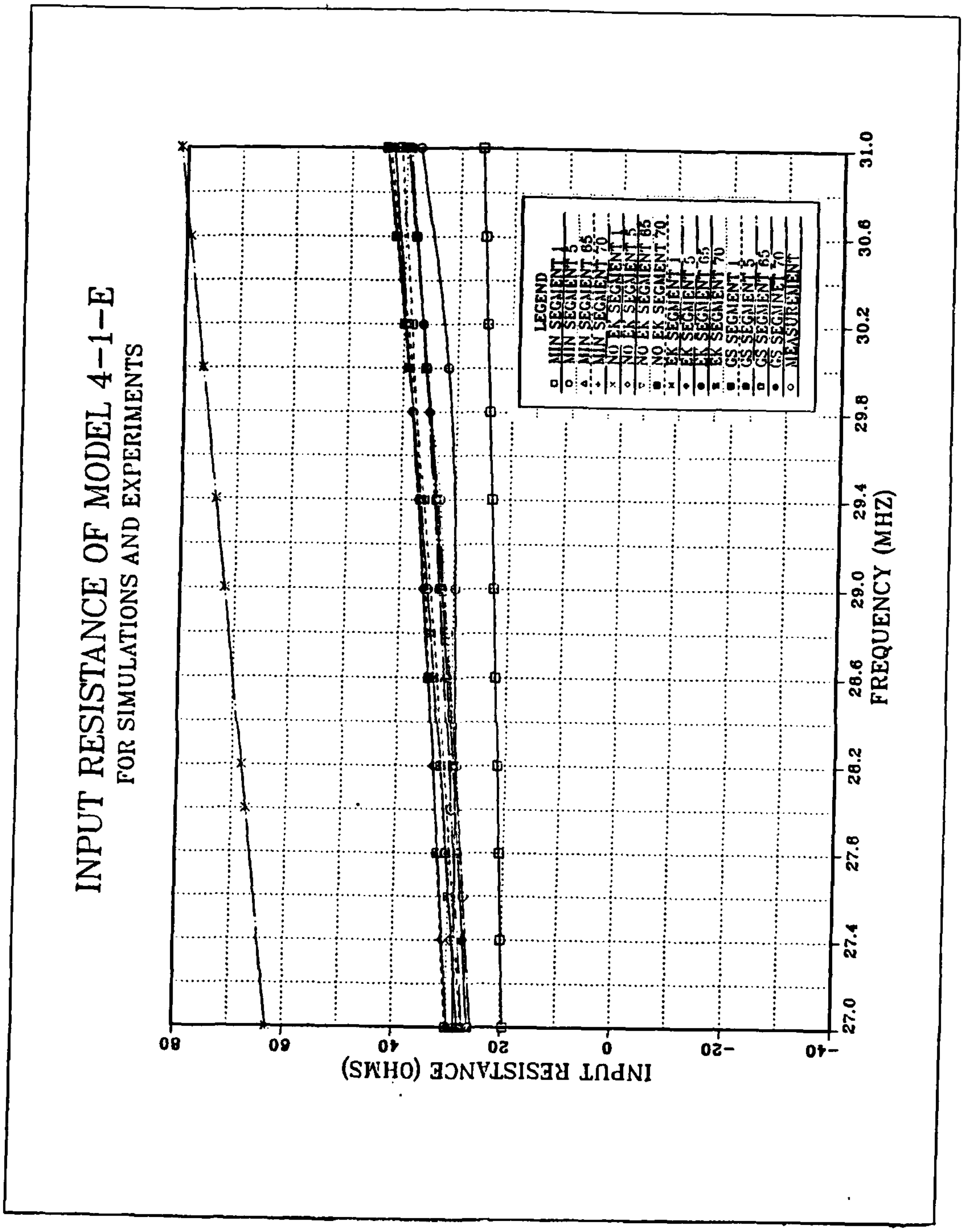

Figure 67. Model 4-1-E Input Resistance vs. Frequency (27-31 MHz) for all Computer Simulations and the Experiment

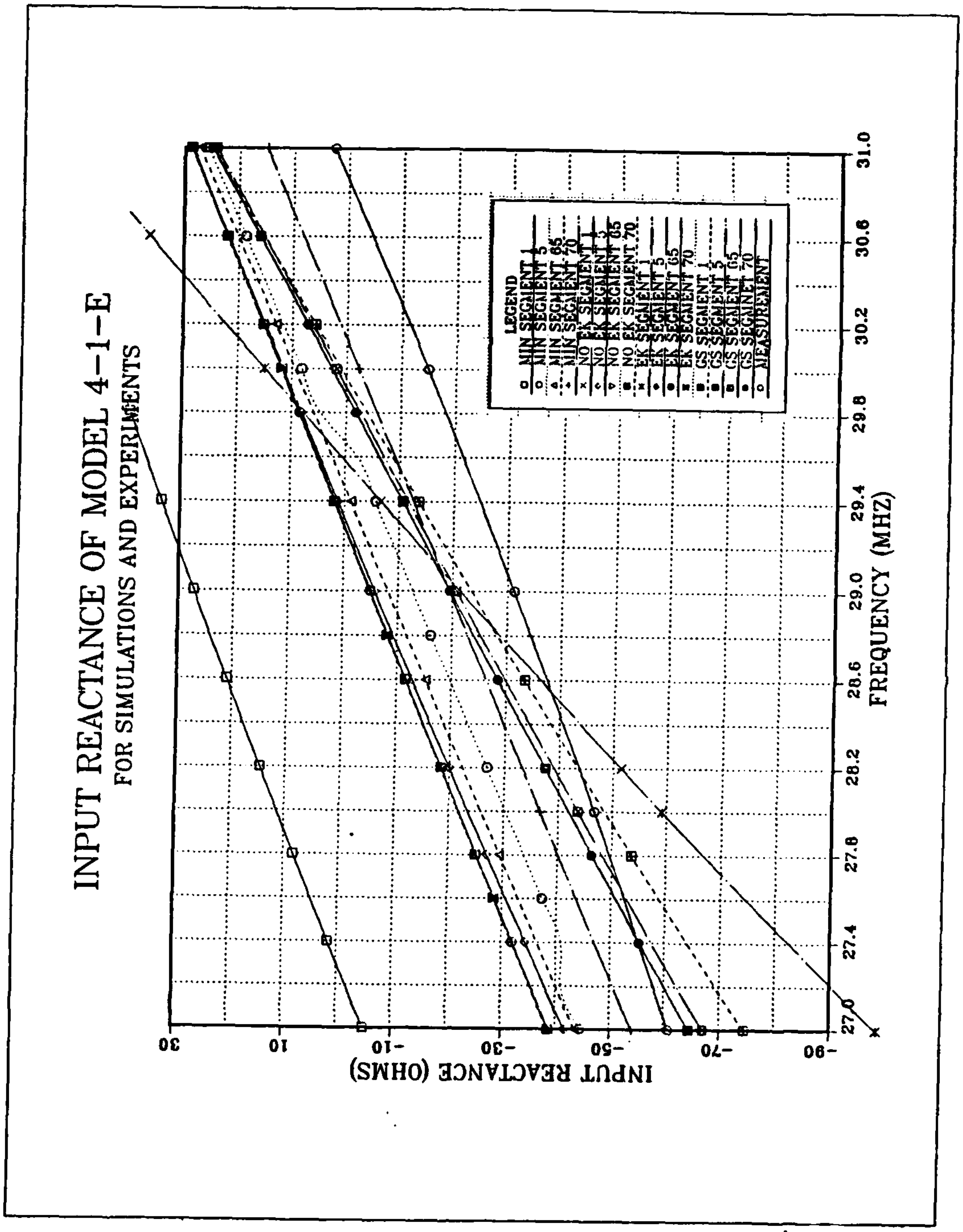

Figure 68. Model 4-1-E Input Reactance vs. Frequency (27-31 MHz) for all Computer Simulations and the Experiment

4. Model 4-2-E results

Model 4-2-E is an equivalent average constant radius (7/8 inch) version of Model 4-2. Figure 69 shows that input resistance values of all computer results are close to those of the experiment. Figure 70 shows that input reactance values do not agree well with those of the experiment. The results of MININEC are reasonably close, however, for this model.

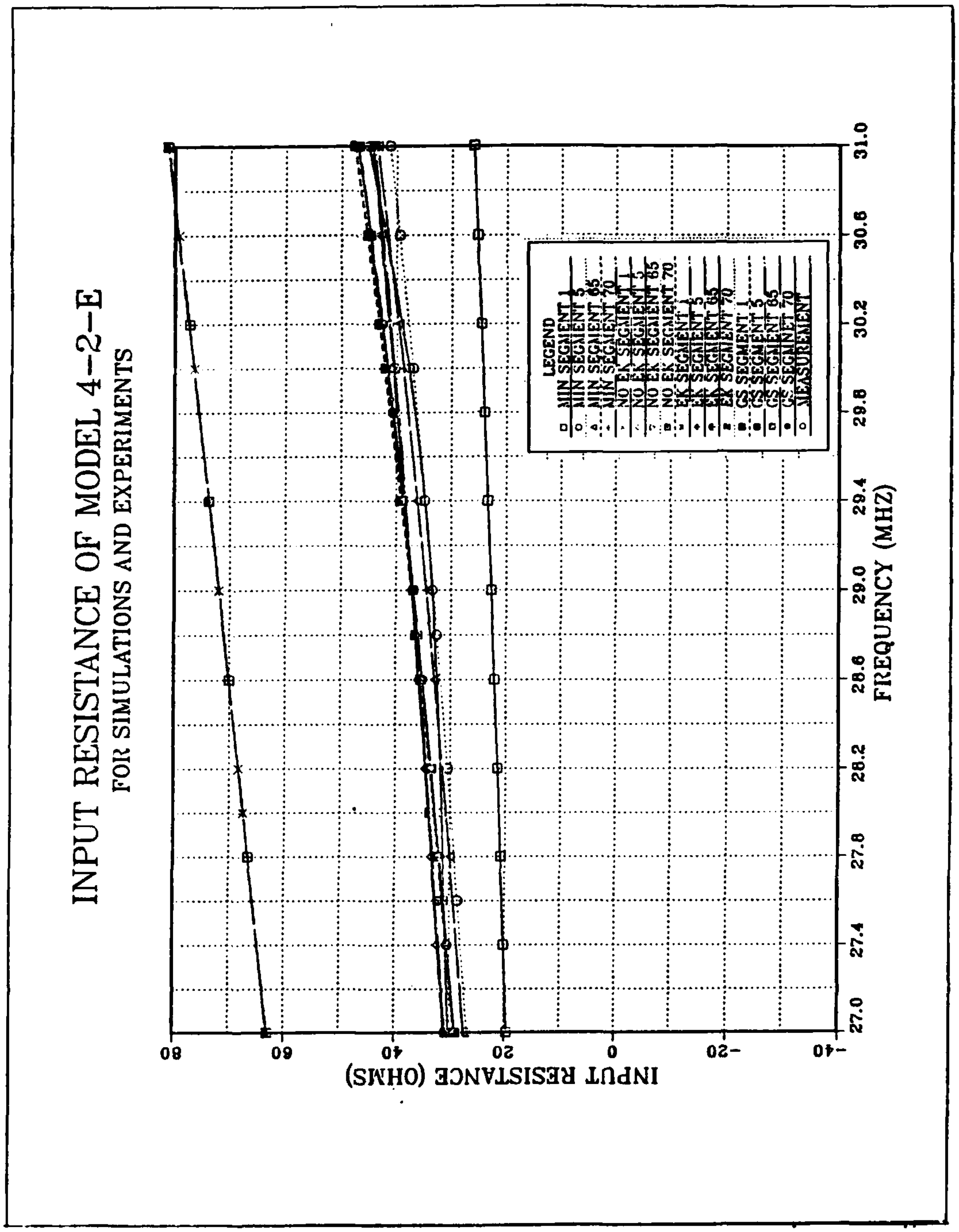

Figure 69. Model 4-2-E Input Resistance vs. Frequency (27-31 MHz) for all Computer Simulations and the Experiment

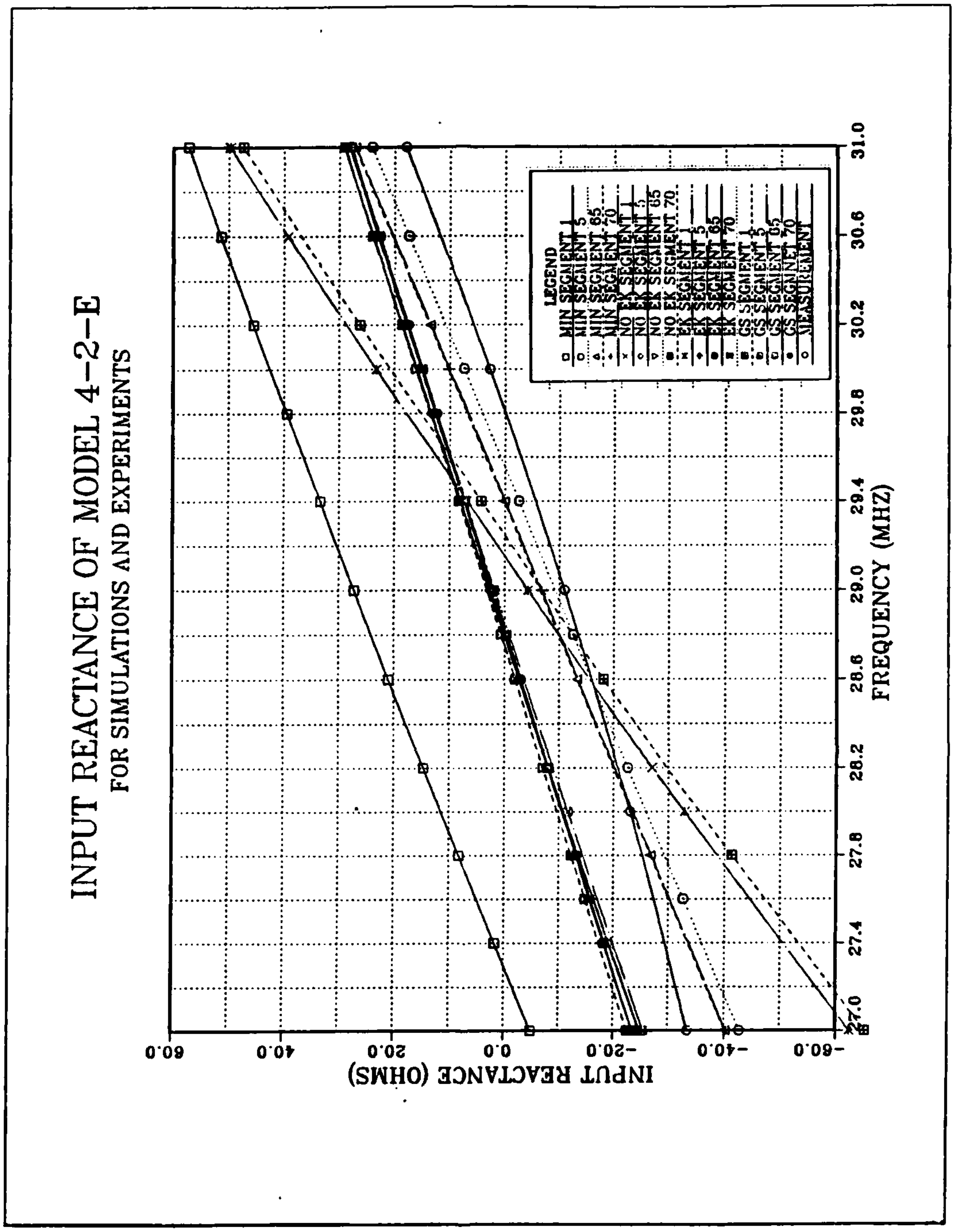

Figure 70. Model 4-2-E Input Reactance vs. Frequency (27-31 MHz) for all Computer Simulations and the Experiment

V. CONCLUSIONS AND RECOMMENDATIONS

This thesis has developed 4 computer model groups and 7 experimental models for stepped radius monopoles. Thin-wire modeling using NEC, MININEC, and NECGS produced results for input impedance over a 10% frequency range (27-31 MHz) and segmentations of 1-70 segments.

A. CONCLUSIONS

Throughout this study, stepped radius antennas show more sensitivity in the imaginary part of the input impedance than the real part when frequency is swept. When comparing results of computer modeling to results of the experiment, more errors occur for larger ratios of adjacent radii especially for the imaginary part of the input impedance which can seriously affect antennas such as the Yagi. This is because the impedance directly controls proper current ratios and phasings which are essential for a clean pattern with low side lobes. Slight changes in these current ratios and phasings have considerable effect on the sidelobes. The results of MININEC are close to results of our experiments which included r/λ's up to 0.0026. This is surprising since NEC has been adopted by many as the most accurate and powerful code available for wire antenna modeling. MININEC is clearly the best code to use for step radius antenna problems. The results of NECGS are the next closest to those of the experiment. The results of simulating the equivalent average constant radius of different radii with the same total length are very different from those of experiments. The results of NEC are the furthest from those of other computer code results and the experiments. In summary, MININEC is recommended for the design of tapered or stepped Yagi's, and Log Periodic (LP) antennas where the equivalent lengths at constant radius can be calculated and input to NEC which has transmission lines to connect LP elements.

B. RECOMMENDATIONS

Many aspects of this study warrant futher investigation:

- The treatment of step charge on the annulus and the charge discontinuty at the junction of radius step changes and the effect on current at match points in NEC is needed.

- More measurements of input impedance on complicated antennas (Yagi's and LP's) are needed.
- The development of subroutines for swept frequency in MININEC is needed.
- The development of subroutines for plotting impedance vs. frequency for MININEC is needed.
- NECGS wire-cage models might be improved if the criteria for equivalence between a normal stepped radius element and a cage model were varied. The present choice for equivalence is based on equal surface area, which has been proven inadequate for short monopoles.

APPENDIX A. COMPUTER CODE DESCRIPTIONS

1. Introduction

Integral equations are used for solving for currents on conducting objects.

$$X + Y = \int_s XKds \qquad (14)$$

where

- X is the unknown current,
- Y is the driven field (electric field or magnetic field),
- K is the kernel containing the geometry of the system, and
- s is the surface of the system.

The electric field type equation for wires is:

$$\hat{T} \bullet \vec{E} + \int \vec{I} \bullet \vec{K} ds \qquad (15)$$

.

where $\hat{T}$ is a unit vector.

The magnetic field type uses the following equation for closed surfaces

$$\vec{I} = 2\hat{n} \times \vec{H} + \int \vec{I} \bullet \vec{K} ds. \qquad (16)$$

Different computer codes use various basis functions and weighting factors for the Electric Field Integral Equations (EFIE's) or Magnetic Field Integral Equations (MFIE's). MININEC uses the Galerkin procedure and NEC uses point-matching for the EFIE in the case of the thin-wire model. Both use the method of moments. This appendix explains the method of moments, MININEC, NEC, and NECGS briefly.

2. The Method of Moments

All wire antenna problems can be expressed initially in the form of a linear integral equation derived from Maxwell's equations and the boundary conditions by the following equation:

$$F(\overline{r}, t) = \frac{1}{\pi}\int_0^{\infty} Re[\phi(\overline{r}, \omega)e^{j\omega t}]d\omega \tag{17}$$

where

- $F(\overline{r}, t)$ is a function of position and time,
- $\overline{r}$ is position,
- t is time, and
- $\phi(\overline{r}, \omega)$ is the Fourier transform of $F(\overline{r}, t)$.

The method of moments [Ref. 1] is a general procedure for solving linear equations and so-named because the process of taking moments is multiplied by appropriate weighting functions and then integrated. The use of the method of moments in electromagnetics and related matrix methods has become popular since the work of J. H. Richmond and R. F. Harrington showed how powerful and versatile such techniques could be [Ref. 1].

Following Harrington, consider the inhomogeneous equation:

$$L_{\omega}\phi_j = \Gamma, \tag{18}$$

where

- L_ω is an integral or integro-differential linear operator.
- Γ is a known function (an impressed field or voltage source), and
- ϕ is a function to be determined (a distribution of electric current).

Here ϕ and Γ are functions of the spatial coordinates and of frequency. The quantity ϕ is expressed in terms of known functions using undetermined parameters; for example, as a linear combination of a finite number of basis functions ϕ_j in the domain of L_ω.

For the current case, it will be expressed as follows:

$$I(\ell) = \sum_{i=1}^{N} I_i \mathcal{I}i(\ell) \qquad (19)$$

where

- N is the number of basis functions which cover the wires.
- I_i are the amplitudes of the unknowns which need to be found, and
- $\mathcal{I}i(\ell)$ are known basis functions.

Different numerical electromagnetic computer codes have a choice of their own special combination of basis and amplitude (weighting).

3. MININEC

MININEC is a BASIC program for the PC using the method of moments for the analysis of thin wire antennas, suitable for small problems (less than 75 unknowns and 10 wires, depending on the computer memory and compiler). MININEC solves the impedance and the current on arbitrarily oriented wires, including configurations with multiple wire junctions, in free space and over a perfectly conducting ground plane. Other options include lumped parameter impedance loading of wires and calculation of near or far zone electric fields. Both near or far electric and magnetic fields can be determined for free space and a perfectly conducting ground.

MININEC uses a Galerkin procedure for the current representation. Currents on the wires are expanded in terms of a finite series of known basis functions with unknown amplitudes. Since a finite number of basis functions have been chosen, N equations need to be derived from the EFIE to obtain a solution for the unknown amplitudes, I_i. This is done by multiplying the EFIE equation in turn by N weighting functions and integrating over the wire length. These weighting functions could be delta functions positioned at the center of each basis function, and in this way the EFIE equation would be satisfied at these points. However, the solution could be badly in error and it has been reported that better results are obtained if the basis functions themselves are equal to the weighting functions. In this way, the overall error of the solution for the current is minimized in the least squares sense. This scheme is known as the Galerkin procedure. Refer to [Ref. 1] for more information on the Galerkin procedure.

4. NUMERICAL ELECTROMAGNETICS CODE (NEC)

The Numerical Electromagnetics Code (NEC) is a user-oriented computer code for the analysis of the electromagnetic response of antennas and other metal structures. It is built around the numerical solution of integral equations for the current induced on structures by sources or incident fields. This approach avoids many of the simplifying assumptions required by other solution methods and provides a highly accurate and versatile tool for electromagnetic analysis.

The code combines an integral equation for smooth surfaces to provide convenient and accurate modeling of a wide range of structures. A model may include nonradiating networks and transmission lines connecting parts of the structure, perfect or imperfect conductors, and lumped element loading. A structure may also be modeled over a ground plane that may be either a perfect or imperfect conductor.

The excitation may be either voltage sources on the structure or an incident plane wave of linear or elliptic polarization. The output may include induced currents and charges, near electric or magnetic fields, and radiated fields. Hence the program is suited to either antenna analysis or scattering and Electro-Magnetic Pulse (EMP) studies.

The integral equation approach is best suited to structures with dimensions up to several wavelengths. Although there is no theoretical size limit, the numerical solution requires a matrix equation of increasing order as the structure size is increased relative to 1 wavelength. Hence, modeling very large structures may require more computer time and file storage than is practical on a particular machine. In such cases, standard high-frequency approximations such as the geometrical optics, physical optics, or geometrical theory of diffraction may be more suitable than the integral equation approach used in NEC.

a. Structure Modeling

The basic elements for modeling structures in NEC are short straight segments for wires and flat patches for surfaces. An antenna and any conducting object in its vicinity that affect its performance must be modeled with strings of segments following the paths of wires and with patches covering surfaces. Proper choice of the segments and patches for a model is the most critical step in obtaining accurate results. In this thesis, thin wire modeling by NEC is used. Refer to the NEC manual [Ref. 2] for more information.

b. Wire Modeling

A wire segment is defined by the coordinates of its two end points and its radius. Modeling a wire structure with segments involves both geometrical and electrical factors. Geometrically, the segments should follow the paths of conductors as closely as possible, using a piece-wise linear fit on curves. The following are electrical considerations for wire segment modeling :

- The segment length Δ relative to the wavelength λ is:
  - Δ should be less than about 0.1 λ in order to get accurate results in most of the cases.
  - A somewhat longer segment may be acceptable on long wires with no abrupt changes while a shorter segment, 0.05 λ or less, may be needed in modeling critical regions of antenna.
  - Δ less than 0.001 λ should be avoided since the similarity of the constant and cosine components of the current expansion leads to numerical inaccuracy.
- The wire radius, r, relative to λ is limited by the approximations used in the kernel of the electric field integration equation. The segment radius α relative to both segment length Δ and wavelength λ are :
  - α should be less than 0.1 λ
  - α should be less than 0.125 Δ
  - α can be less than 0.5 Δ, but this requires the extended thin wire kernel option by placing the EK card in the input data set.
- Connected segments must have identical coordinates for connected ends. NEC assumes two end segments connected if the separation between the end segments is less than 0.001 times the length of the shortest segment.
- Segment intersections other than at their ends do not allow currents to flow from one segment to another.
- Large wire radius changes should be avoided particularly for adjacent segments. If the segment has a large radius, then sharp bends should be avoided as well.
- When modeling a solid structure with a wire grid, a large number of segments should be used.

- A segment is needed at the point where a network connection, a voltage or a current source, is going to be located.
- Base fed wires connected to ground should be vertical.
- The segments on either side of the excitation source should be parallel and have the same length and radii.
- Parallel wires should be several radii apart.
- Before modeling a structure, the limit of the number of segments and the number of connection points should be checked for the particular version of NEC.

5. NECGS

NECGS is a quick and very efficient special- purpose version of NEC3 for limited applications [Ref. 2]. It was developed for a vertical monopole on a uniform radial wire ground screen. The radial wires can include top-hat wires and other conductors but they must lie in the X-Z plane. NECGS works like NEC3 except:

a. Geometry

- In the geometry section, the only acceptable cards are GW, GC, GR, GM (limited use), GS, and GE.
- GR works differently and goes before the wires to be rotated. Examples below:
  "GW" card(s) to define the monopole in the Z-axis
  "GR" ITG, NS
  "GW" card(s) for radial wires in X-Z plane.
- ITG on "GR" cards has no effect.
- "GR" card may be omitted to run a monopole on a ground stake.
- A thick tower may be modeled by "rotating" an "L" shaped object.
- A top load wire may also be defined in the X-Z plane along with the ground screen. The number of top loads must be the same as the number of ground screen wires; NR on GR card-unless a GM card is used.
- "GM" allows limited move capability and will move RADIAL parts only, not axial wires. This is good for the number of top-load wires not equal to the number of radial wires.

b. Main Code Section

- NT, TL, CP, and WG are not supported.
- EK card does not apply.
- Voltage source excitation only is allowed. A source on a radial wire will be duplicated on all radial wires.
- A load on a radial wire will be duplicated on all radials.

c. Dimension Limitation

- The number of input wire segments on the monopole and one radial is limited to 150.
- There is no dimension limit on the number of radials, except for computer time limitations.

APPENDIX B. INPUT IMPEDANCE CONVERGENCE GRAPH

These are the convergence test graphs for MININEC and NEC.

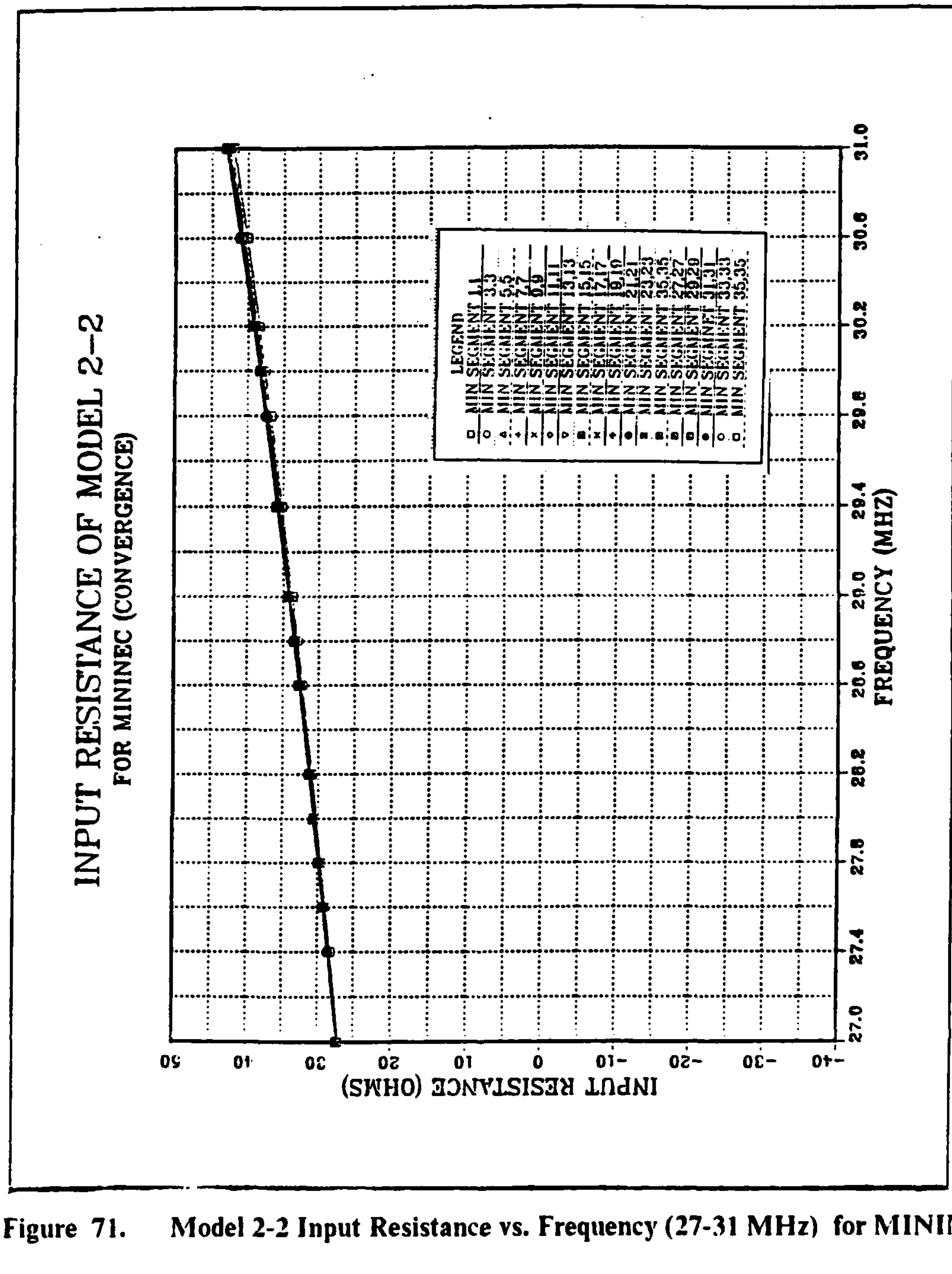

Figure 71. Model 2-2 Input Resistance vs. Frequency (27-31 MHz) for MININEC

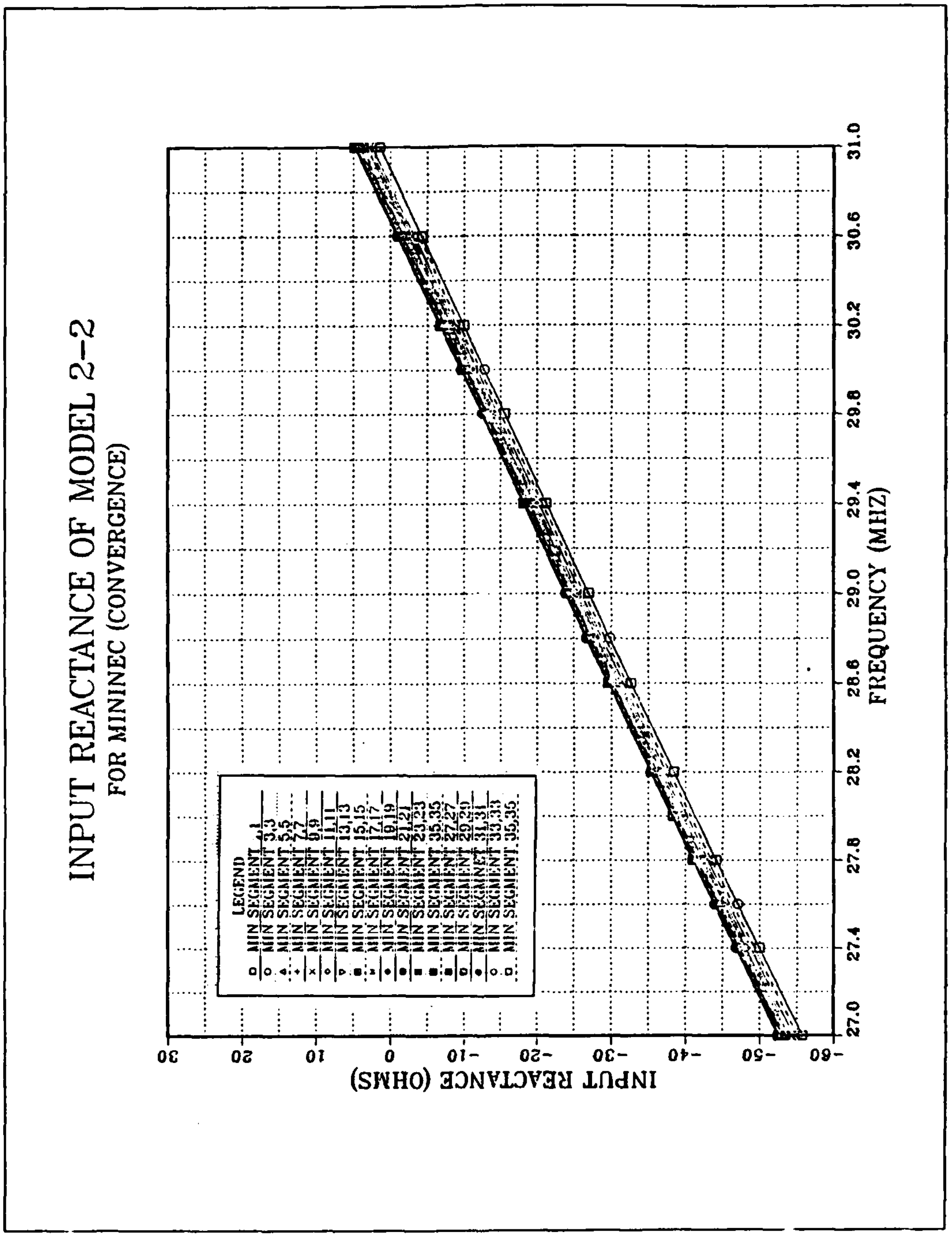

Figure 72. Model 2-2 Input Reactance vs. Frequency (27-31 MHz) for MININEC

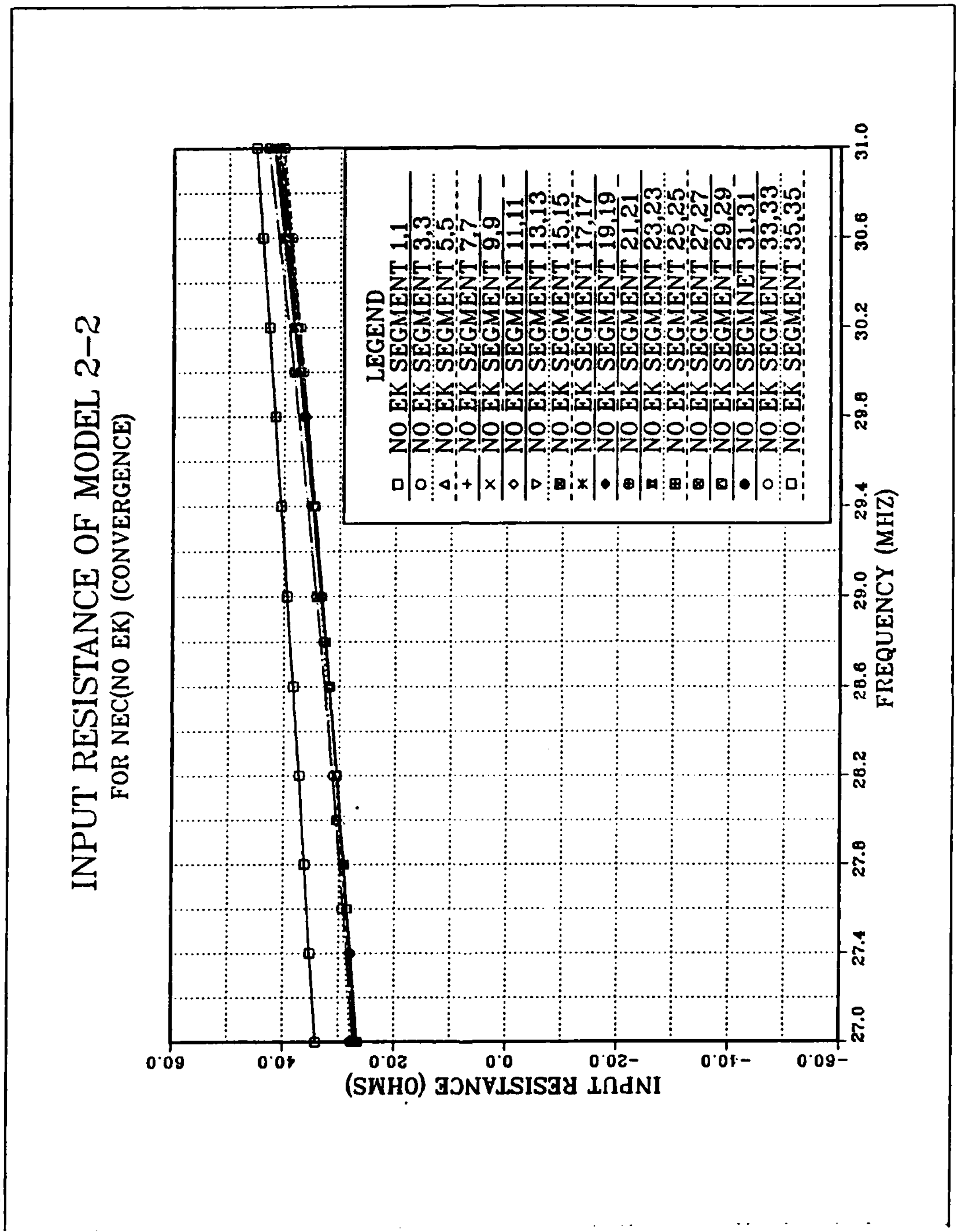

Figure 73. Model 2-2 Input Resistance vs. Frequency (27-31 MHz) for NEC (no EK card)

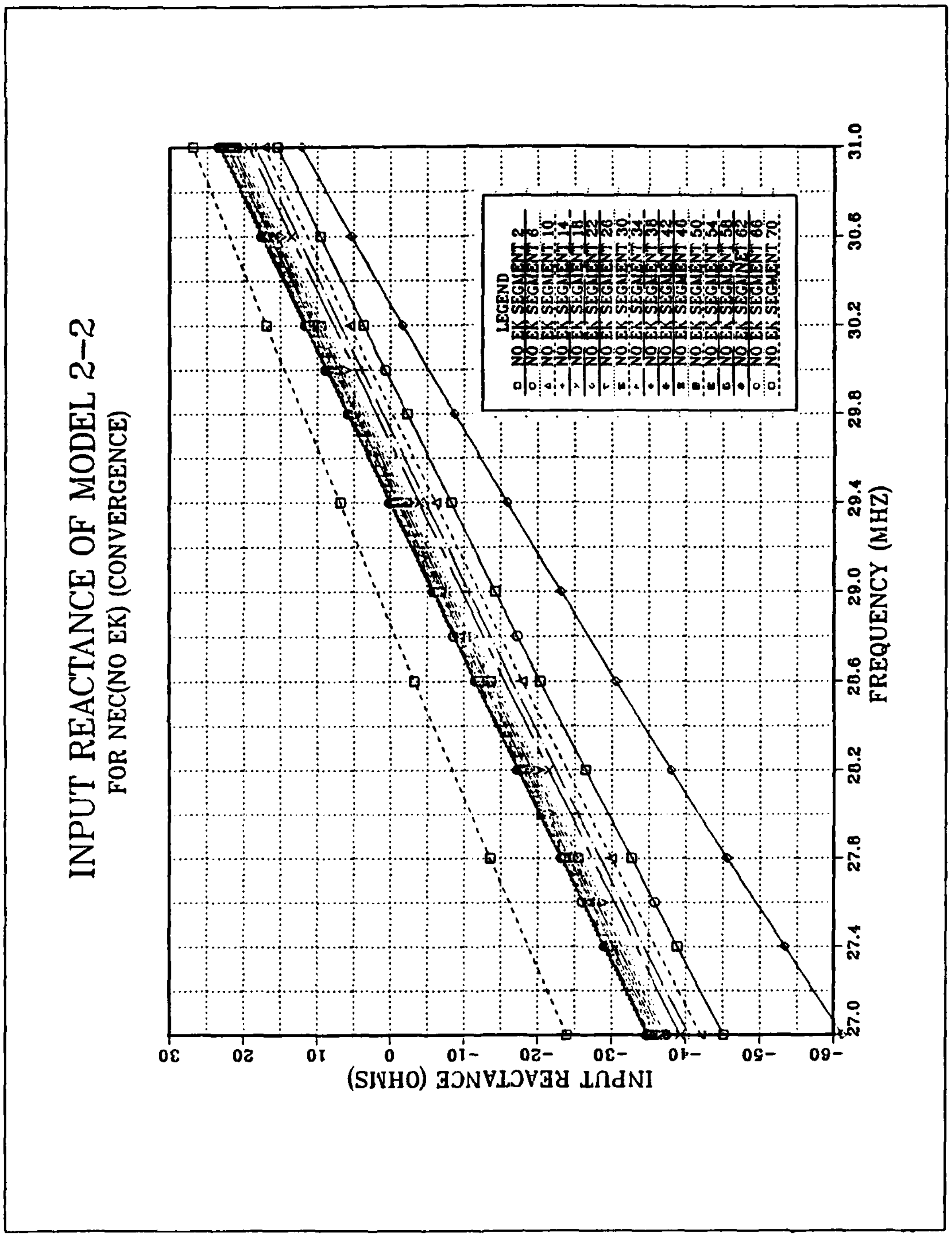

Figure 74. Model 2-2 Input Reactance vs. Frequency (27-31 MHz) for NEC (no EK card)

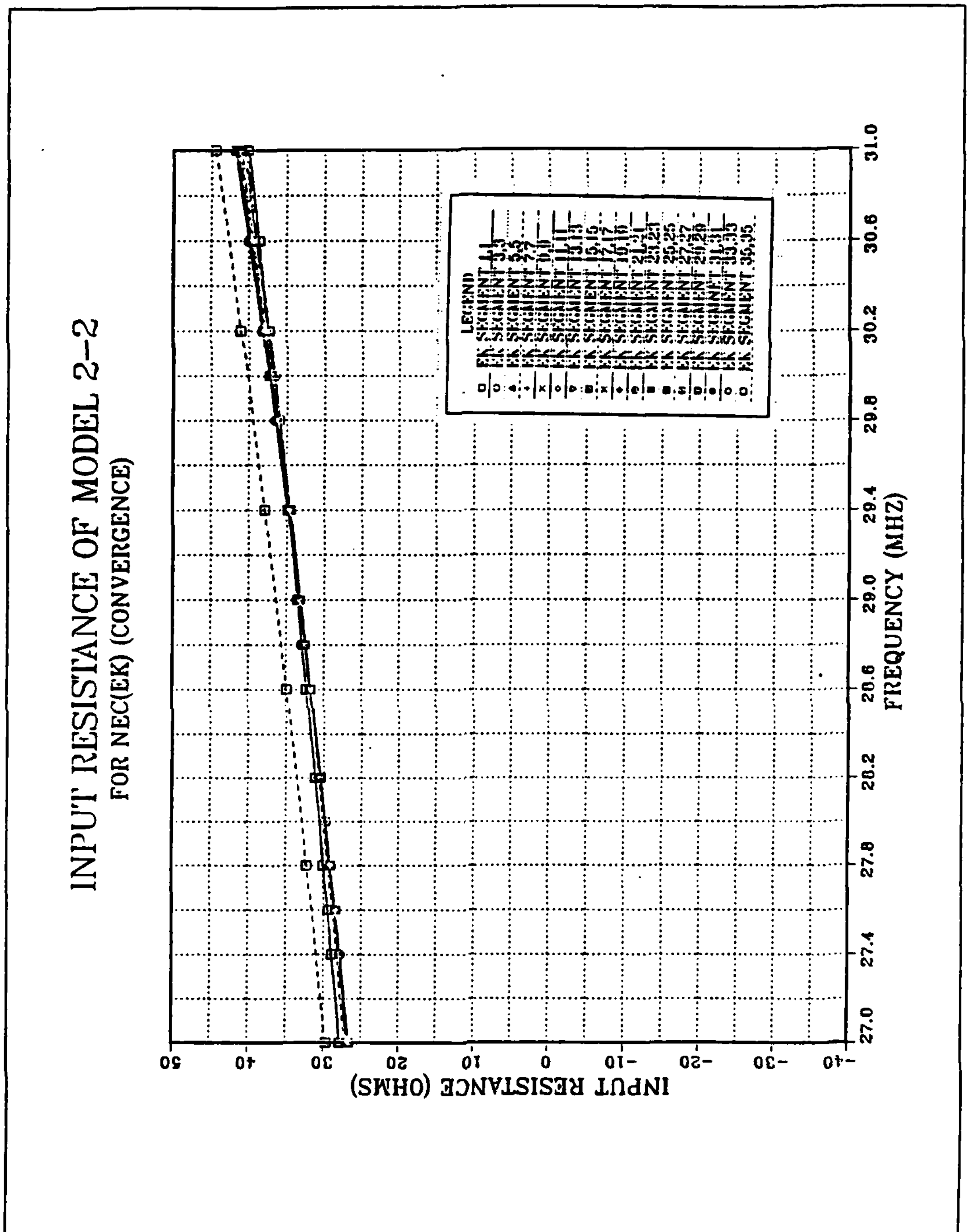

Figure 75. Model 2-2 Input Resistance vs. Frequency (27-31 MHz) for NEC (EK card)

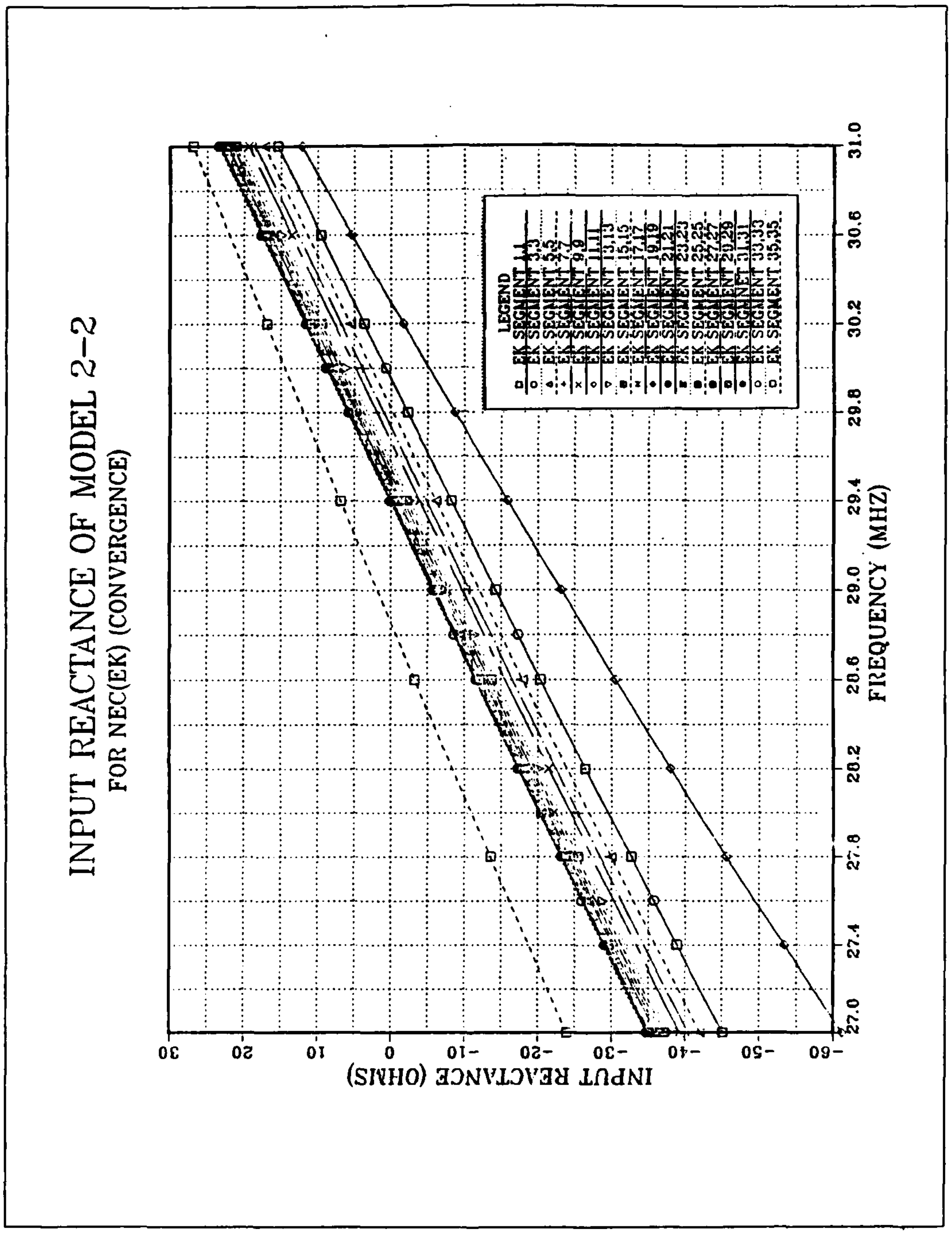

Figure 76. **Model 2-2 Input Reactance vs. Frequency (27-31 MHz) for NEC (EK card)**

APPENDIX C. GEOMETRY DATA SETS

This section of the Appendix has the geometry data set samples of each computer simulation model.

1. MININEC

Following are the sample geometry data sets and the sample results of Model 4-2 with various segments. The other data sets are different from these in segment number (1-70 segments), geometry, and frequencies (27-31 MHz).

```
**************************************
MINI-NUMERICAL ELECTROMAGNETICS CODE
          MININEC (3)
 10-13-1988            21:29:59
**************************************

FREQUENCY (MHz): 27
  WAVE LENGTH =  11.1037  METERS

ENVIRONMENT (+1 FOR FREE SPACE, -1 FOR GROUND PLANE): -1
NUMBER OF MEDIA (0 FOR PERFECTLY CONDUCTING GROUND):  0

NO. OF WIRES: 5

WIRE NO. 1
        COORDINATES                          END        NO. OF
 X         Y         Z        RADIUS    CONNECTION   SEGMENTS
 0         0         0                 -1
 0         0        .48768    .0254      0           13

WIRE NO. 2
        COORDINATES                          END        NO. OF
 X         Y         Z        RADIUS    CONNECTION   SEGMENTS
 0         0        .48768                1
 0         0        .97536    .0238125   0           13

WIRE NO. 3
        COORDINATES                          END        NO. OF
 X         Y         Z        RADIUS    CONNECTION   SEGMENTS
 0         0        .97536                2
 0         0        1.46304   .022225    0           13

WIRE NO. 4
        COORDINATES                          END        NO. OF
 X         Y         Z        RADIUS    CONNECTION   SEGMENTS
 0         0        1.46304               3
 0         0        1.95072   .0206375   0           13

WIRE NO. 5
        COORDINATES                          END        NO. OF
 X         Y         Z        RADIUS    CONNECTION   SEGMENTS
 0         0        1.95072               4
 0         0        2.4384    .01905     0           13

        **** ANTENNA GEOMETRY ****

WIRE NO.  1  COORDINATES                CONNECTION PULSE X      Y      Z      RADIUS     END1
END2  NO.
 0         0        0              .0254      -1   1   1
 0         0        3.751385E-02   .0254       1   1   2
 0         0        7.502769E-02   .0254       1   1   3
 0         0        .1125415       .0254       1   1   4
```

0	0	.1500554	.0254	1	1	5
0	0	.1875692	.0254	1	1	6
0	0	.2250831	.0254	1	1	7
0	0	.2625969	.0254	1	1	8
0	0	.3001108	.0254	1	1	9
0	0	.3376246	.0254	1	1	10
0	0	.3751385	.0254	1	1	11
0	0	.4126523	.0254	1	1	12
0	0	.4501661	.0254	1	0	13

WIRE NO. 2 COORDINATES CONNECTION PULSE X Y Z RADIUS END1 END2 NO.

0	0	.48768	.0238125	1	2	14
0	0	.5251938	.0238125	2	2	15
0	0	.5627077	.0238125	2	2	16
0	0	.6002215	.0238125	2	2	17
0	0	.6377354	.0238125	2	2	18
0	0	.6752492	.0238125	2	2	19
0	0	.7127631	.0238125	2	2	20
0	0	.7502769	.0238125	2	2	21
0	0	.7877908	.0238125	2	2	22
0	0	.8253046	.0238125	2	2	23
0	0	.8628184	.0238125	2	2	24
0	0	.9003323	.0238125	2	2	25
0	0	.9378461	.0238125	2	0	26

WIRE NO. 3 COORDINATES CONNECTION PULSE X Y Z RADIUS END1 END2 NO.

0	0	.97536	.022225	2	3	27
0	0	1.012874	.022225	3	3	28
0	0	1.050388	.022225	3	3	29
0	0	1.087901	.022225	3	3	30
0	0	1.125415	.022225	3	3	31
0	0	1.162929	.022225	3	3	32
0	0	1.200443	.022225	3	3	33
0	0	1.237957	.022225	3	3	34
0	0	1.275471	.022225	3	3	35
0	0	1.312985	.022225	3	3	36
0	0	1.350498	.022225	3	3	37
0	0	1.388012	.022225	3	3	38
0	0	1.425526	.022225	3	0	39

WIRE NO. 4 COORDINATES CONNECTION PULSE X Y Z RADIUS END1 END2 NO.

0	0	1.46304	.0206375	3	4	40
0	0	1.500554	.0206375	4	4	41
0	0	1.538068	.0206375	4	4	42
0	0	1.575582	.0206375	4	4	43
0	0	1.613095	.0206375	4	4	44
0	0	1.650609	.0206375	4	4	45
0	0	1.688123	.0206375	4	4	46
0	0	1.725637	.0206375	4	4	47
0	0	1.763151	.0206375	4	4	48
0	0	1.800665	.0206375	4	4	49
0	0	1.838178	.0206375	4	4	50
0	0	1.875692	.0206375	4	4	51
0	0	1.913206	.0206375	4	0	52

WIRE NO. 5 COORDINATES CONNECTION PULSE X Y Z RADIUS END1 END2 NO.

0	0	1.95072	.01905	4	5	53
0	0	1.988234	.01905	5	5	54
0	0	2.025748	.01905	5	5	55
0	0	2.063262	.01905	5	5	56
0	0	2.100775	.01905	5	5	57
0	0	2.138289	.01905	5	5	58
0	0	2.175803	.01905	5	5	59
0	0	2.213317	.01905	5	5	60
0	0	2.250831	.01905	5	5	61
0	0	2.288345	.01905	5	5	62
0	0	2.325859	.01905	5	5	63
0	0	2.363372	.01905	5	5	64
0	0	2.400886	.01905	5	0	65

```
NO. OF SOURCES : 1 PULSE NO., VOLTAGE MAGNITUDE, PHASE (DEGREES): 1 , 1 , 0 NUMBER OF LOADS 0

FILL MATRIX : 6:39 FACTOR MATRIX: 0:34

********************  SOURCE DATA  ******************** PULSE 1    VOLTAGE = ( 1 , 0 J)
        CURRENT = ( 1.547403E-02 , 1.856772E-02 J)
        IMPEDANCE = ( 26.48729 ,-31.78284 J)
        POWER = 7.737014E-03 WATTS

********************  CURRENT DATA  ********************

WIRE NO. 1 : PULSE     REAL        IMAGINARY    MAGNITUDE    PHASE
NO.        (AMPS)      (AMPS)      (AMPS)       (DEGREES)
1          1.547403E-02 1.856772E-02 2.417035E-02 50.19273
2          1.547006E-02 1.775532E-02 2.354939E-02 48.93464
3          1.545813E-02 1.760352E-02 2.342729E-02 48.71275
4          1.543827E-02 1.741042E-02 2.326935E-02 48.43576
5          1.541045E-02 1.723926E-02 2.312302E-02 48.20596
6          .0153747     1.707298E-02 2.297538E-02 47.99606
7          1.533101E-02 1.690883E-02 2.282429E-02 47.80183
8          .0152794     .0167445     .022668      47.61948
9          1.521985E-02 1.657854E-02 2.250538E-02 47.44667
10         1.515239E-02 .01641       2.233569E-02 47.28177
11         1.507698E-02 1.623815E-02 2.215836E-02 47.12358
12         1.499358E-02 1.606241E-02 .0219729     46.97112
13         1.490193E-02 1.588188E-02 2.177847E-02 46.82331 J        1.480133E-02 1.569505E-02 2.157345E-02 46.67861

WIRE NO. 2 : PULSE     REAL        IMAGINARY    MAGNITUDE    PHASE
NO.        (AMPS)      (AMPS)      (AMPS)       (DEGREES) J        1.480133E-02 1.569505E-02 2.157345E-02 46.67861
15         1.469922E-02 1.551504E-02 .0213725     46.54668
16         1.458832E-02 1.532832E-02 2.116073E-02 46.41695
17         1.446935E-02 1.513607E-02 .0209395     46.2901
18         .0143426     1.493869E-02 2.070929E-02 46.16623
19         1.420817E-02 1.473625E-02 .0204702     46.04522
20         1.406612E-02 1.452874E-02 2.022226E-02 45.92688
21         1.391652E-02 .0143162     1.996555E-02 45.81104
22         .0137594     1.409858E-02 1.970002E-02 45.69756
23         1.359476E-02 1.387587E-02 1.942569E-02 45.5863
24         1.342259E-02 1.364799E-02 1.914245E-02 45.47704
25         1.324282E-02 .0134148     1.885018E-02 45.36965
26         1.305497E-02 1.317571E-02 1.854809E-02 45.26375 J        1.285735E-02 1.292859E-02 1.823348E-02 45.15829

WIRE NO. 3 : PULSE     REAL        IMAGINARY    MAGNITUDE    PHASE
NO.        (AMPS)      (AMPS)      (AMPS)       (DEGREES) J        1.285735E-02 1.292859E-02 1.823348E-02 45.15829
28         1.266537E-02 1.269244E-02 1.793069E-02 45.06117
29         1.246383E-02 1.244835E-02 1.761558E-02 44.96439
30         1.225453E-02 .0121985     1.729095E-02 44.86874
31         1.203792E-02 1.194349E-02 1.695755E-02 44.77439
32         1.181423E-02 1.168354E-02 1.661569E-02 44.68133
33         1.158353E-02 1.141874E-02 1.626547E-02 44.58954
34         1.134592E-02 .0111492     1.590706E-02 44.49895
35         1.110144E-02 1.087495E-02 1.554048E-02 44.40952
36         1.085012E-02 1.059602E-02 1.516577E-02 44.32116
37         1.059191E-02 1.031236E-02 1.478287E-02 44.23381
38         .0103267     1.002383E-02 1.439159E-02 44.14736
39         1.005389E-02 9.729826E-03 1.399107E-02 44.06157 J        9.770452E-03 9.427121E-03 .0135769     43.97543

WIRE NO. 4 : PULSE     REAL        IMAGINARY    MAGNITUDE    PHASE
NO.        (AMPS)      (AMPS)      (AMPS)       (DEGREES) J        9.770452E-03 9.427121E-03 .0135769     43.97543
41         9.49992E-03  9.140683E-03 1.318334E-02 43.89595
42         9.219228E-03 8.845924E-03 1.277672E-02 43.81619
43         8.93122E-03  8.545893E-03 1.236119E-02 43.73698
44         8.636565E-03 8.241302E-03 1.193773E-02 43.65844
45         8.335444E-03 7.93235E-03  .0115066     43.58058
46         8.027976E-03 7.619171E-03 1.106798E-02 43.5034
47         7.71418E-03  7.301796E-03 .0106219     43.42688
48         7.394065E-03 6.98024E-03  1.016838E-02 43.35096
49         7.06756E-03  6.654447E-03 9.707321E-03 43.27559
50         6.734514E-03 6.324282E-03 9.238519E-03 43.20069
51         6.394623E-03 5.989468E-03 8.761568E-03 43.12619
52         6.047111E-03 5.649277E-03 8.275373E-03 43.05189 J        5.687214E-03 5.299101E-03 7.773344E-03 42.97675
```

```
WIRE NO. 5 : PULSE       REAL       IMAGINARY    MAGNITUDE    PHASE
 NO.        (AMPS)      (AMPS)      (AMPS)       (DEGREES) J          5.687214E-03  5.299101E-03  7.773344E-03  42.97675
 54         5.34661E-03  4.969657E-03 7.299571E-03 42.90736
 55         4.993802E-03 4.630358E-03 6.810159E-03 42.83733
 56         4.632752E-03 4.28509E-03  6.310657E-03 42.76746
 57         4.263678E-03 3.934116E-03 5.801397E-03 42.69788
 58         3.886295E-03 3.577207E-03 5.282017E-03 42.62855
 59         3.499946E-03 3.213797E-03 4.751643E-03 42.55945
 60         3.103633E-03 2.84301E-03  4.208948E-03 42.4905
 61         2.695801E-03 2.463468E-03 3.651851E-03 42.4216
 62         2.273904E-03 2.072911E-03 3.076946E-03 42.35258
 63         1.834579E-03 1.668344E-03 2.479728E-03 42.283
 64         1.364095E-03 1.237447E-03 1.841746E-03 42.21295
 65         8.906736E-04 8.057465E-04 1.201052E-03 42.13402 E       0        0        0        0

FILENAME (NAME.OUT): MB51327.OUT
```

2. NEC

Following are the sample geometry data sets for each model of NEC.

a. *Model 1-1 Geometry Data Set (6 segment)*

```
CM NEC SIMULATION FOR EXPERIMENT(Model 1-1)
CM IMPEDANCE VS RADIUS CHANGE WHEN SEGMENTS ARE 6.
CM RADIUS CHANGE FROM E-05 WAVELENGTH TO 1 WAVELENGTH
CM CENTER FREQUENCY 30.757874 MHz
CM LAMDA = 32 FEET AT 30.757874 MHz
CE
GW1,6, 0,0,0, 0,0,8., 32E-05      TAG1 6SEG 8FEET
GS1                              CHANGE SCALE(FEET TO METER)
GE1                              GROUND(CHARGE AT BASE ZERO)
EX0,1,1,01,1,0,75                FEED. 1V AT 1ST SEG IMPEDANCE
GN1                              PERFECTLY CONDUCTING GROUND
FR0,3,0,0,29.757874,1            CENTER FREG. 30.757874MHz
PL4                              IMPEDANCE and SWR
XQ
EN
```

**** These are 21 different raius data in wavelength for Model 1 ****

(1) 1E-05 (12) 0.75E-02

(2) 0.25E-04 (13) 1E-02

(3) 0.50E-04	(14) 0.25E-01
(4) 0.75E-04	(15) 0.50E-01
(5) 1E-04	(16) 0.75E-01
(6) 0.25E-03	(17) 1E-01
(7) 0.50E-03	(18) 0.25E-00
(8) 0.75E-03	(19) 0.50E-00
(9) 1E-03	(20) 0.75E-00
(10) 0.25E-02	(21) 1E-00
(11) 0.50E-02	

b. Model 2-1 Geometry Data Set (1, 1 segment)

```
CM NEC(NO EK) SIMULATION FOR EXPERIMENT
CE
GW1,1, 0,0,0, 0,0,4., .0208   TAG1 1SEG 4FEET R=.0208FEET
GW2,1, 0,0,4, 0,0,8., .0104   TAG2 1SEG 4FEET R=.0104FEET
GS1                           CHANGE SCALE(FEET TO METER)
GE1                           GROUND(CHARGE AT BASE ZERO)
EX0,1,1,01,1,0,75             FEED. 1V AT 1ST SEGMENT
GN1                           PERFECTLY CONDUCTING GROUND
FR0,21,0,0,27,.2              FREG. SWEEP. 27-31MHz
PL4                           IMPEDENCE AND  SWR
XQ
EN
```

c. Model 2-2 Geometry Data Set (3, 3 segment)

```
CM NEC(NO EK) SIMULATION FOR EXPERIMENT
CE
GW1,3, 0,0,0, 0,0,4., .0416  TAG1 3SEG 4FEET R=.0416FEET
GW2,3, 0,0,4, 0,0,8., .0208  TAG2 3SEG 4FEET R=.0208FEET
GS1                          CHANGE SCALE(FEET TO METER)
GE1                          GROUND(CHARGE AT BASE ZERO)
EX0,1,1,01,1,0,75            FEED. 1V AT 1ST SEGMENT
```

```
GN1                     PERFECTLY CONDUCTING GROUND
FR0,21,0,0,27,.2          FREG. SWEEP. 27-31MHz
PL4                     IMPEDENCE AND SWR
XQ
EN
```

d. Model 2-1-E Geometry Data Set (10 segment)

```
CM NEC SIMULATION FOR EXPERIMENT (MODEL 2-1-E)
CM AVERAGE RADIUS OF .0208 FEET AND .0104 FEET = 0.0156 FEET
CE
GW1,10, 0,0,4, 0,0,8., .0156   TAG1 10SEG 8FEET R=.0156FEET
GS1                     CHANGE SCALE(FEET TO METER =0.3048)
GE1                     GROUND(CHARGE AT BASE ZERO)
EX0,1,1,01,1,0,75          FEED. 1V AT 1ST SEGMENT
GN1                     PERFECTLY CONDUCTING GROUND
FR0,21,0,0,27,.2      FREG. SWEEP. 27-31MHz BY 0.2MHz INCREMENTS
PL4                     IMPEDANCE AND SWR
XQ
EN
```

e. Model 2-2-E Geometry Data Set (18 segment)

```
CM NEC SIMULATION FOR EXPERIMENT (MODEL 2-2-E)
CM (AVERAGE RADIUS OF .0416 FEET AND .0208 FEET = 0.0312 FEET)
CE
GW1,18, 0,0,0, 0,0,8., .0312   TAG1 18SEG 8FEET R=.0312FEET
GS1                     CHANGE SCALE(FEET TO METER =0.3048)
GE1                     GROUND(CHARGE AT BASE ZERO)
EX0,1,1,01,1,0,75          FEED. 1V AT 1ST SEGMENT
GN1                     PERFECTLY CONDUCTING GROUND
FR0,21,0,0,27,.2       FREG. SWEEP. 27-31MHz BY .2MHz INCREMENTS
PL4                     IMPEDANCE AND SWR
```

```
XQ
EN
```

f. Model 3-1 Geometry Data Set (7, 7, 7 segment)

```
CM NEC SIMULATION FOR TELESCOPING ANT. EXPERIMENT (MODEL
3-1)
CM IMPEDANCE VS FREQUENCY CHANGE WHEN SEGMENTS ARE 7,7,7
(3TAG).
CM FREQUENCY CHANGE FROM 27MHz TO 31 MHz
CE
GW1,7, 0,0,0, 0,0,2.666667, 2.083333E-2        TAG1 7SEG
GW2,7, 0,0,2.666667, 0,0,5.333333, 1.5625E-2   TAG2 7SEG
GW3,7, 0,0,5.333333, 0,0,8., 1.041667E-2       TAG3 7SEG
GS1                        CHANGE SCALE(FEET TO METER)
GE1                        GROUND(CHARGE AT BASE ZERO)
EX0,1,1,01,1,0,75          FEED. 1V AT 1ST SEGMENTS
GN1                        PERFECTLY CONDUCTING GROUND
FR0,21,0,0,27,.2           FREQ. SWEEP. 27-31MHz
PL4                        IMPEDANCE AND SWR
XQ
EN
```

g. Model 3-2 Geometry Data Set (9, 9, 9 segment)

```
CM NEC SIMULATION FOR TELESCOPING ANT. EXPERIMENT
CM IMPEDANCE VS FREQUENCY CHANGE WHEN SEGMENT 9,9,9
(3TAG)
CM FREQUENCY CHANGE FROM 27MHz TO 31 MHz
CE
GW1,9, 0,0,0, 0,0,2.666667, 8.333333E-2        TAG1 9SEG
GW2,9, 0,0,2.666667, 0,0,5.333333, 7.8125E-2   TAG2 9SEG
GW3,9, 0,0,5.333333, 0,0,8., 7.291667E-2       TAG3 9SEG
```

```
GS1                 CHANGE SCALE(FEET TO METER)
GE1                 GROUND(CHARGE AT BASE ZERO)
EX0,1,1,01,1,0,75   FEED. 1V AT 1ST SEG IMPEDANCE
GN1                 PERFECTLY CONDUCTING GROUND
FR0,21,0,0,27,.2    FREQ. SWEEP. 27-31MHz
PL4                 IMPEDANCE and SWR
XQ
EN
```

h. Model 3-1-E Geometry Data Set (33 segment)

CM NEC SIMULATION FOR TELESCOPING ANT. EXPERIMENT (MODEL 3-1-E)

CM IMPEDANCE VS FREQUENCY CHANGE WHEN SEGMENTS ARE 11,11,11 (1TAG).

CM EQUAL RADIUS OF M3SE?=(1/2+3/8+1/4)/3 =3/8 INCH =1.5625E-2 FEET

CM FREQUENCY CHANGE FROM 27MHz TO 31 MHz

```
CE
GW1,33, 0,0,0, 0,0,8., 1.5625E-2   TAG1 33SEG
GS1                 CHANGE SCALE(FEET TO METER)
GE1                 GROUND(CHARGE AT BASE ZERO)
EK                  EK CARD
EX0,1,1,01,1,0,75   FEED. 1V AT 1ST SEGMENT
GN1                 PERFECTLY CONDUCTING GROUND
FR0,21,0,0,27,.2    FREQ. SWEEP. 27-31MHz
PL4                 IMPEDANCE AND SWR
XQ
EN
```

i. Model 3-2-E Geometry Data Set (39 segment)

```
CM NEC SIMULATION FOR TELESCOPING ANT. EXPERIMENT
CM IMPEDANCE VS FREQUENCY CHANGE WHEN SEGMENT 13,13,13
(1TAG)
CM EQUAL RADIUS OF M3S? =(1+15/16+7/8)/3=15/16 INCH =7.8125E-2
FEET
CM FREQUENCY CHANGE FROM 27MHz TO 31 MHz
CE
GW1,39, 0,0,0, 0,0,8., 7.8125E-2   TAG1 39SEG
GS1                  CHANGE SCALE(FEET TO METER)
GE1                  GROUND(CHARGE AT BASE ZERO)
EX0,1,1,01,1,0,75      FEED. 1V AT 1ST SEG IMPEDANCE
GN1                  PERFECTLY CONDUCTING GROUND
FR0,21,0,0,27,.2       FREQ. SWEEP. 27-31MHz
PL4                  IMPEDANCE AND SWR
XQ
EN
```

j. Model 4-1 Geometry Data Set (45 segment)

```
CM NEC SIMULATION FOR TELESCOPING ANT. EXPERIMENT
CM IMPEDANCE VS FREQUENCY CHANGE WHEN SEGMENT
9,9,9,9,9(5TAG)
CM FREQUENCY CHANGE FROM 27MHz TO 31 MHz
CE
GW1,9, 0,0,0, 0,0,1.6, 0.03125          TAG1 9SEG
GW2,9, 0,0,1.6, 0,0,3.2, 2.60417E-2     TAG2 9SEG
GW3,9, 0,0,3.2, 0,0,4.8, 2.0833E-2      TAG3 9SEG
GW4,9, 0,0,4.8, 0,0,6.4, 1.5625E-2      TAG4 9SEG
GW5,9, 0,0,6.4, 0,0,8., 1.0416667E-2    TAG5 9SEG
GS1                  CHANGE SCALE(FEET TO METER)
GE1                  GROUND(CHARGE AT BASE ZERO)
EX0,1,1,01,1,0,75      FEED. 1V AT 1ST SEG IMPEDANCE
```

```
GN1                     PERFECTLY CONDUCTING GROUND
FR0,21,0,0,27,.2        FREQ. SWEEP. 27-31MHz
PL4                     IMPEDANCE AND SWR
XQ
EN
```

k. Model 4-2 Geometry Data Set (50 segment)

```
CM NEC SIMULATION FOR TELESCOPING ANT. EXPERIMENT
CM IMPEDANCE VS FREQUENCY CHANGE WHEN SEGMENT 10,10,10,10,10(5TAG)
CM FREQUENCY CHANGE FROM 27MHz TO 31 MHz
CE
GW1,10, 0,0,0, 0,0,1.6, 8.33333E-2      TAG1 10SEG
GW2,10, 0,0,1.6, 0,0,3.2, 7.8125E-2     TAG2 10SEG
GW3,10, 0,0,3.2, 0,0,4.8, 7.2917E-2     TAG3 10SEG
GW4,10, 0,0,4.8, 0,0,6.4, 6.7708E-2     TAG4 10SEG
GW5,10, 0,0,6.4, 0,0,8., 6.25E-2        TAG5 10SEG
GS1                     CHANGE SCALE(FEET TO METER)
GE1                     GROUND(CHARGE AT BASE ZERO)
EX0.1,1,01,1,0,75       FEED. 1V AT 1ST SEG IMPEDANCE
GN1                     PERFECTLY CONDUCTING GROUND
FR0,21,0,0,27,.2        FREQ. SWEEP. 27-31MHz
PL4                     IMPEDANCE AND SWR
XQ
EN
```

l. Model 4-1-E Geometry Data Set (51 segment)

```
CM NEC SIMULATION FOR TELESCOPING ANT. EXPERIMENT (MODEL 4-1-E)
CM IMPEDANCE VS FREQUENCY CHANGE WHEN SEGMENTS ARE 17,17,17 (1TAG).
```

```
CM EQUAL RADIUS OF M3S?=(1/2+3/8+1/4)/3=3/8 INCH =1.5625E-2
FEET
CM FREQUENCY CHANGE FROM 27MHz TO 31 MHz
CE
GW1,51, 0,0,0, 0,0,8., 1.5625E-2   TAG1 51SEG
GS1                   CHANGE SCALE(FEET TO METER)
GE1                   GROUND(CHARGE AT BASE ZERO)
EK                    EK CARD
EX0,1,1,01,1,0,75       FEED. 1V AT 1ST SEGMENT
GN1                   PERFECTLY CONDUCTING GROUND
FR0,21,0,0,27,.2        FREQ. SWEEP. 27-31MHz
PL4                   IMPEDANCE AND SWR
XQ
EN
```

m. Model 4-2-E Geometry Data Set (60 segment)

```
CM NEC SIMULATION FOR TELESCOPING ANT. EXPERIMENT
CM IMPEDANCE VS FREQUENCY CHANGE WHEN SEGMENT 61(1TAG)
CM EQUAL RADIUS = (1+15/16+7/8+13/16+3/4)/5 = 7/8 INCH
CM 7/8 INCH = 7.2916667E-02 FEET = 2.2225E-02 METER
CM FREQUENCY CHANGE FROM 27MHz TO 31 MHz
CE
GW1,60, 0,0,0.0, 0,0,8.0, 7.2917E-2    TAG1 60SEG
GS1                   CHANGE SCALE(FEET TO METER)
GE1                   GROUND(CHARGE AT BASE ZERO)
EX0,1,1,01,1,0,75       FEED. 1V AT 1ST SEG IMPEDANCE
GN1                   PERFECTLY CONDUCTING GROUND
FR0,21,0,0,27,.2        FREQ. SWEEP. 27-31MHz
PL4                   IMPEDANCE AND SWR
XQ
EN
```

3. NECGS

Following are the sample geometry data sets for each model of NECGS.

a. Model 1 Geometry Data Set (constant radius modeling with no end cap)

```
CM NEC SIMULATION FOR EXPERIMENT (NECGS : 6 WIRE)
CM IMPEDANCE VS RADIUS CHANGE WHEN SEGMENT 6
CM RADIUS CHANGE FROM E-05 LAMDA TO 1 LAMDA
CM CENTER FREQUENCY 30.757874 MHz
CM LAMDA = 32 FEET AT 30.757874 MHz
CE
GR0,6
GW1,6, 32E-5,0,0, 32E-5,0,8., 5.333333334E-05      TAG1 6SEG 8FEET
GS1                          CHANGE SCALE(FEET TO METER)
GE1                          GROUND(CHARGE AT BASE ZERO)
EX0,1,1,01,1,0,75              FEED. 1V AT 1ST SEG IMPEDANCE
GN1                          PERFECTLY CONDUCTING GROUND
FR0,3,0,0,29.757874,1          CENTER FREG. 30.757874MHz
PL4                          IMPEDANCE AND SWR
XQ
EN
```

b. Model 2-1 Geometry Data Set (equal radius modeling with no end cap)

```
CM NEC SIMULATION FOR TELESCOPING ANT. EXPERIMENT (NECGS
: 6 WIRE)
CM IMPEDANCE VS FREQUENCY CHANGE WHEN SEGMENTS ARE 35
CM FREQUENCY CHANGE FROM 27MHz TO 31 MHz
CE
GR0,6
GW1,17, 2.0833333E-2,0,4, 2.0833333E-2,0,0, 0.
GC0,0,1.3287,3.472222E-3,3.472222E-3
GW2,1, 2.0833333E-2,0,4., 1.0416667E-2,0,4., 2.604167E-3
GW3,17, 1.0416667E-2,0,4, 1.0416667E-2,0,8, 0.
```

```
GC0,0,1.3287,1.736111E-3,1.736111E-3
GS1                   CHANGE SCALE(FEET TO METER)
GE1                   GROUND(CHARGE AT BASE ZERO)
EX0,1,17,01,1,0,75       FEED. 1V AT 1ST SEG IMPEDANCE
GN1                   PERFECTLY CONDUCTING GROUND
FR0,21,0,0,27,.2        FREQ. SWEEP. 27-31MHz
PL4                   IMPEDANCE AND SWR
XQ
EN
```

c. Model 2-2 Geometry Data Set (different radii modeling with an end cap)

```
CM NEC SIMULATION FOR TELESCOPING ANT. EXPERIMENT (NECGS : 6
WIRE)
CM IMPEDANCE VS FREQUENCY CHANGE WHEN SEGMENTS ARE 36
CM FREQUENCY CHANGE FROM 27MHz TO 31 MHz
CE
GR0,6
GW1,17, 4.1666667E-2,0,4, 4.1666667E-2,0,0, 0.
GC0,0,1.3287,6.944444E-3,6.944444E-3
GW2,1, 4.1666667E-2,0,4., 2.0833333E-2,0,4., 5.208333E-3
GW3,17, 2.0833333E-2,0.4, 2.0833333E-2,0,8, 0.
GC0,0,1.3287,3.472222E-3,3.472222E-3
GW4,1, 2.0833333E-2,0,8, 0,0,8, 3.472222E-3
GS1                   CHANGE SCALE(FEET TO METER)
GE1                   GROUND(CHARGE AT BASE ZERO)
EX0,1,17,01,1,0,75       FEED. 1V AT 1ST SEG IMPEDANCE
GN1                   PERFECTLY CONDUCTING GROUND
FR0,21,0,0,27,.2        FREQ. SWEEP. 27-31MHz
PL4                   IMPEDANCE AND SWR
XQ
EN
```

d. Model 2-1-E Geometry Data Set (equal radius modeling with no end cap)

```
CM NEC SIMULATION FOR EXPERIMENT (NECGS : 6 WIRE)
CM AVERAGE RADIUS OF .0208 FEET AND .0104 FEET = 0.0156 FEET
CE
GR0,6
GW1,14, 1.5625E-2,0,0, 1.5625E-2,0,8., 2.601667E-3 TAG1 1SEG 8FEET
GS1                    CHANGE SCALE(FEET TO METER =0.3048)
GE1                    GORUND(CHARGE AT BASE ZERO)
EX0,1,1,01,1,0,75        FEED. 1V AT 1ST SEG IMPEDENCE
GN1                    PERFECTLY CONDUCTING GROUND
FR0,21,0,0,27,.2       FREG. SWEEP. 27-31MHz BY 0.2MHz INCREMENT
PL4                    IMPEDANCE AND SWR
XQ
EN
```

e. Model 2-2-E Geometry Data Set (equal radius modeling with an end cap)

```
CM NEC SIMULATION FOR EXPERIMENT (NECGS : 6 WIRE)
CM AVERAGE RADIUS OF .0208 FEET AND .0104 FEET = 0.0156 FEET
CE
GR0,6
GW1,2, 3.125E-2,0,0, 3.125E-2,0,8., 5.208E-3 TAG1 1SEG 8FEET
GS1                    CHANGE SCALE(FEET TO METER =0.3048)
GE1                    GORUND(CHARGE AT BASE ZERO)
EX0,1,1,01,1,0,75        FEED. 1V AT 1ST SEG IMPEDENCE
GN1                    PERFECTLY CONDUCTING GROUND
FR0,21,0,0,27,.2       FREG. SWEEP. 27-31MHz BY 0.2MHz INCREMENT
PL4                    IMPEDANCE AND SWR
XQ
EN
```

f. Model 3-1 Geometry Data Set (different radii modeling with no end cap)

```
CM NEC SIMULATION FOR TELESCOPING ANT. EXPERIMENT (NECGS :
6 WIRE)
CM IMPEDANCE VS FREQUENCY CHANGE WHEN SEGMENT
CM FREQUENCY CHANGE FROM 27MHz TO 31 MHz
CE
GR0,6
GW1,13, 2.0833333E-2,0,2.66666667, 2.0833333E-2,0,0, 0
GC0,0,1.5050,3.472222E-3,3.472222E-3
GW2,1, 2.0833333E-2,0,2.66666667, 1.5625E-2,0,2.66666667, 3.038194E-3
GW3,10, 1.5625E-2,0,2.666667, 1.5625E-2,0,4, 0
GC0,0,1.5050,2.604167E-3,2.604167E-3
GW4,10, 1.5625E-2,0,5.333333334, 1.5625E-2,0,4, 0
GC0,0,1.5050,2.604167E-3,2.604167E-3
GW5,1, 1.5625E-2,0,5.333333334, 1.041667E-2,0,5.333333334,2.170139E-3
GW6,13, 1.041667E-2,0,5.33333334, 1.041667E-2,0,8, 0
GC0,0,1.5050,1.736111E-3,1.736111E-3
GS1                  CHANGE SCALE(FEET TO METER)
GE1                  GROUND(CHARGE AT BASE ZERO)
EX0,1,13,01,1,0,75      FEED. 1V AT 1ST SEG IMPEDANCE
GN1                  PERFECTLY CONDUCTING GROUND
FR0,21,0,0,27,.2       FREQ. SWEEP. 27-31MHz
PL4                  IMPEDANCE AND SWR
XQ
EN
```

g. Model 3-2 Geometry Data Set (different radii modeling with an end cap)

```
CM NEC SIMULATION FOR TELESCOPING ANT. EXPERIMENT (NECGS
: 6 WIRE)
CM IMPEDANCE VS FREQUENCY CHANGE WHEN SEGMENT
```

```
CM FREQUENCY CHANGE FROM 27MHz TO 31 MHz
CE
GR0,6
GW1,13, 8.3333333E-2,0,2.66666667, 8.3333333E-2,0,0, 0
GC0,0,1.5050,1.3888889E-2,1.3888889E-2
GW2,1,8.3333333E-2,0,2.66666667,7.8125E-2,0,2.66666667,1.3454861E-2
GW3,10, 7.8125E-2,0,2.666667, 7.8125E-2,0,4, 0
GC0,0,1.5050,1.3020833E-2,1.3020833E-2
GW4,10, 7.8125E-2,0,5.333333334, 7.8125E-2,0,4, 0
GC0,0,1.5050,1.3020833E-2,1.3020833E-2
GW5,1,7.8125E-2,0,5.33333334,7.291667E-2,0,5.33333334,1.2586805E-2
GW6,13, 7.2916667E-2,0,5.33333334, 7.2916667E-2,0,8, 0
GC0,0,1.5050,1.2152777E-2,1.2152777E-2
GW7,1, 7.2916667E-2,0,8, 0,0,8, 1.2152777E-2
GS1                   CHANGE SCALE(FEET TO METER)
GE1                   GROUND(CHARGE AT BASE ZERO)
EX0,1,13,01,1,0,75       FEED. 1V AT 1ST SEG IMPEDANCE
GN1                   PERFECTLY CONDUCTING GROUND
FR0,21,0,0,27,.2        FREQ. SWEEP. 27-31MHz
PL4                   IMPEDANCE AND SWR
XQ
EN
```

h. Model 3-1-E Geometry Data Set (equal radius modeling with no end cap)

```
CM NEC SIMULATION FOR TELESCOPING ANT. EXPERIMENT (NECGS : 6 WIRE)
CM IMPEDANCE VS FREQUENCY CHANGE WHEN SEGMENT 5,5,5 (1TAG)
CM EQUAL RADIUS OF M3S?=(1/2+3/8+1/4)/3=3/8 INCH = 1.5625E-2 FEET
CM FREQUENCY CHANGE FROM 27MHz TO 31 MHz
CE
```

```
GR0,6
GW1,15, 1.5625E-2,0,0, 1.5625E-2,0,8., 2.6041667E-3   TAG1 15SEG
GS1                    CHANGE SCALE(FEET TO METER)
GE1                    GROUND(CHARGE AT BASE ZERO)
EX0,1,1,01,1,0,75        FEED. 1V AT 1ST SEG IMPEDANCE
GN1                    PERFECTLY CONDUCTING GROUND
FR0,21,0,0,27,.2         FREQ. SWEEP. 27-31MHz
PL4                    IMPEDANCE AND SWR
XQ
EN
```

i. Model 3-2-E Geometry Data Set (different radii modeling with an end cap)

```
CM NEC SIMULATION FOR TELESCOPING ANT. EXPERIMENT (NECGS : 6 WIRE)
CM IMPEDANCE VS FREQUENCY CHANGE WHEN SEGMENT 5,5,5 (1TAG)
CM EQUAL RADIUS OF M3S? =(1/2+3/8+1/4)/3=3/8 INCH =1.5625E-2 FEET
CM FREQUENCY CHANGE FROM 27MHz TO 31 MHz
CE
GR0,6
GW1,3, 7.8124998E-2,0,0, 7.8124998E-2,0,8., 1.3020833E-3
GS1                    CHANGE SCALE(FEET TO METER)
GE1                    GROUND(CHARGE AT BASE ZERO)
EX0,1,1,01,1,0,75        FEED. 1V AT 1ST SEG IMPEDANCE
GN1                    PERFECTLY CONDUCTING GROUND
FR0,21,0,0,27,.2         FREQ. SWEEP. 27-31MHz
PL4                    IMPEDANCE AND SWR
XQ
EN
```

j. Model 4-1 Geometry Data Set (equal radius modeling with no end cap)

```
CM NECGS SIMULATION FOR TELESCOPING ANT. EXPERIMENT
(MODEL 4-1)
CM IMPEDANCE VS FREQUENCY CHANGE
CM FREQUENCY CHANGE FROM 27MHz TO 31 MHz
CE
GR0,6                     6 WIRE
GW1,9, 3.1253E-2,0,1.6, 3.1253E-2,0,0, 0
GC0,0,1.7675,3.472222E-3,3.472222E-3
GW2,1, 3.125E-2,0,1.6, 2.6041667E-2,0,1.6, 3.472222E-3
GW3,8, 2.6041667E-2,0,1.6, 2.6041667E-2,0,2.4, 0
GC0,0,1.7574,3.472222E-3,3.472222E-3
GW4,8, 2.6041667E-2,0,3.2, 2.6041667E-2,0,2.4, 0
GC0,0,1.7574,3.472222E-3,3.472222E-3
GW5,1, 2.6041667E-2,0,3.2, 2.083333E-2,0,3.2, 3.4722222E-3
GW6,8, 2.083333E-2,0,3.2, 2.083333E-2,0,4, 0
G C0,0,1.7574,3.472222E-3,3.472222E-3
G W7,8, 2.083333E-2,0,4.8, 2.083333E-2,0,4, 0
G C0,0,1.7574,3.472222E-3,3.472222E-3
G W8,1, 2.083333E-2,0,4.8, 1.5625E-2,0,4.8, 3.472222E-3
G W9,8, 1.5625E-2,0,4.8, 1.5625E-2,0,5.6, 0
G C0,0,1.7574,3.4722222E-3,3.4722222E-3
G W10,8, 1.5625E-2,0,6.4, 1.5625E-2,0,5.6, 0
GC0,0,1.7574,3.4722222E-3,3.4722222E-3
GW11,1, 1.5625E-2,0,6.4, 1.0416667E-2,0,6.4, 3.4722222E-3
GW12,9, 1.0416667E-2,0,6.4, 1.0416667E-2,0,8, 0
GC0,0,1.7675,3.472222E-3,3.472222E-3
GS1                  CHANGE SCALE(FEET TO METER)
GE1                  GROUND(CHARGE AT BASE ZERO)
EX0,1,9,01,1,0,75      FEED. 1V AT 1ST SEGMENT
GN1                  PERFECTLY CONDUCTING GROUND
FR0,21,0,0,27,.2       FREQ. SWEEP. 27-31MHz
PL4                  IMPEDANCE AND SWR
```

XQ
EN

k. Model 4-2 Geometry Data Set (different radii modeling with an end cap)

```
CM NECGS SIMULATION FOR TELESCOPING ANT. EXPERIMENT
(MODEL 4-2)
CM IMPEDANCE VS FREQUENCY CHANGE
CM FREQUENCY CHANGE FROM 27MHz TO 31 MHz
CE
GR0,6                                   6 WIRE
GW1,9, 8.3333333E-2,0,1.6, 8.3333333E-2,0,0, 0
GC0,0,1.7675,1.3888888E-2,1.3888888E-2
GW2,1, 8.333333E-2,0,1.6, 7.8125E-2,0,1.6, 1.3454861E-2
GW3,8, 7.8125E-2,0,1.6, 7.8125E-2,0,2.4, 0
GC0,0,1.7574,1.3020833E-2,1.3020833E-2
GW4,8, 7.8125E-2,0,3.2, 7.8125E-2,0,2.4, 0
GC0,0,1.7574,1.3020833E-2,1.3020833E-2
GW5,1, 7.8125E-2,0,3.2, 7.2916667E-2,0,3.2, 1.2586805E-2
GW6,8, 7.2916667E-2,0,3.2, 7.2916667E-2,0,4, 0
GC0,0,1.7574,1.2152778E-2,1.2152778E-2
GW7,8, 7.2916667E-2,0,4.8, 7.2916667E-2,0,4, 0
GC0,0,1.7574,1.2152778E-2,1.2152778E-2
GW8,1, 7.2916667E-2,0,4.8, 6.7708333E-2,0,4.8, 1.171875E-2
GW9,8, 6.7708333E-2,0,4.8, 6.770833E-2,0,5.6, 0
GC0,0,1.7574,1.1284722E-2,1.1284722E-2
GW10,8, 6.7708333E-2,0,6.4, 6.770833E-2,0,5.6, 0
GC0,0,1.7574,1.1284722E-2,1.1284722E-2
GW11,1, 6.7708333E-2,0,6.4, 6.25E-2,0,6.4, 1.0850694E-2
GW12,9, 6.25E-2,0,6.4, 6.25E-2,0,8, 0
GC0,0,1.7675,1.0416667E-2,1.0416667E-2
GW13,1, 6.25E-2,0,8, 0,0,8, 1.0416667E-2     A CAP
GS1                   CHANGE SCALE(FEET TO METER)
```

```
GE1                    GROUND(CHARGE AT BASE ZERO)
EX0,1,9,01,1,0,75       FEED. 1V AT 1ST SEGMENT
GN1                    PERFECTLY CONDUCTING GROUND
FR0,21,0,0,27,.2        FREQ. SWEEP. 27-31MHz
PL4                    IMPEDANCE AND SWR
XQ
EN
```

l. Model 4-1-E Geometry Data Set (equal radius modeling with no end cap)

```
CM NECGS SIMULATION FOR TELESCOPING ANT. EXPERIMENT
(MODEL 4-1-E)
CM IMPEDANCE VS FREQUENCY CHANGE WHEN SEGMENT 70(1TAG)
CM EQUAL RADIUS OF (3/8+5/16+1/4+3/16+1/8) = 1/4 INCH
CM 1/4 INCH = 2.08333333E-02 FEET = 6.3499999E-03 METER
CM FREQUENCY CHANGE FROM 27MHz TO 31 MHz
CE
GR0,6                  6 WIRE
GW1,70, 2.0833333E-2,0,0.0, 2.0833333E-2,0,8., 3.472222E-3
GS1                    CHANGE SCALE(FEET TO METER)
GE1                    GROUND(CHARGE AT BASE ZERO)
EX0,1,1,01,1,0,75       FEED. 1V AT 1ST SEGMENT
GN1                    PERFECTLY CONDUCTING GROUND
FR0,21,0,0,27,.2        FREQ. SWEEP. 27-31MHz
PL4                    IMPEDANCE AND SWR
XQ
EN
```

m. Model 4-2-E Geometry Data Set (different radii modeling with no end cap)

```
CM NEC SIMULATION FOR TELESCOPING ANT. EXPERIMENT (NECGS :
6 WIRE)
CM IMPEDANCE VS FREQUENCY CHANGE WHEN SEGMENT IS 1(1TAG).
CM EQUAL RADIUS = (1+15/16+7/8+13/16+3/4)/5 = 7/8 INCH
```

```
CM 7/8 INCH = 7.2916667E-02 FEET = 2.2225E-02 METER
CM FREQUENCY CHANGE FROM 27MHz TO 31 MHz
CE
GR0,6
GW1,1, 7.2916667E-2,0,0., 7.2916667E-2,0,8., 1.2152777E-2
GS1                  CHANGE SCALE(FEET TO METER)
GE1                  GROUND(CHARGE AT BASE ZERO)
EX0,1,1,01,1,0,75      FEED. 1V AT 1ST SEGMENT
GN1                  PERFECTLY CONDUCTING GROUND
FR0,21,0,0,27,.2       FREQ. SWEEP. 27-31MHz
PL4                  IMPEDANCE AND SWR
XQ
EN
```

APPENDIX D. INPUT IMPEDANCE CALCULATION AND RVAL PROGRAM

1. Input Impedance Calculation Program

```
C  THIS PROGRAM CALCULATES  THE REAL AND THE IMAGINARY VALUE OF
C  THE INPUT IMPEDANCE FROM MEASURING DATA, REFLECTION COEFFICIENT
C    KL( )  = MEASURED REFLECTION COEFFCIENT
C    KLM( )  = MEASURED MAGNITUDE OF REFLECTION COEFFCIENT
C    KLP( )  = MEASURED PHASE OF REFLECTION COEFFCIENT
C    KLR( )  = MEASURED REAL VALUE OF REFLECTION COEFFCIENT
C    KLI( )  = MEASURED IMAGINARY VALUE OF REFLECTION COEFFCIENT
C    ZIN( )  = CALCULATED INPUT IMPEDANCE ( COMPLEX )
C    ZR( )  = CALCULATED INPUT IMPEDANCE ( REAL )
C    ZI( )  = CALCULATED INPUT IMPEDANCE ( IMAGINARY )
C    KC( )  = MEASURED CORRECTION REFLECTION COEFFICIENT
C    KCM( )  = MEASURED MAGNITUDE CORRECTION REFLECTION COEFFICIENT
C    KCP( )  = MEASURED PHASE CORRECTION REFLECTION COEFFICIENT
C    KF( )  = CALCULATED FINAL REFLECTION COEFFICIENT
C    KFM( )  = CALCULATED FINAL MAGNITUDE OF REFLECTION COEFFICIENT
C    KFP( )  = CALCULATED FINAL PHASE OF REFLECTION COEFFICIENT
C    KFR( )  = CALCULATED FINAL REAL VALUE OF REFLECTION COEFFICIENT
C    KFI( )= CALCULATED FINAL IMAGINARY VALUE OF REFLECTION COEFFICIENt
C    F1 ( ) = F2( ) = FREQUENCY
      COMPLEX KL(100),ZIN(100),KC(100),KF(100)
      REAL  KLM(100),KLP(100),ZR(100),ZI(100),K CM(100),KCP(100)
      REAL  KLR(100),KLI(100),F1(100),F2(100),K CR(100),KCI(100)
      REAL  KFM(100),KFP(100),KFR(100),KFI(100)
      INTEGER L1(100),L2(100)
C     OPEN ( UNIT = 10 , FILE = 'IMP SHORT' , STATUS = 'OLD' )
C     OPEN ( UNIT = 11 , FILE = 'IMP EX1' , STATUS = 'OLD' )
C     OPEN ( UNIT = 15 , FILE = 'IMPEX1RI DATA')
C     OPEN ( UNIT = 16 , FILE = 'IMPEX1MP DATA')
      OPEN ( UNIT = 10 , FILE = 'IMP CAP1 SHORT1' , STATUS = 'OLD' )
      OPEN ( UNIT = 11 , FILE = 'IMP CAP1 NOEX1' , STATUS = 'OLD' )
      OPEN ( UNIT = 15 , FILE = 'IMP C1RI DATA')
      OPEN ( UNIT = 16 , FILE = 'IMP C1MP DATA')
      N = 23
      DO 10 I = 1,N
        READ (10,*) L1(I),F1(I),K CM(I),KCP(I)
        READ (11,*) L2(I),F1(I),KLM(I),KLP(I)
10      CONTINUE
      PI = 4.*ATAN(1.0)
```

```
      DTR = PI 180.
      DO 20 J = 1,N
C         KLR(J) = KLM(J)*COS(DTR*KLP(J))
C         KLI(J) = KLM(J)*SIN(DTR*KLP(J))
C         KL(J) = CMPLX(KLR(J),KLI(J))
C         KCR(J) = KCM(J)*COS(DTR*KCP(J))
C         KCI(J) = KCM(J)*SIN(DTR*KCP(J))
C         KC(J) = CMPLX(KCR(J),KCI(J))
C         KF(F) = KL(J) KC(J)
C         ZIN(J) = 50.*(1.+KF(J)) (1.-KF(J))
C         ZR(J) =REAL(ZIN(J))
C         ZI(J) =AIMAG(ZIN(J))
C         WRITE (16,100) F1(J),ZR(J),ZI(J)
C
50     KFM(J) = KLM(J) K CM(J)
      KFP(J) = KLP(J)-(-180.+K CP(J))
      KFR(J) = KFM(J)* COS(DTR*KFP(J))
      KFI(J) = KFM(J)*SIN(DTR*KFP(J))
      KF(J) =  CMPLX(KFR(J),KFI(J))
      ZIN(J) = 50.*(1.+KF(J)) (1.-KF(J))
      ZR(J) =REAL(ZIN(J))
      ZI(J) =AIMAG(ZIN(J))
20     CONTINUE
      WRITE (15,105)
      WRITE (16,115)
      WRITE (15,110)
      WRITE (16,120)
      DO 30 K = 1,N
      WRITE (15,100) L1(K),F1(K),ZR(K),ZI(K)
      WRITE (16,100) L2(K),F1(K),KFM(K),KFP(K)
30     CONTINUE
100    FORMAT(3X,I4,3(5X(E16.7)))
105    FORMAT (20X,' INPUT IMPEDAN CE     ')
115    FORMAT (15X,'  CALCULATED FINAL REFLECTION COEFFICIENT  ')
110    FORMAT (3X,'NO. OF TEST',6X,'FREQ.',16X,'REAL',13X,'IMAGINARY')
120    FORMAT (3X,'NO. OF TEST',6X,'FREQ.',14X,'MAGNITUDE',14X,'PHASE')
      STOP
      END
```

2. RVAL Program

```
****  THIS PROGRAM COMES FROM NEC LIBRARY AT NPS.  ****
C     PROGRAM RVAL - CALCS TAPERED SEGMENT PARMS FOR GC CARD
C
C              USE IT FOR SMALL TO BIG STEPPING, ONLY
```

```
C
      REAL*4      S1
      REAL*4      SN
      REAL*4      L
C
C   GET INPUTS
C
      CALL FRTCMS('FILEDEF ', 'FT05F001', 'TERMINAL')
      CALL FRTCMS('FILEDEF ', 'FT06F001', 'TERMINAL')
 1005 CONTINUE
      WRITE(6,'(1X,A)') 'PLEASE ENTER FIRST SEGMENT LENGTH',
     !             '              LAST SEGMENT LENGTH',
     !             '                  TOTAL LENGTH'
      READ(5,*,END=1005) S1, SN, L
      SNOVS1 = SN / S1
C
C     CALCULATE THE ANALYTIC SOLUTION
C
      R = 1. / (1. - ((SN - S1) / L))
      N = LOG(SNOVS1) / LOG(R) + 1.
C
C     PRINT SOLUTION
C
      WRITE(6,'(1X,A,I5)') 'N = ', N
      WRITE(6,'(1X,A,F10.4)') 'R = ', R
C
      S1 = L * (1. - R) / (1. - (R ** N))
      WRITE(6,( " S(",I3,") = ", F10.4)') 1, S1
      SSUM = S1
C
      DO 1010 I = 2, N
C
        S = S1 * (R ** (I - 1))
        SSUM = SSUM + S
        WRITE(6,'(" S(",I3,") = ", 2F10.4)') I, S, SSUM
C
 1010 CONTINUE
      WRITE(6,'(1X,A,F10.4)') 'WIRE LENGTH = ', SSUM
      STOP
      END
```

LIST OF REFERENCES

1. Moore, J. and Pizer, R., *Moment Methods in Electromagnetics Techniques and Applications*, Research Studies Press, June 1983.

2. Burke, G. J. and Poggio, A. J., Naval Ocean Systems Center Technical Document 116, Volume 2., *Numerical Electromagnetics Code (NEC) "Method of Moments"* , Lawrence Livermore Lavoratory, January 1981.

3. Logan, J. C. and Rockway, J. W., Naval Ocean System Center Technical Document 938, *The New MININEC (Version 3): A Mini-Numerical Electromagnetic Code*, September 1986.

4. Butler, C. M., Duff, B. M., King, R. W. P., Yung, E. K., and Singarayer, S., *Theoretical and Experimental Investigations of Thin-wire Structures: Junction Connections, Current, and Charges*, AFWL Interaction Note 238, February 1975.

5. King, R. W. P., and Wu, T. T., "The Tapered Antenna and its Application to the Junction Problem for Thin Wires", *IEEE Trans. Antennas and Propagation*, Vol. AP - 24, No. 1, pp. 42 - 45, January 1976.

6. Curtis, W. L., "Charge Distribution on a Dipole with a Stepped Change in Radius", *1976 AP-S International Symposium Digest*, Amherst, Massachusetts, pp. 189 - 192, October 1976.

7. Glisson, A. W., and Wilton, D. R., *Numerical Procedures for Handling Stepped Radius Wire Junctions*, University of Mississippi Final Report for Contract N-66001-77-C-0156, March 1979.

8. Breakall, J. K., and Adler, R. W., "A Comparison of NEC and MININEC on the Stepped Radius Problem", *Applied Computational Electromagnetics Society Journal & Newsletter*, Vol. 2 No. 2, Fall 1987.

9. Rockway, J. W., Logan, J. C., Tam, D. W. S., and Li, S. T., *The MININEC System:Microcomputer Analysis of Wire Antennas*, Artech House, 1988

10. Favorite, J., *Naval Postgraduate School Report MVS-01, User's Guide to MVS at NPS*, Naval Postgraduate School Report MVS-01, November 1983.

11. *Signal Generator(8640) Operating and Service Manual*, Hewlett Packard, 1972

12. *Vector Voltmeter(8605A) Operating and Service Manual*, Hewlett Packard, 1971

13. *Measurement of Complex Impedance (Application Note 77-3)*, Hewlett Packard, 1967

14. Brown, R. G., Shapre, R. A., Hughes, W. L., and Post, R. E., *Lines,Waves, and Antennas(2nd edition)*, The Ronald Press Company, New York, 1973

15. Thomson, D.D, *Electromagnetic Near Field Computations for a Broadcast Mononploe using the Numerical Electromagnetics Code(NEC)* , M.S.E.E. Thesis, Naval Postgraduate School, Monterey, California, Semptember, 1983

INITIAL DISTRIBUTION LIST

		No. Copies
1.	Defense Technical Information Center Cameron Station Alexandria, VA 22304-6145	2
2.	Library, Code 0142 Naval Postgraduate School Monterey, CA 93943-5002	2
3.	Chairman, Code 62 Department of Electrical and Computer Engineering Naval Postgraduate School Monterey, CA 93943-5000	1
4.	Research Administration, Code 012 Naval Postgraduate School Monterey, CA 93943-5000	1
5.	Dr. Richard W. Adler, Code 62Ab Department of Electrical and Computer Engineering Naval Postgraduate School Monterey, CA 93943-5000	20
6.	Dr. James K. Breakall, Code 62Bk Department of Electrical and Computer Engineering Naval Postgraduate School Monterey, CA 93943-5000	20
7.	John Belrose CRC/DRC, Bldg 2A, Rm 330 3701 Carling Avenue, Box 11490 STA H Ottawa ON Canada K2H8S2	1
8.	Al Christman Grove City College Electrical Engineering Department Grove City, PA 16127	1
9.	Roger E. Cox Telex Communications Inc.	1

8601 Northeast Hwy 6
Lincoln, NE 68505

10. E. Cummins, Jr. 1
19020 Quail Valley Blvd.
Gaithersburg, MD 20879

11. Dr. S. J. Kubina 1
Concordia University
7141 Sherbrooke ST West
Montreal, Quebec
Canada H4B1R6

12. Mr. Jim Logan 1
NOSC Code 822 (T)
271 Catalina Blvd.
San Diego, CA 92152

13. Commander, Janet McDonald 1
USAISEC.ASB-SET-P
FT. Huachuca, AZ 85613-5300

14. E. K. Miller 1
519 Innwood Road
Simi Valley, CA 93065

15. Ric Thowless 1
NOSC Code 822 (T)
271 Catalina Blvd.
San Diego, CA 92152

16. Bill Werner 1
Andrew Calif. Corp.
2028 Old Middlefield Way
Mountain View, CA 94043

17. Prof. Don Wilton 1
University of Houston/EE Dept.
4800 Calhoun
Houston, TX 77004

18. Yim, Jae Yong 2
Chung Book Chung Joo City Bong Whang Dong 1339

(Young Mi Super 2nd floor)
Republic of Korea, ZIP-Code 360-140

19. Libray. P.O.Box 77 1
Gong Neung Dong, Dobong Ku
Seoul 130-09
Republic of Korea

20. Libray. P.O.Box 77 1
Doon San Dong, Joong Ku
Dae Jun city. Cuoong Chung Nam Do
Republic of Korea

21. Mr. G. J. Burke 1
L-156 LLNL
P.O. Box 808
Livermore, CA 94550